Chen Tan

Towards a Versatile and Sustainable Platform for Tailor-Made Adhesives

Åbo Akademi University

Towards a Versatile and Sustainable Platform for Tailor-Made Adhesives

Chen Tan

Laboratory of
Molecular Science and Engineering
Faculty of Science and Engineering
Åbo Akademi University
Åbo, Finland, 2022

Supervised by

Professor Carl-Eric Wilén
Polymer Technology
Molecular Science and Engineering
Åbo Akademi University, Finland

Co-supervised by

Laboratory Engineer Teija Tirri
Polymer Technology
Molecular Science and Engineering
Åbo Akademi University, Finland

Pre-examiner and Opponent

Docent Sami Hietala
Department of Chemistry
Helsinki University, Finland

Pre-examined by

Professor Mikael Skrifvars
Faculty of Textiles, Engineering and Business
University of Borås, Sweden

ISBN 978-952-12-4196-3 (PRINT)
ISBN 978-952-12-4197-0 (PDF)
Painosalama Oy, Åbo, Finland, 2022

"If you plan for one year, plant rises.

If you plan for 10 years, plant trees.

If you plan for 100 years, educate mankind."

书山有路勤为径，学海无涯苦作舟。

Acknowledgements

This thesis was carried out at the Laboratory of Polymer Technology, Åbo Akademi University (ÅA) in collaboration with different industrial companies.

I would like to express my great appreciation to my supervisor, Teija Tirri, for her great supervision and systematic instruction as well as great support and help both in my PhD work and life. We worked together as workmates and friends. I was greatly grateful to my supervisor, Prof. Carl-Erik Wilén, for his great trust and support during my PhD study. Without his insistence and inclusion, I cannot complete my doctoral thesis.

I would like to thank all my colleagues, the personnel at the Polymer Technology Laboratory, for their strong help and guidance both in my work and life, especially the best time we spent together I will never forget.

Finally, I would like to express my deepest feeling to my family, my parents and my dearest little princess Nicole who have always supported and accompanied me. Without you all, I can not achieve and arrive this destiny. Special thanks go to all my Chinese friends in Finland and China (especially during my stay in Changshu). You all make my life more colorful.

Too many thanks and cannot be expressed properly by word. After all, I would like to say: love you all forever~!

At last but not least, this is a hard moment for us all, due to the COVID-19 crisis. I wish all of you: a healthier, safer, and happier all the time. Hopefully, meet you somewhere and someday!

To myself: this is an end and also a start. Move on and never stop!

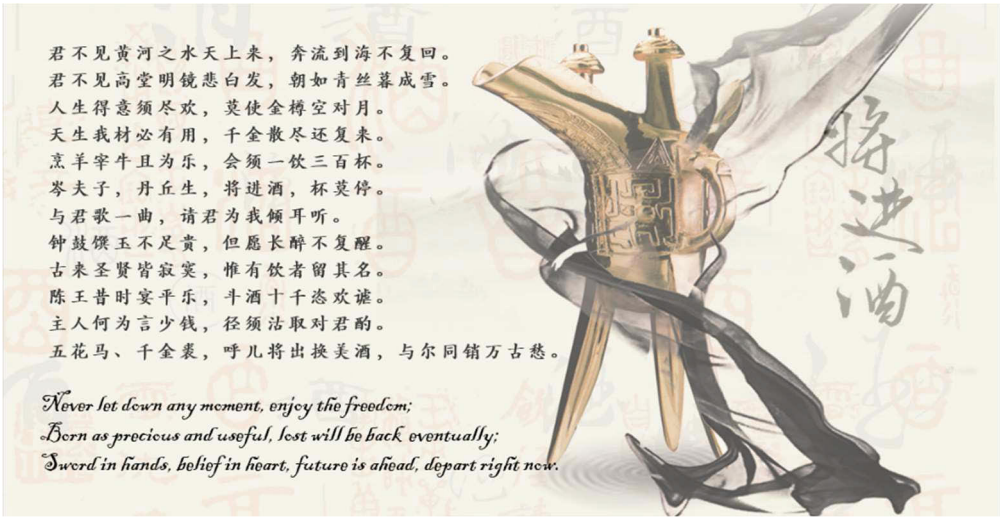

Feb. 2022 Changshu, China

Chen Tan

Abstract

The main objective of the present thesis work was to explore the possibility to design and synthesize versatile environmental-friendly adhesives and to adjust their properties to be suitable for different purposes by studying the adhesives structure-property relationships. The thesis consists of a summary part and three articles. Three different types of adhesives were developed in this study and the main results have been published in three articles.

In the first part of this study, the aim was to develop poly(styrene-co-butyl acrylate) emulsion based adhesives that simultaneously exhibit high cohesive and adhesive strength via structured core–shell particle design. The structure–property relationship was examined by various characterization methods including size-exclusion chromatography (SEC), cryogenic transmission electron microscopy (cryoTEM), differential scanning calorimetry (DSC) and dynamic mechanical analysis (DMA). Optimized properties were achieved by changing the core–shell ratio, degree of crosslinking of the core by using different concentrations of ethylene glycol dimethacrylate (EGDMA) and modification of the soft shell by varying the concentration of a thiol based chain transfer agent (CTA). Crosslinking of the core part enabled high cohesive strength of the adhesive, whilst the relatively soft shell facilitated high adhesion by enabling the proper wetting of the substrate. The optimal adhesive performance in terms of tack, peel strength and shear strength were achieved when the latex particles had a crosslinked core, a shell prepared without CTA and a core–shell ratio of 1:1.5. Thus, the goal of combining sufficient energy storage and energy dissipation properties in one particle through structured particle design was successful.

In the second part, a number of chain-extended moisture-curable urethane prepolymers were synthesized in order to develop isocyanate terminated urethane prepolymer formulations that would at the same time display both high adhesive strength and low viscosity. Proton nuclear magnetic resonance spectroscopy (1H-NMR), size exclusion chromatography (SEC), differential scanning calorimetry (DSC), and Brookfield viscometry were utilized for characterizing the prepared urethane prepolymers. In addition, the adhesion strength of the cured prepolymers was determined by tensile shear strength test according to the DIN 1465 standard. Especially, the role of different types of linear (butanediol, pentanediol) and branched chain extenders (di-propylene glycol (di-PPG), tri-propylene glycol (tri-PPG) and the influence of their dosage on the degree of microphase separation between hard segments (HS) and soft segments (SS) in urethane prepolymers were studied. Furthermore, the benefits of utilizing a one-step versus a two-step polymerization process were investigated. The results revealed that the extent of phase separation of different urethane prepolymers was dependent on the extent of hydrogen bonding

interactions which was extensively studied by attenuated total reflectance infrared spectroscopy (ATR-FTIR). The incorporation of branched chain extenders (di-PPG and tri-PPG) did not result in notable phase separation between hard segments and soft segments, while linear chain extenders (pentanediol and butanediol) readily promoted phase separation. The degree of phase separation was particularly pronounced for butanediol, and when the linear chain extender ratio was higher than or equal to 0.74. Compared with a two-stage process, one-stage process produced more randomly distributed polymer chains with highly dispersed hard segments. Thus, urethane prepolymers exhibiting strong adhesive strength with simultaneously low viscosity were successfully developed by systematic adjustment of structural parameters.

The third research work explored the possibility of synthesizing moisture-curable silane-terminated poly(urethane-urea)s (SPURs) of low viscosity. First, NCO-terminated urethane prepolymers were prepared, followed by silane end-capping. The impact of polyol molecular weight and the ratio of isocyanate to polyol (NCO/OH) on viscosity and the properties of SPUR were examined. As alternatives to the organotin catalysts traditionally used for the polyurethane synthesis and curing processes, a toxicological more favourable bismuth carboxylate catalyst was evaluated. In addition, the effect of organofunctional groups in the aminosilane structure (R_1–NH–R_2–Si(OR_3)$_3$), i.e., R_1 (alkyl, aryl or trimethoxysilylpropyl), the spacer R_2 (α or γ) and alkyl group R_3 (methyl or ethyl), was examined. The chemical structures of the SPURs were investigated by nuclear magnetic resonance spectroscopy (NMR), Fourier transform infrared spectroscopy (FT-IR) and the mechanical properties were evaluated by tensile tests. The results show that silane-terminated, moisture-curable polyurethanes can be efficiently synthesized and cured with bismuth carboxylate catalyst. Thus, SPUR exhibiting low viscosity, with adequate tensile strength and elongation could be prepared using environmentally benign bismuth carboxylate catalyst having a high metal content of 19%–21%, by utilizing secondary aminosilane end-cappers and an optimal combination of the polyol molecular weight and NCO/OH ratio.

Sammanfattning

Huvudsyftet med denna doktorsavhandling var att undersöka möjligheten att syntetisera skräddarsydda och miljövänliga högkvalitativa lim samt att optimera deras egenskaper genom att studera limmets struktur-egenskapsförhållanden. Avhandlingen består av en sammanfattande del och tre artiklar. Tre olika typer av lim utvecklades i denna studie och huvudresultaten publicerades i tre internationella fackliga tidskrifter.

I den första delen av denna studie var syftet att tillverka poly(styren-sam-butylakrylat) emulsionsbaserade lim som samtidigt skulle uppvisa hög kohesions- och vidhäftningsstyrka via optimering av emulsionspartiklarnas morfologi och kemiska sammansättning hos kärnan och skalet. Struktur-egenskapsförhållandet undersöktes med hjälp av olika analysmetoder såsom storleks uteslutningskromatografi (SEC), kryogen transmissions elektronmikroskopi (cryoTEM), svepkalorimetri (DSC) och dynamisk mekanisk analys (DMA). Resultaten uppvisar att dispersionslim med både hög kohesion och vidhäftningsegenskaper kunde tillverkas genom syntes av heterogena partiklar som hade ett hårt och delvis tvärbunden kärna och ett mjukt skal. Tvärbindning av kärndelen möjliggjorde hög kohesions styrka hos limmet, medan det relativt mjuka skalet underlättade hög vidhäftning genom att möjliggöra god vätning till underlaget.

I den andra delen av avhandlingen syntetiserades ett antal fukthärdande polyuretanlim som samtidigt skulle uppvisa både hög vidhäftningshållfasthet och låg viskositet. Proton kärnmagnetisk resonansspektroskopi (^{1}H-NMR), SEC, DSC och Brookfield-viskometri användes för att karakterisera de framställda uretan prepolymererna. Vidhäftningshållfastheten för de härdade prepolymererna undersöktes sedan enligt DIN 1465-standarden. Särskilt inverkan av olika typer av linjära (butandiol, pentandiol) och förgrenade kedjeförlängare (di-propylenglykol (di-PPG), tri-propylenglykol (tri-PPG) och effekten av deras dosering på graden av mikrofas separation mellan hårda segment (HS) och mjuka segment (SS) i uretanprepolymerer studerades. Vidare undersöktes fördelarna med att använda en en-stegs kontra en tvåstegs polymerisationsprocess. Resultaten visade att graden av fasseparation av olika uretaner prepolymerer var starkt beroende av vätebindningsinteraktioner som sedan studerades omgående med hjälp av total reflektans infraröd spektroskopi (ATR-FTIR). Inkorporering av förgrenade kedjeförlängare (di-PPG och tri-PPG) resulterade inte i märkbar fasseparation mellan hårda segment och mjuka

segment, medan linjära kedjeförlängare (pentandiol och butandiol) främjade fasseparationen. Graden av fasseparation var särskilt markant för butandiol när det linjära kedjeförlängningsförhållandet var högre än eller lika med 0,74. Jämfört med en tvåstegsprocess producerade enstegsprocessen mer slumpmässigt fördelade polymerkedjor med starkt dispergerade hårda segment. Uretanprepolymerer som uppvisar stark vidhäftningsstyrka med samtidigt låg viskositet utvecklades framgångsrikt genom systematisk justering av de strukturella parametrarna.

Det tredje forskningsarbetet undersökte möjligheten att syntetisera fukthärdbara silylterminerade poly(uretan-urea) (SPUR) med låg viskositet. Först framställdes NCO-terminerade uretanprepolymerer som sedan reagerades vidare med sekundära aminoalkoxysilaner. Effekten av polyolens molekylvikt och förhållandet mellan isocyanat och polyol (NCO/OH) på viskositeten och egenskaperna hos SPUR undersöktes. Som alternativ till de tennkatalysatorer som traditionellt används för polyuretansyntes- och härdningsprocesser, utvärderades möjligheterna att alternativt använda en miljövänligare vismutkarboxylatkatalysator. Dessutom undersöktes effekten av organofunktionella grupper i aminoalkoxysilanstrukturen (R1–NH–R2–Si(OR3)3), dvs R1 (alkyl, aryl eller trimetoxisilylpropyl), spacern R2 (α eller γ) och alkylgrupp R3 (metyl eller etyl) inverkan på SPUR limmets egenskaper. De kemiska strukturerna hos SPURerna studerades med kärnmagnetisk resonansspektroskopi (NMR), Fourier-transform infraröd spektroskopi (FT-IR) och de mekaniska egenskaperna utvärderades genom dragförsök. Detta arbete visar att silanterminerade, fukthärdbara polyuretaner effektivt kan syntetiseras och härdas med vismutkarboxylatkatalysator. SPUR som uppvisar låg viskositet, med god draghållfasthet och töjning kunde således framställas med användning av miljövänlig vismutkarboxylatkatalysator med en hög metallhalt på 19 %–21 %, genom att använda sekundära aminoalkoxysilaner och en optimal kombination av polyolens molekylvikt och NCO/OH-förhållande.

Resultaten från dessa studier kan utnyttjas för att vidare utveckla nya miljövänligare lim som även uppvisar förbättrade adhesions egenskaper.

List of original publications

This thesis is based on the work contained in the following publications, referred to by Roman numerals in the text:

I) C. Tan, T. Tirri, C-E. Wilen. The effect of core-shell particle morphology on adhesive properties of poly(styrene-co-butylacrylate), Journal of Adhesion and Adhesives 2015.

II) C. Tan, Teija Tirri, C-E.Wilen, Investigation on the Influence of Chain Extenders on the Performance of One-Component Moisture-Curable Polyurethane Adhesives, Polymers 2017, 9, 184.

III) C. Tan, V. Luona, T. Tirri, C-E. Wilen, The Synthesis of Low-Viscosity Organotin-Free Moisture-Curable Silane-Terminated Poly(Urethane-Urea)s, Polymers 2018, 10, 781.

The author´s contribution to the publications:

For all publications C. Tan was responsible for designing the research plans together with the co-authors. C. Tan synthesized and characterized most of the adhesives and planned as well as performed most of the analytical studies. C. Tan analyzed the data as well as results and she wrote the first drafts of the manuscripts and finalized them together with the co-authors.

Abbreviations

SEC	Size-exclusion chromatography
GPC	Gel permeation chromatography
cryoTEM	Cryogenic transmission electron microscopy
DSC	Differential scanning calorimetry
DMA	Dynamic mechanical analysis
EGDMA	Ethylene glycol dimethacrylate
CTA	Chain transfer agent
1H-NMR	Proton nuclear magnetic resonance spectroscopy
Di-PPG	Di-propyleneglycol
Tri-PPG	Tri-propyleneglycol
HS	Hard segment
SS	Soft segment
ATR-FTIR	Attenuated total reflectance - Fourier transform infrared spectroscopy
SPURs	Poly(urethane-urea)s
PUR	Polyurethane
NMR	Nuclear magnetic resonance spectroscopy
PSA	Pressure sensitive adhesive
VOC	Volatile organic compound
DLVO	Derjaguin, Landau, Verwey, and Overbeek theory
WBLs	Weak boundary layers
Tg	Glass transition temperature
SDS	Sodium dodecyl sulfate
2-EHA	2-ethyl hexyl acrylate
APEO	Alkylphenol ethoxylates
AA	Acrylic acid
MFFT	Minimum film formation temperature
CO_2	Carbon dioxide
TDI	Toluene diisocyanate

BO	Butylene oxide
EO	Ethylene oxide
PO	Propylene oxide
PTMOs	Polytetramethylene oxides
HMDI	Hexamethylene diisocyanate
hMDI	Hydrogenated methylene diphenyl diisocyanate
IPDI	Isophorone diisocyanate
TMXDI	Tetramethylxylene diisocyanate
MDI	Methylene diphenyl diisocyanate
pMDI	Polymeric methylene diphenyl diisocyanate
MCPUs	Moisture-curable urethane prepolymers
MF	Melamine-formaldehyde
PFR	Phenol-resorcinol-formaldehyde
DBT(D)L	Dibutyltin dilaurate
BuA	Butyl acrylate
St	Styrene
EGDMA	Ethylene glycol dimethacrylate
KPS	Potassium persulfate
TBHP	Tert-butyl hydroperoxide
THF	Tetra hydrofuran
DLS	Dynamic light scattering
LT-ELSD	Low temperature evaporative light scattering detector
Mn	Number-average molecular weight
Mw	Weight-average molecular weight
PDI	Polydispersity index
VTMO	Vinyl trimethoxysilane
DOTL	Dioctyltin dilaurate
PTFE	Polytetrafluoroethylene
CE	Chain extender
Mc	Molecular weight between crosslinks

COSY	Correlation spectroscopy
HSQC	Heteronuclear single quantum coherence
HMBC	Heteronuclear multiple bond correlation
p-NCO	Primary isocyanate
s-NCO	Secondary isocyanate
P-UR	Primary urethane
S-UR	Secondary urethane

Table of contents

1. Introduction

The adhesion science deals with understanding material properties that are associated with formation of interfacial interlocking, changes in the interfaces by time and events leading to failure of adhesive/cohesive joints. Adhesion science is a multidisciplinary subject where different aspects are studied in a holistic approach in an attempt to understand the fundamental mechanisms of interatomic and intermolecular interactions at the interface of two surfaces that make them to stick together. It is important to make a distinction between adhesion and cohesion, i.e. adhesion involves molecular interactions at the interface of two dissimilar materials bonding together, whereas cohesion describes the intermolecular attractions between like materials sticking together via primary and often also via secondary bonding such as hydrogen bonding. Thus, cohesion refers to the internal strength of an adhesive due to various interactions within the adhesive that binds the substrates together. While adhesion refers to the bonding of one material to another, that is, an adhesive to a substrate, through a number of different possible interactions at the adhesive-substrate surface interface. In this context, it is important to remember that in every situation involving an adhesive and a substrate, the combination of adhesion and cohesion determines the overall bonding effectiveness.

Adhesive joints can be achieved both by chemical and mechanical bonding. When uncured, adhesives are fluid and they can flow over the substrate, filling the voids/pores of the surface and attach or "bond" to that surface by mechanical interlocking, i.e. the adhesive penetrating into the adherent gives raise to mechanical adhesion. A classic example of a process for mechanical interlocking is extrusion coating, where molten polymer film is applied onto the surface of a moving paper whereby the molten polymer is penetrating into the pores of the paper and so becoming mechanically interlocked during cooling and solidification of the polymeric adhesive.

When there are chemical bonds within the adhesive joints, they may involve covalent, ionic, metallic or chelation bonding. It follows from the above that the adhesive bonded chemically to a substrate often has a modified molecular structure at the bonding interface. This interfacial region, the so-called adhesion zone, is characterized by some changes in the adhesive structure due to bonding interactions.

To promote chemical adhesion, one may use various synthetic polymeric adhesives. The phenol-formaldehyde resins invented by Baekeland were the first synthetic polymer used as adhesives. Even today, phenol formaldehyde, urea-formaldehyde and melamine formaldehyde resins are widely used as adhesives for the bonding of plywood, structural wood products such as laminates and mineral wool. Epoxy based polymer is an example of high-performance adhesives exhibiting high temperature resistance and mechanical properties in conjunction with excellent resistance towards most acids, alkalis, solvents and

corrosive agents. Otto Bayer developed another important family of adhesives, namely, polyurethane based adhesives for bonding of wood, glass, composites and leather. (Dennis G. Lay, Polyurethane Adhesives, 2018) Moreover, organo-silane agents have been utilized to enhance chemical adhesion.

Acrylic adhesives were introduced in 1930s and later they formed the basis for a complex series of adhesives including cyanoacrylates, acrylic cements, structural adhesives, pressure-sensitive adhesives, hardening adhesives and two-part toughened adhesives. Acrylic adhesives are either thermoplastics, which can be molded above a certain temperature, or thermosetting polymer, which 'cure' once and cannot be re-molded. Acrylic adhesives are capable of adhering a number of different materials from polymers to glass. The acrylic adhesives can be produced by emulsion polymerization using different monomers such as ethyl acrylates, 2-ethyl-hexylacrylates, butyl acrylate and co-monomers e.g. vinyl acetate, vinyl ethers and styrene. Besides polymer composition, the molecular weight of the acrylate polymer also affects adhesion properties. A steadily growing segment of adhesives is pressure-sensitive adhesives (PSAs) that are also based on waterborne acrylate dispersions. PSAs are highly viscoelastic liquids that adhere to virtually any surfaces when lightly pressed down and they can be detached without leaving traces. They exhibit permanent tack and sufficient cohesion to be used as, for example, self-adhesive adhesion labels after removal from a release liner.

Formulators of adhesives are looking for new adhesives that better meet stricter performance demands, the more stringent restrictions of chemical substances, recycling and other sustainable requirements, low–migration tendency of adhesive compounds, solvent free or waterborne solutions, adhesives with reduced or zero- volatile organic compounds (VOC), formulations with reduced weight and cost, fast processing and easy of handling, etc.

2. Scope of the Thesis

The aim of this thesis is as follows: 1) to design core-shell type of emulsion adhesives that exhibit simultaneously high cohesive and adhesive properties, 2) to prepare isocyanate terminated urethane prepolymers that exhibit high adhesive strength in combination with low viscosity by rational adjusting the length and type of chain extenders, and 3) to develop low viscous organotin-free high performance one-component silane-terminated polyurethane adhesives.

The overall intent of the thesis has been to increase the knowledge of modifying adhesives in order to provide more sustainable adhesive solutions as well as adhesives exhibiting enhanced and tailor-made set of desired properties.

The thesis is divided into 5 chapters. First an introductory part and a general background to this thesis are given in chapter 1. The theoretical background of tailoring adhesives and its properties are presented in chapter 2, whereas the materials and methods used to conduct the research are described in chapter 3. Chapters 4 and 5 present the obtained results, conclusion and prospects.

In publication I, a series of water-borne poly(styrene-co-butyl acrylate) adhesives with a core-shell type of morphology was prepared in an effort to design and synthesize a load bearing adhesive showing both sufficient energy storage and energy dissipation. Thus, core-shell type of acrylic adhesives was successfully synthesized, and designed that exhibit an optimal balance between tack, peel strength and shear strength compared to conventional latex particles with a uniform composition. The core-shell morphology was optimized by changing the core-shell ratio, by crosslinking the core and by adjusting the softness of the shell via using a chain transfer agent.

In publication II, segmented moisture curable polyurethane adhesives have been prepared using diisocyanates, polyols and chain extenders. The produced hard segments (HS) originating from the diisocyanate moiety provide the cohesive strength and the soft segment (SS) that contribute with the flexibility and softness is made up of polyols/chain extenders. In particular, the role of different types of linear and branched chain extenders and their dosage on the degree of micro-phase separation between hard and soft segments were studied as well as the influence of the synthesis process itself. This work demonstrated that selective chain extenders enable the preparation of one-component polyurethane adhesives with an architecture that simultaneously provides low viscosity and improved shear strength after curing.

In publication III, the synthesis of moisture-curable silane-terminated poly(urethane-urea)s (SPUR)s using environmentally benign bismuth carboxylate catalyst has been studied. The effects of polyol molecular weight, NCO/OH ratio and the types of catalysts and aminosilanes used in the synthesis of SPUR were investigated. The mechanical properties of the cured SPUR samples, in terms of tensile strength and elongation, were mainly impacted by the flexibility of polymer chains, the content and type of silane, and variety of hard segments, as well as extent of hydrogen bonding. The presented results

provide and insight as to the synthesis of low viscous organotin-free high-performance moisture-curable silane-terminated polyurethanes with an optimal performance balance between flexibility and toughness.

3. Literature review

3.1 Adhesion and Adhesives

Adhesive bonding belongs to the science of joining and it becomes increasingly popular over other joining ways such as riveting, welding, soldering, nailing, etc. The advantages of adhesive bonding are obvious, i.e. uniform distribution of stress, lightweight assemblies, cost effectiveness, corrosion free, etc.

Already early humans have been utilizing natural glues (such as pitch and bitumen) to join articles for the manufacture of simple tools and building materials. The consciousness of the importance of adhesion was the drive for humans to study its fundamentals and behaviors of different materials. From the past century until now, the joining by sticky substances have been extensively developed due to recent advancements in material science and technologies and therefore various adhesives are utilized in a wide variety of applications.

The adhesion bonding involves two main elements: the adhesive and the adherents (the materials to be joined). The adhesion bonding processes are quite complexed dependent on several variables such as adherent materials and processes as well as any specific and functional requirements, and thus no single mechanism can elaborate on. For better understanding of adhesive bonding, it is required to obtain a comprehensive knowledge on the bulk and surface of adherents as well as the material property of the adhesive.

3.1.1 Practical and Fundamental Adhesion and Their Relationships

Generally, two types of adhesions, i.e. practical and fundamental adhesion, have been extensively compared and discussed. The practical adhesion is concerned with the real mechanical forces or energy to be applied to separate the bonded components, which is generally assessed by measuring the force required for an adhesive joint's failure in the laboratory. Whereas the fundamental adhesion relates to the forces or mechanisms on a molecular level involved in holding together the components of an adhesive bond. Generally, the practical adhesion is closely related to and very dependent on the fundamental adhesion.

The theories of adhesion can be classified into two main categories: mechanical interlocking or entanglement and charge interactions, which are defined by type of interaction and relative to its length scale. According to Table 1, it shows that the adhesion interactions via interlocking occur over greater length scales than the adhesion interactions via charge interactions. The length scale plays an important role in the understanding of adhesion bonding mechanism. Although the practical adhesion occurs at macroscopic length scales in millimeter to meter, many fundamental aspects of adhesion occur at the smaller length scale in nanometer to micrometer, which both contribute to the final performance of adhesives in different ways and degrees. It is commonly accepted that there are seven adhesion mechanism theories: mechanical

interlocking (hooking), electrostatic (electronics or electrical double layer), adsorption (thermodynamic or wetting), diffusion, chemical covalent bonding, acid-base and weak boundary layers. (Gardner, 2018) It is well-known that these mechanisms do not individually form strong adhesive bonds but worked simultaneously in an adhesive bonding, and which one contributed most very much depending on the specific bonding scenario.

Table 1 Comparison of Adhesion Interactions Relative to Length Scale (Gardner, 2018)

Category of Adhesion Mechanism	Type of Interaction	Length Scale
Mechanical	Interlocking or entanglement	0.01-1000 μm
Diffusion	Interlocking or entanglement	10 nm-2 μm
Electrostatic	Charge	0.1-1 μm
Covalent bonding	Charge	0.1-0.2 nm
Acid-base interaction	Charge	0.1-0.4 nm
Hydrogen bonding	Charge	0.235-0.27 nm
Lifshitz-van der Waals	Charge	0.5-1 nm

The mechanical interlocking theory was first proposed in early last century, and since then it has aroused much of interests. It constitutes a very important mechanism for understanding of adhesive bonding. In adhesion science, the perceptions of mechanical interlocking have evolved with the development of analytical methods and with the increased fundamental knowledge and understanding. There are two types of mechanical interlocking: locking by friction and locking by dovetailing. (Gardner, 2018) The main factors that determine the mechanical interlocking are the surface properties such as geometry and surface roughness of adherents and absorption of adhesives. Adhesives with moderate viscosity penetrate and/or absorb into the irregularities, pores, or crevices on the adherent's surfaces to yield a high-level adhesion. Consequently, adhesives exhibiting enhanced absorption onto substrate with a rough surface form strong mechanical interlocking.

Electrostatic theory is another important mechanism, which was proposed in 1948. It postulates that the adhesion strength is due to electrostatic forces, i.e., by the transfer of charges occurring between electropositive materials to electronegative materials when they are adhered. The DLVO (Derjaguin, Landau,

Verwey, and Overbeek) theory is commonly utilized to describe the force interactions between charged surfaces in a liquid medium and it explains the particle aggregation in aqueous dispersion in a quantitative way. Due to the existence of double layer counterions, it combines the effects of the van der Waals attraction and the electrostatic repulsion and thus the total adhesion force is defined as a sum of the van der Waals forces and the electric double layer forces.

Thermodynamic adhesion or wetting is another important mechanism, and it is believed that good wetting is the prerequisite for high adhesive bonding. Wetting provides the formation of atomic and molecular interactions between adhesives and adherents, manifested by surface tension or surface free energy as the fundamental material properties. There is a consensus that the spontaneous wetting of the adhesive occurred when surface energy of the substrate is greater. The forces contributing to wetting mainly are acid-base interactions, weak hydrogen bonding and van der Waals forces.

The diffusion theory, which was first proposed by Voyutskii and Vakula, is intended to explain the interactions or adhesion forces between materials, which are compatible when they are brought into close contact and are dissolved with each other. The key factor that affects the diffusion process is that the solubility parameters for the adhesive and adherent must be similar. Different ways of welding can illustrate this phenomenon, such as solvent welding or thermal welding. However, this mechanism is not applicable for an adherent that is not absorbable, like glass.

Defined by the International Union of Pure and Applied Chemistry (IUPAC), interpenetrating polymer network (IPN) is a polymer comprising two or more networks that are at least partially interlaced on a molecular scale, but not covalently bonded to each other and are inseparable from each other unless chemical bonds are broken. It is worthy to mention, that polymer interdiffusion plays an important role in the formation of IPNs. Examples of IPNs are the interactions during wood bonding and fiber-reinforced polymer composites.

The formation of adhesive bonds via chemical (also referred to as covalent interactions) is believed to provide a strong adhesive strength and adhesion durability, which is estimated to be 1000 times greater than the surface energy of the same material. A usual way to realize this is by the use of coupling agents that can bridge the two dissimilar materials via chemical interactions together. Hydrogen bonding, which was previously well recognized as a type of physical bonding interaction, has been noted to also contribute to chemical bonding interactions significantly.

The acid-base theory was proposed by Drago et al. and later modified by Fowkes and Mostafa. It postulates bond formation by an interaction between an electron-acceptor and an electron-donor. The Lewis acid-base concept has been broadly applied and it has received significant attention among researchers developing surface and wetting chemistries. Several models to calculate the work of adhesion such as Fowlkes method, the Good method, the van Oss method and the Chang-Chen method have been developed.

Bikerman was the first to introduce the concept of weak boundary layers (WBLs). WBL can be roughly classified into two types: mechanical and chemical WBLs. Where the former one involves e.g. air bubbles and damaged surface, whereas the latter one refers to chemical contamination such as lubricant or plasticizer as well as an aged or inactivated or weathered surfaces. Although, WBL is considered to play a negative role in adhesion, adhesives can be formulated to accommodate WBLs under certain conditions. For example, moisture curable adhesives are suitable for a wet WBL.

For good adhesive performance, basic requirements must be fulfilled such as proper rheology to ensure surface wetting and adhesion, but also good cohesion to deliver mechanical strength. From a practical viewpoint, they can be collectively expressed in terms of proper combination of tack, peel and shear strength. (Roberge S, 2006)

3.1.2 Classification and General Applications

There are several ways of classification for adhesives. In the broadest way of classification, they are classified into structural and non-structural adhesives. The structural adhesives are characterized by long-term integrity and durability of adhesion, i.e. their unaltered performance during the service life of the product assembly. Thus, no significant change upon moderate aging of adhesion, whereby the high shear strength (usually above 6900 kPa) is vital for structural adhesives. The structural adhesives include epoxy based, polyurethanes, acrylate based, resorcinol, phenolics based, and polyaromatic high temperature resins. The non-structural adhesives have limited durability and require a sheltered or relatively mild application environment. For instance, pressure sensitive adhesives belonging to non-structural adhesives, commonly utilized in packaging. In general, non-structural adhesives involve natural or synthesized rubbers, silicones, polyvinyl acetal, acrylics, polyesters, polyvinyl acetate, ethylene-vinyl acetate copolymer, and polyolefins, etc. By the chemical or physical nature of adhesives, they can be divided into thermoplastics, thermosets, elastomers and hybrids. The difference between thermoplastics and thermosets lies in their polymer structure and performance: thermoplastics are non-crosslinked and thermally reversible, while thermosets are crosslinked and therefore thermally irreversible. Elastomeric adhesives have high elongation and low tensile strength, with representatives such as formulated natural or synthetic rubbers. By methods of application and subsequent treatment, adhesives can be classified as non-reactive and reactive adhesives: the non-reactive adhesives refer to the ones that are set by water or solvent evaporation (such as solvent-based or water-based) or cooling (thermoplastics such as rubber-based hotmelts); the reactive adhesives refer to the ones are set by external curing processes such as by water or UV light. (Dubé, 2007)

3.1.3 Waterborne Polyacrylate Adhesives

3.1.3.1 Emulsion polymerization

Today water-borne dispersions manufactured by emulsion polymerization are widely employed as coatings, inks, paints and adhesives. (JM., 2004; HB., 2013; J., 2008; Ma J, 2013; Tong Yu C, 1997; K., 2003; CS, 2006) The characteristics of the acrylic dispersions can be tailored-made to meet different end-uses by careful selection of initiators, monomers, the stabilization system, additives and design of particle morphology as well as polymerization process. The selection of these parameters has a significant influence on dispersion properties such as glass transition temperature, adhesion profile, degree of crosslinking (use of di-functional monomers), molecular weight and molecular weight distribution, particle size and its distribution as well as particle morphology. Thus, with proper recipe the particles obtained exhibit optimal size, composition, morphology and molecular weight for the utilization as adhesives. (Dubé, 2007)

The emulsion polymerization can be conducted in a batch, semi-continuous or continuous reactor. The system of emulsion polymerization is initially comprised of mainly water (continuous phase), monomer(s) droplets (discontinuous phase), water-soluble initiator and amphiphilic surfactants (anionic/cationic or non-ionic surfactants or combinations thereof). Typically, a mixture of anionic (such as sodium dodecyl sulfate, also known as SDS) and non-ionic (e.g. fatty alcohol ethoxylates)) surfactants. The anionic surfactant is responsible for controlling the particle nucleation step, whereas the non-ionic provides additional electrolyte tolerance, mechanical shear stability and freeze-thaw stability. In fact, dispersion stability during storing over long periods can be achieved by combining charged and non-charged surfactants that can simultaneously provide both electrostatic and steric stabilization. (Dubé, 2007)

According to Harkin´s emulsion polymerization model (Daniels, 2003), the polymerization process can be divided into three distinct intervals as shown in Figure 1.

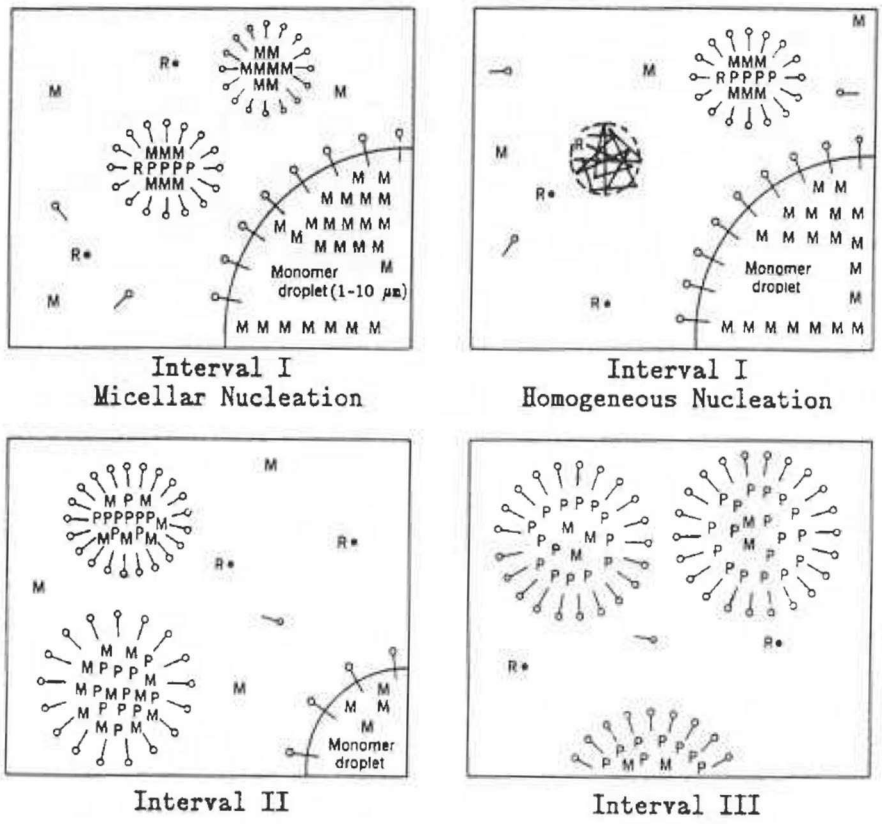

Figure 1. Harkin´s emulsion polymerization model. It divides the emulsion polymerization process into three distinct intervals: Interval I – micellar nucleation and homogeneous nucleation; Interval II – polymer chain propagation and particle growth; Interval III – polymer chain termination.

The first interval corresponds to the nucleation stage where sufficient amount of surfactant(s) has been added to stabilize the formed monomer droplets and micelles in the aqueous phase. The monomer droplet size is typically in the order of 1 – 10 μm diameter (concentration of droplets per unit volume is ca. 10^{11}/mL) and the micelle size is in the order of 10-100 nm (concentration of droplets per volume unit is ca. 10^{18}/mL). Therefore, the specific area of monomer swollen micelles are several hundred times greater than for the monomer droplets. After the introduction of water-soluble initiator and upon heating, free radicals are formed due to thermal decomposition of initiator. The formed radical R • reacts with the first monomers to yield oligo-radicals. The initially formed oligo-radicals are too hydrophilic to enter in the organic phase and start polymerization. However, by time they become hydrophobic enough to get in the organic phase, whereby polymer particle nucleation and polymerization is

taking place. The particle nucleation can take place either via homogenous or heterogeneous processes. In the homogeneous nucleation polymer particles start to form when the oligo-radicals grow beyond the length at which they are no longer water soluble. The homogeneous nucleation process is more common when using partially water-soluble monomers like methyl methacrylate (MMA) than for example scarcely water-soluble styrene. In contrast, heterogeneous nucleation takes place when the formed oligo-radicals diffuse into the micelles to start the polymerization within the micelle particles. Inside the micelles, the oligo-radicals will be fed by the presence of the high concentration of monomers in the droplets. The monomer conversion in the first interval is between 0 to 15 %. The number of micelles will decline as a function of conversion, as the entrance of oligo-radicals turns them into polymer particles. In parallel, the micelles will be destroyed as they provide surfactants to the growing polymer particles. Therefore, after this first interval, the number of polymer particles stay constant.

In the second interval, the monomer droplets and polymer particles coexist. The polymer particles grow as more monomer is diffusing from the monomer droplets into polymer particles and they will be consumed. The monomer conversion in the second interval is between 15 to 85 %. At the end of the second interval, all the monomer droplets have disappeared since all monomer has diffused into polymer particles.

The third interval is characterized by termination of polymerization as the monomer concentration is sharply decreasing in the polymer particles until the monomer has been almost fully consumed.

The most common type of emulsion polymerization is an oil-in-water system, yielding polymer particles of 50-200 nm that are dispersed in water (also called latex) and showing a milk-like appearance. The nature of emulsion polymers is referred to as “products by process” which implies that the main properties of latex are determined during the polymerization process itself. (JM., 2004)

3.1.3.2 Environment and sustainability of polymer dispersions

Despite solvent-based adhesives have been well developed and commercially produced for many years, they practically emit harmful volatile organic compounds (VOCs) during production and application, which significantly limit their broad use in today's society.

Due to increased public consciousness and more strict governmental regulations, the replacement of solvent-based adhesives by more environmentally friendly alternatives are in high demand. Therefore, emulsion polymerization has gain popularity and aqueous polymer emulsions have found increasingly wide use as binders, adhesives, paints and inks.

However, in recent years the adhesive industry has faced yet another challenge related to the elimination of so-called secondary emissions from construction adhesives. One recent representative example of such a secondary pollution compound is 2-ethyl-1-hexanol, which may be hazardous, pose a risk to human health and/or environment. (John B. Sullivan Jr. MD, 1999; Assessment report on 2-ethylhexanol for developing ambient air quality objectives, 2004) This indoor air pollution component arises from the decomposition of poly (2-ethyl hexyl acrylate) or its copolymers via hydrolysis under strongly alkaline conditions (pH 13) (Figure 2). Unfortunately, still today, 2-ethyl hexyl acrylate (EHA) is a commonly used monomer in commercial waterborne adhesive emulsions. (Chino S, 2013; Yokota T, 2013; Sjöberg A, 2007)

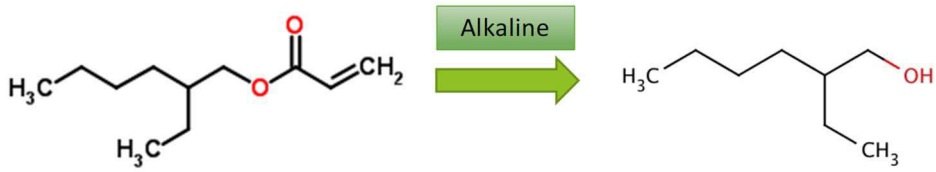

2-ethyl hexyl acrylate

2-ethyl-1-hexanol

Figure 2. The scheme of 2-EHA's decomposition reaction. 2-EHA is potentially decomposed into 2-ethyl-1-hexanol under strongly alkaline conditions.

In addition, special attention has been paid on the emulsifier systems, and endocrine disruptive compounds such as alkylphenol ethoxylates (APEO) are increasingly forbidden and replaced by alternative non-ionic emulsifiers that comply with the concept of sustainability. (Rawlins JW, 2013; Priac A, 2014)

3.1.3.3 Waterborne polyacrylate based adhesive

Among various emulsion-based adhesives, poly(styrene-co-acrylate) latexes are well-known for their versatility as adhesives and coatings. (K., 2003) Latexes with different combinations of soft and hard segments provide diversity in performance, as the soft polyacrylate promotes tack and the hard polystyrene enhances mechanical strength. In addition to the main monomers, a small quantity of an acid-functional monomer (no more than 1.5% of dry polymer), such as acrylic acid (AA), is required in the latex formulation. The repulsive

negative charges on the latex particle surfaces enhance the colloidal stability and also improve peel and shear strength by enabling ionic bonding. (K., 2003; Foster AB, 2009) Additional components such as emulsifiers, initiators, redox agents and pH adjusters are also of great importance for achieving optimal properties of the final latex.

In most cases, the aqueous latexes are dried into films while they perform their function as adhesives. Thus, the so-called minimum film formation temperature (MFFT) of waterborne adhesives is a vital parameter to their adhesive performance. MFFT is required to be lower than the application temperature to attain film formation. The fulfillment of the prerequisites as a good waterborne adhesive is closely related to the structural features of latexes such as particles size, particle morphology, crosslink density, gel content, molecular weight and its distribution as well as the glass transition temperature (Tg). (Kajtna J, 2009; Pérez-Carrillo L, 2007) These characteristics in turn mainly depend on the polymer's chemical composition and process condition. Consequently, the choice of latex components, polymerization parameters and the design of latex particles are critical for optimizing adhesive properties and the adhesive´s performance in the intended end-use applications.

Particle design

Today, poly(styrene-co-acrylate) based emulsions with a uniform particle morphology are most commonly applied as pressure sensitive adhesives (PSAs) and because of their relatively low mechanical strength they are not ideal as load bearing adhesives per se. On the other hand, high strength poly (styrene-co-acrylate) latexes intended for construction adhesives can be prepared via proper design of particle morphology. Thus, core–shell type of emulsions is becoming increasingly important in comparison to conventional uniform emulsion particles, since owing to their heterogeneous structures one can design emulsion polymers with versatile properties. (Ma J, 2013; Pérez-Carrillo L, 2007; Ferguson CJ, 2002) The difference in the micro structure of the core and the shell enables the combination of sufficient energy storage and dissipation properties in the same particle. (da Silva LF, 2011; Ji W, 2012) In addition to different ratios of soft and hard monomers in the core and the shell, crosslinkers and chain transfer agents (CTAs) can be used to further create distinctive properties in the named layers. Crosslinkers improve cohesive strength by creating a rigid polymer network structure, whereas the use of CTA enhances polymer chain flexibility and mobility, which in turn enables enhanced adhesion by allowing the polymer chains to interpenetrate into the voids of the substrate. Generally, the core–shell particles can be built-up of a rigid core and a soft shell or vice versa. In the case of an emulsion based adhesive, the rigid core–soft shell type is preferable, as the crosslinked core offers sufficient cohesive strength, and the flexible shell consisting of a low molecular weight polymer simultaneously provides enhanced wetting and adhesion to a substrate. (K., 2003)

Pressure sensitive Adhesives (PSA)

Pressure sensitive adhesives have found their forte as an easy-to-use family of adhesives with permanent tack at room temperature (in dry solvent free form) that adheres to a wide variety of material surfaces upon mere contact without the need of more than finger pressure. Thus, PSAs exhibit sufficient cohesive strength and elastic properties that it can be adhered to many materials by using mild pressure and it can be removed from the surface without leaving any residue. PSAs can be described as soft solids that are able to deform sufficiently to achieve good wetting to the surface to which they are applied, and they retain some elastic properties to resist debonding from the substrate. The bonding forces are normally weak and consist mainly of dispersion interactions between the adhesive and substrate surface. (Dubé, 2007)

Release linear is an essential component of PSA when they used in products such as tapes and labels. The release linear can be considered as PSA delivery system protecting the pressure sensitive adhesive from contamination and unintentional contact until it is applied. Normally the release linear has a coating (typically silicone or fluoroalkyl containing copolymers) having a surface energy less than the PSA that enables a shift and easy removal of PSA from the release linear with only applying a light force.

In addition, the pressure sensitive adhesives comprise of base polymer, tackifiers, potential fillers, plasticizers and antioxidants. The base polymer usually consists of acrylic copolymers or elastomers (such as natural rubber, polybutadiene) and the composition thereof determines its glass transition temperature and the cohesive strength of the adhesive. Whereas the role of the tackifiers and plasticizers is to adjust the viscoelastic properties of the system. In contrast to conventional adhesives, PSA do not undergo a change in physical state between wetting, bonding and de-bonding processes.

Moreover, if the pressure sensitive adhesives have been obtained by emulsion polymerization it contains some surfactants. In emulsion polymerizations the nature and type of surfactants, play a vital role by providing the colloidal stability of the latex particles, while surfactant residues in the pressure sensitive adhesive are general unwanted. Thus, by migration of the surfactant residues to the surface of the adhesive, they may change its properties and its ability to form good contact and adhere to various substrates. In addition, the surfactants may also act as plasticizers and thereby change the adhesives bulk properties in a negative way.

3.1.4 Polyurethane Adhesives

In 1937, Otto Bayer and coworkers invented polyurethane resins, and by further refining its structure they were able to extend its application range towards adhesives in 1940. In general, polyurethane adhesives are capable of bonding different types of substrates. The first urethane prepolymers were utilized to bond porous substrates such as wood and fabrics in the early 1950s, and soon after the first two component urethane adhesives were developed for metal-to-metal bonding. In 1961, researchers at Du Pont invented waterborne polyurethanes, and four years later W.R. Grace launched the product into the market. Whereas polyurethane pressure-sensitive adhesives commercialized in the early 1970s. (Dennis G. Lay, Polyurethane Adhesives, 2018)

During the development of polyurethane adhesives, they gained increasing attention due to their excellent adhesion, flexibility, low temperature performance, high cohesive strength and high cure speeds, which further expanded their application range. Polyurethane adhesives effectively wet different substrate surfaces and they also readily penetrate into porous substrates, they form hydrogen bonds and even form covalent bonds with substrates containing active hydrogens. Thereby polyurethanes exhibit good adhesion performance in many applications.

Without a doubt, polyurethane adhesives are globally among the most versatile adhesives. Owing to the fact, urethane can effectively join a wide variety of substances together. Depending on their chemical compositions, polyurethane adhesives that are either rigid or flexible or a combination thereof can be prepared, and they may exhibit from slow to fast curing profiles depending on the end application requirements. Moreover, there are almost infinitive variations of one-component and two-component polyurethanes that are able to fulfill the desired adhesion and physical properties of specific products. Property/structure studies of polyurethane adhesives have shown that its morphology is key to understanding how polyurethane adhesives function. With rational design, polyurethane adhesives can be manufactured that exhibit high adhesion to various substrates in combination with exerting high attraction between themselves (cohesion forces).

Due to the versatility and characteristics of polyurethanes adhesives, they are widely applied in a wide variety of applications such as textiles, packaging, construction, transportation, furniture, etc.

3.1.4.1 Chemistry of polyurethane

Polyurethane is prepared by addition polymerization of isocyanates reacting with compounds with active hydrogens such as the ones containing hydroxyl groups, as shown in Figure 3.

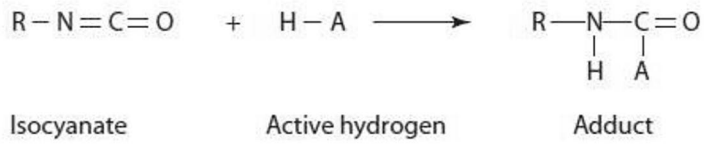

Figure 3. Reaction of isocyanate with active hydrogen. (Dennis G. Lay, Polyurethane Adhesives, 2018)

The reactivity increases with the activity of active hydrogens, for example, amines' reactivity is higher as compared to hydroxyl groups while primary alcohols react faster than secondary alcohols. Other factors such as solvent, temperature and the presence of catalysts have also great impact on the reaction rate.

The formation of urethane prepolymer is accomplished by the reaction between an isocyanate with a polyol as depicted in Figure 4. Besides the main reaction, several side reactions such as branching or crosslinking occur simultaneously, resulting in a variety in viscosity, gelation and exotherms. For example, unreacted isocyanate easily reacts with moisture to give urea under liberation of carbon dioxide (CO_2), which results in a significant viscosity increase and uncontrolled gassing. The formed urea can further react with excess isocyanate to give biuret. The urethane groups react with excess isocyanates to give allophanate, which in turn can continue to react with excess isocyanate to yield isocyanurate. These side reactions are usually unfavorable, due to their significant contribution to increased viscosity and generation of heat. Therefore, the formation of urethane and urea must be adjusted via control of reaction temperature and stoichiometry of chemicals. (Lapprand, Boisson, Delolme, Méchin, & Pascault, 2005; Heintz, et al., Effects of reaction temperature on the formation of polyurethane prepolymer structures, 2003)

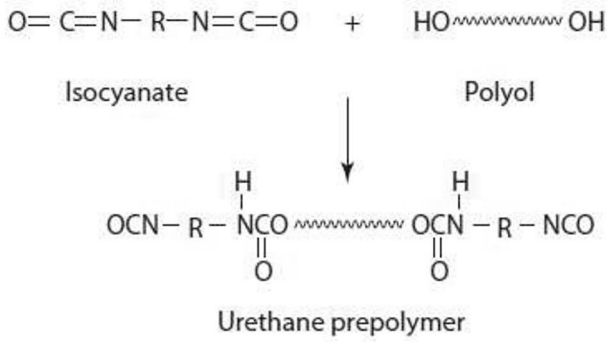

Figure 4. Reaction of polyol with an isocyanate to form a urethane prepolymer (Dennis G. Lay, Polyurethane Adhesives, 2018)

Polyurethane adhesives are classified into one-component and two-component adhesives. Both categories include several subclasses of adhesives, as shown in Table 2. The basic raw materials for the synthesis of polyurethane are polyols, isocyanates and potentially catalysts. For the synthesis of polyurethane elastomer, chain extenders are usually applied. Organosilane can also be applied to make a hybrid urethane polymer combining benefits of organic and inorganic components. Other additives such as fillers can be added in the polyurethane adhesives to further optimize application specific properties.

Table 2 Different types of urethane adhesives

One component	Two Component
Moisture-curing liquid urethane adhesives	Structural urethane adhesives
Moisture-curing hot melt adhesives	Water-borne urethane adhesives
Solvent-borne urethane adhesives	"Modified" two-component urethane adhesives
Blocked urethane adhesives	
Thermoplastic polyurethane adhesives	

3.1.4.2 Catalyst

There are two types of commercial catalysts used for preparation of polyurethane: organometallics and tertiary amines. In general, the catalytic activity is affected by electronic and steric effects. From the electronic aspect, the catalysts containing empty electronic orbitals (especially in transition metals) enable the reactants coordination to the metal center and thereby activating the bonds for a faster reaction. Subsequently, the molecule's ability to donate or accept electronics determine the catalytic activity. Steric effects impact on the catalytic activity in terms of structural interactions between the substituents on the catalysts and the reactants. The easier for the electrons to access the reactants in a less shielded position, the more efficient is the catalyst, which explains why the catalytic activity of triethylenediamine is higher than that of triethylamine.

The organometallic catalysts for polyurethane are generally based on Sn, Bi, Hg, Zn, Fe and Co complexes, and the most common one is Sn carboxylates. However, due to increasing attention to the environment and health care, alternative organometallic catalysts to replace Sn are highly demanded.

Table 3 Gelation times in minutes at 70° C for different catalyzed isocyanates. (Dennis G. Lay, Polyurethane Adhesives, 2018) The shorter gelation time indicates faster reaction and more efficient catalysis.

Catalyst	TDI*	m-Xylene Diisocyanate	Hexamethylene Diisocyanate
None	>240	>240	>240
Triethylamine	120	>240	>240
Triethylenediamine	4	80	>240
Stannuous octoate	4	3	4
Dibutyltin di(ethylhexoate)	6	3	3
Bismuth nitrate	1	0.5	0.5
Zinc naphthenate	60	6	10
Ferric chloride	6	0.5	0.5
Ferric 2-ethylhexoate	16	5	4
Cobalt 2-ethylhexoate	12	4	4

*TDI: Toluene di-isocyanate

It is well known that the function of catalysts is not only to promote the reaction rates but also to affect the selectivity of reactions and even can change the order of reactivity. For example, Hg catalysts accelerate the reaction of isocyanate-hydroxyl more efficiently than the reaction of isocyanate-water, which is very suitable to for cast applications where pot-life and bubble-free reactions are required. Moreover, some organometallic catalysts such as Zn, Fe and Co complexes are very effective in promoting the reactivity of aliphatic than aromatic isocyanates, according to Table 3 (Dennis G. Lay, Polyurethane Adhesives, 2018).

3.1.4.3 Polyol

The polyols for the synthesis of polyurethane are divided into polyether polyols, polyester polyols, and polybutadiene polyols. The chemical structure of the different polyols gives them specific characteristics that are optimal for different applications.

The most common are polyether polyols, due to their balance of performance and cost. Polyether polyols are synthesized via ring-opening polymerization of ethylene, propylene and butylene oxides initiated with active proton in the presence of a strong base. Dependent on the initiator and the type and amount of oxide, polyether polyols have variable functionality, molecule weights and hydrophobicity. The commercially available capped and mixed-oxide feed polyols are shown in Figure 5, their characteristics are determined by their structure and manufacturing process. Polyether polyols exhibit many benefits such as good low-temperature performance (the glass transition temperature (Tg) of around -60° C range), good flexibility (rotating polymer backbone), low viscosity and good substrate wetting, as well as good resistance to alkali hydrolysis. The molecular weights of polyether polyols are ranging between 500-2000 for difunctional and between 250-3000 for trifunctional. The lower molecular weight and higher-functionality polyols are typically utilized in rigid-foam application or as crosslinkers for two-component urethane adhesives. Polytetramethylene oxides (PTMOs) are premium priced, and they offer good physical properties and excellent hydrolysis resistance among polyether polyols.

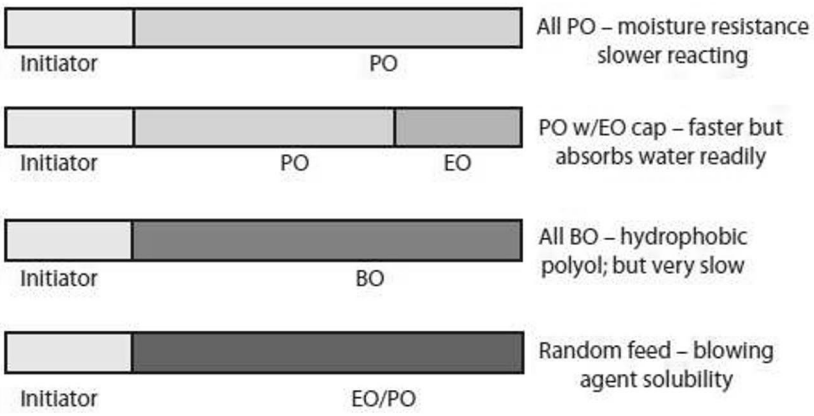

Figure 5. Various commercially available capped products and mixed-oxide feed polyols. BO: butylene oxide; EO: ethylene oxide; PO: propylene oxide. (Dennis G. Lay, Polyurethane Adhesives, 2018)

Compared with polyether polyols, polyester polyols provide better tensile strength and heat resistance to urethane adhesives, but their shortcoming is limited low-temperature performance and relatively poor hydrolysis and chemical resistance. Polyester polyols are synthesized by the reaction of diols with diacids. Among polyester polyols, polycaprolactones provide improved hydrolysis resistance and tensile strength but exhibit both higher viscosity and cost.

Polybutadiene polyols are hydroxyl-terminated liquid polybutadiene resins that exhibit exceptional good low-temperature properties as their Tg is below -70^{o} C. Polybutadiene polyols exhibit excellent hydrolytic stability and low-temperature properties, but their price is 40-50 % premium over polyether polyols which limit their extensive application in urethane adhesives.

3.1.4.4 Isocyanate

The isocyanates can be classified simply into aliphatic and aromatic ones. Examples of aliphatic isocyanates are hexamethylene diisocyanate (HMDI), hydrogenated methylene diphenyl diisocyanate (MDI), isophorone diisocyanate (IPDI), and tetramethylxylene diisocyanate (TMXDI), and representatives of aromatic isocyanates are toluene diisocyanate (TDI) and methylene diphenyl diisocyanate (MDI). The main differences between aliphatic and aromatic lies in their reactivity, UV-stability, cost and toxicity. Aromatic isocyanates are cheaper and react faster than the aliphatic isocyanates, and thus they have been more widely utilized as polyurethane adhesives. Aliphatic isocyanates are usually applied when UV resistance of polyurethanes is demanded.

TDI is colourless, volatile and a low-viscosity liquid, which has been used to manufacture low-viscosity urethane prepolymers as adhesives. TDI consists of a mixture of 2,4 and 2,6 isomers in 80:20. The two isocyanates groups in TDI exhibit different reactivity´s due to unalike steric hindrances, leading to an improved shelf stability for the urethane prepolymers. TDI synthesized urethane prepolymers are commonly applied as adhesives for textile and food packaging industries where low viscosity and low cost are required. However, the high volatility of TDI has limited its extensive growth in adhesive applications.

MDI is less volatile than TDI and it has been used where high tensile strength and toughness as well as heat resistance are demanded. Pure MDI is commonly supplied as 4,4'-isomer, with a melting point at 38 ^{o}C that contains two equivalent isocyanates with the same reactivity. Several other versions of MDI products such as uretonimine and a mixture of 35% 2,4'- and 4,4'- isomers that are supplied in a liquid form for ease of handling. Besides, these liquid MDI products offer other advantages such as slower reactivity, longer pot-life and giving raise to lower-viscosity prepolymers with lower residues and improved shelf stability. Polymeric MDIs, which are made during the manufacturing of monomeric MDI, are dark brown oligomers having an average in 2.3-3.2 in functionality and containing 30-32% isocyanate NCO. Polymeric MDIs are liquid at room temperature, more storage stable and cheaper than pure MDI. Polymeric MDIs can individually be issued as binders or adhesives for binding porous substrates such as wood and fabrics. (Gurke, 2002)

The toxicology of isocyanates per se is of primary concern, since it can cause respiratory ill effects, eye, and skin irritations as well as allergic sensitization. Precaution must be taken to prevent exposure during preparation or during use of polyurethane adhesives.

3.1.4.5 Urethane polymer morphology

Polyurethanes generally comprise of two parts of: i.e. long polyol chains that provide softness and flexibility, and short urethane linkages that provide hardness and rigidity. The two parts are referred to as soft and hard segments, respectively. The versatility of polyurethanes is realized by choosing proper raw materials and by fine-tuning of soft and hard segments.

Generally, the soft segments determine low-temperature and room temperature elastomeric properties and thereby controlling flexibility and softness as well as elongation of polyurethane materials. Meanwhile, the tensile strength and hardness decrease as the soft segment concentration increases. The weathering resistance is controlled by the chemical structure of polyols.

The hard segments contribute to the hardness and tensile strength of polyurethane materials. The extent of hard segments can be enhanced by short chain diols or diamines that are called chain extenders. Sufficient amounts of hard segments will aggregate into hard domains, due to their similarity in polarity and ability of hydrogen bonding. The phase separation or phase aggregation greatly promote its mechanical strength.

3.1.4.6 One-component moisture-curable polyurethane adhesive

One-component moisture-curable urethane prepolymers (MCPUs) are widely used adhesives, due to their effective wetting properties, low viscosity, fast curing speed, ease of handling, toughness, good water and chemical resistance. (Šebenik & Krajnc, 2007; Müller & Rath, 2010; Klinedinst, Yilgör, Yilgör, Zhang, & Wilkes, 2012; Clauß, Influence of the adhesive formulation on the mechanical properties and bonding performance of polyurethane prepolymers, 2011; Clauß, et al., 2011; Lehringer & Gabriel, Review of Recent Research Activities on One-Component PUR-Adhesives for Engineered Wood Products. In Materials and Joints in Timber Structures: Recent Developments of Technology, 2014; Sterley, Trey, Lundevall, & Olsson, 2012; Engels, et al., 2013) The unique characteristics of MCPUs originate from their specific dual micro-phase structure, i.e., from the thermodynamic incompatibility of soft segments and hard segments in the block copolymer. The soft segment consists of polyols that provide flexibility and softness, and hard segments derived from isocyanates in turn offer cohesive strength to the polymer matrix as reinforcement units. (Saralegi, et al., 2013; Papon & Villenave, Rheological characterization of thermoplastic polyurethane elastomers, 2000) Consequently, in theory tailored MCPUs that fulfill specific application requirements can be manufactured by varying the composition and length of soft and hard segments and synthesis method thereof. (Chattopadhyay, Sreedhar, & Raju, 2005)

In general, as opposed to the in-situ highly crosslinked rigid adhesives such as melamine-formaldehyde (MF) or phenol-resorcinol-formaldehyde (PFR),

MCPU adhesives have become one of the prominent classes of flexible adhesives. (Lehringer & Gabriel, Review of Recent Research Activities on One-Component PUR-Adhesives for Engineered Wood Products. In Materials and Joints in Timber Structures: Recent Developments of Technology, 2014; Stoeckel, Konnerth, & Gindl-Altmutter, 2013) Since the features of polyurethanes are ultimately controlled by the dual phase structure, the cohesive strength of MCPUs can be enhanced by adjusting the extent of microphase separation between hard and soft segments, for instance via the incorporation of short chain diols called chain extenders. (Müller & Rath, 2010) The incorporation of chain extenders endows greater immiscibility between non-polar soft and highly polar hard segments (HS), and allows hard segments to phase segregate into hard domains via hydrogen bonding interactions. Hence, the physical crosslinking structure of HS domains reinforces the soft segment matrix, and subsequently promotes mechanical strength and physical properties. (Lee, Tsai, Tsai, & Chen, 2007) However, on the other hand, the complete phase separation and substantial hydrogen bonding interactions give rise to high viscosity, and consequently result in poor substrate wetting.

Therefore, a good balance between phase separation and phase mixing of hard and soft segments is vital in order to achieving outstanding bond performance for MCPU based adhesives. (Chattopadhyay, Sreedhar, & Raju, 2005; Delpech & Miranda, 2011; Yoon & Han, 2000; Sheth, Klinedinst, Wilkes, Yilgor, & Yilgor, 2005) Hydrogen bonding interactions between hard segment domains induce phase separation, whereas hydrogen bonds between hard and soft segments favor phase mixing. (Chattopadhyay, Sreedhar, & Raju, 2005; Delpech & Miranda, 2011) Moreover, the miscibility between hard and soft segments can be tuned by either increasing the crystallinity of soft segments by using polyols having carbonate groups along the polymer backbone or decreasing the crystallinity of hard segments by using branched chain extenders or decreasing their dosage. (Lee, Tsai, Tsai, & Chen, 2007) From an economic viewpoint, the latter way provides a possibility to develop an inexpensive MCPU adhesive exhibiting simultaneously high cohesive strength and low viscosity.

3.1.4.7 Silane modified polyurethane adhesive

Polyurethane (PUR) adhesives have a widespread application range due to their ease of use and excellent ability to bind different materials together. Besides their adhesive properties, their mechanical, thermal, and chemical properties are tunable by rational design of the molecular chain structure. However, in recent years, traditional PUR adhesives that contain free isocyanate groups, including isocyanate-terminated urethane prepolymers, have been under scrutiny due to the occupational health concerns related to respiratory and skin exposures. (John B. Sullivan Jr. MD, 1999; Fernandes, 2015; Cornille, 2017; COMMISSION REGULATION (EC) No 552/2009, 2009) Also organotin catalysts used for their production and curing have potential harmful environmental effects. (Guhl D. , Alternatives to DBTL catalysts in polyurethanes A comparative study, 2015; Ravichandran, 2010; Blank, 2002; Commission Regulation (EU) No 276/2010, 2010) Furthermore, the undesired release of CO_2 during moisture curing of NCO

terminated prepolymers also give rise to bubbles within the PUR matrix, and thereby giving raise to porous adhesive joints.

Due to the aforementioned circumstances, there is an urgent need to further refine and develop polyurethane adhesives by utilizing more sustainable chemistries that are free of terminal isocyanate groups and that use more environmentally benign catalysts than dibutyltin dilaurate (DBTL) to accelerate their preparation and/or curing process.

Towards this end, a number of groups have started to develop, moisture-curable silane terminated polyurethanes (SPUR) that consist of a polyurethane backbone terminated by moisture curable alkoxysilanes. (Huber, Kelch, & Berke, 2016; Yuan, et al., Silane-terminated polyurethane applied to a moisture-curable pressure-sensitive adhesive using triethoxysilane, 2016; Yuan, Zhang, Fu, & Lei, Molecular design for silane-terminated polyurethane applied to moisture-curable pressure-sensitive adhesive, 2017; Nomura, Sato, Sato, Mori, & Endo, 2007; Gurunathan & Chung, 2016) Since SPUR contains no isocyanate residues and the curing process of SPUR does not generate carbon dioxide, some demerits can be circumvented that are otherwise inherently present in conventional 1K PUR adhesives. In addition to these benefits, SPUR also possesses hybrid properties as do polyurethanes and silicones.

In general, there are two main synthetic routes to SPURs, as shown in Figure 6: 1) a NCO-terminated urethane prepolymer that is reacted with aminosilane and 2) an OH-terminated urethane prepolymer that is reacted with isocyanate silane. Route 1 yields SPUR with a high viscosity owing to substantial content of hard segments and rigid urea linkages by aminosilane end-capping. The attractiveness of route 1 is that the urea linkages give better mechanical and physical performance to the adhesive than those based on conventional urethane linkages. On the other hand, the high viscosity ranging from 50000 to 200000 mPa*s makes the wetting of surfaces worse. To some extent the increase in viscosity can be reduced by using secondary aminoalkoxysilanes that yield less ordered monodentate urea structures (Figure 6 (i)) instead of primary ones, which result in a highly ordered bidentate urea structures (Figure 6 (ii)). (Nomura, Sato, Sato, Mori, & Endo, 2007)

During application, the produced SPUR cures by atmospheric moisture to yield highly stable siloxane crosslinked network structures. Thus, the formed hybrid system of SPUR combines the unique and beneficial features of inorganic, elastic silicone with organic, tough polyurethane, whereby adhesive formulations exhibiting water resistance, heat resistance, high tensile strength, elongation and excellent adhesion to a variety of substrates can be obtained. (Yuan, Zhang, Fu, & Lei, Molecular design for silane-terminated polyurethane applied to moisture-curable pressure-sensitive adhesive, 2017; Yuan, et al., Silane-terminated polyurethane applied to a moisture-curable pressure-sensitive adhesive using triethoxysilane, 2016; Sardon, Irusta, González, & Fernández-Berridi, 2013; Allauddin, Narayan, & Raju, 2013)

The development of conventional polyurethanes is well documented and thereby insights have been gained on their structure-property relationships.

PUR properties can be tuned over a wide range by adjusting the molecular weight and the composition of polymer main chains as well as the extent of intra- and intermolecular hydrogen bonding. (Tan, Tirri, & Wilen, 2017; Ionescu, 2005; Poljanšek, Fabjan, Moderc, & Kukanja, 2014; He, Xie, & Zhang, 2014; Lehringer & Gabriel, Materials and Joints in Timber Structures: Recent Developments of Technology, 2014; Król, 2007) However, to the best of our knowledge, the effect of organosilane type and bismuth based catalysts on the properties and performance of SPUR has not been systematically studied.

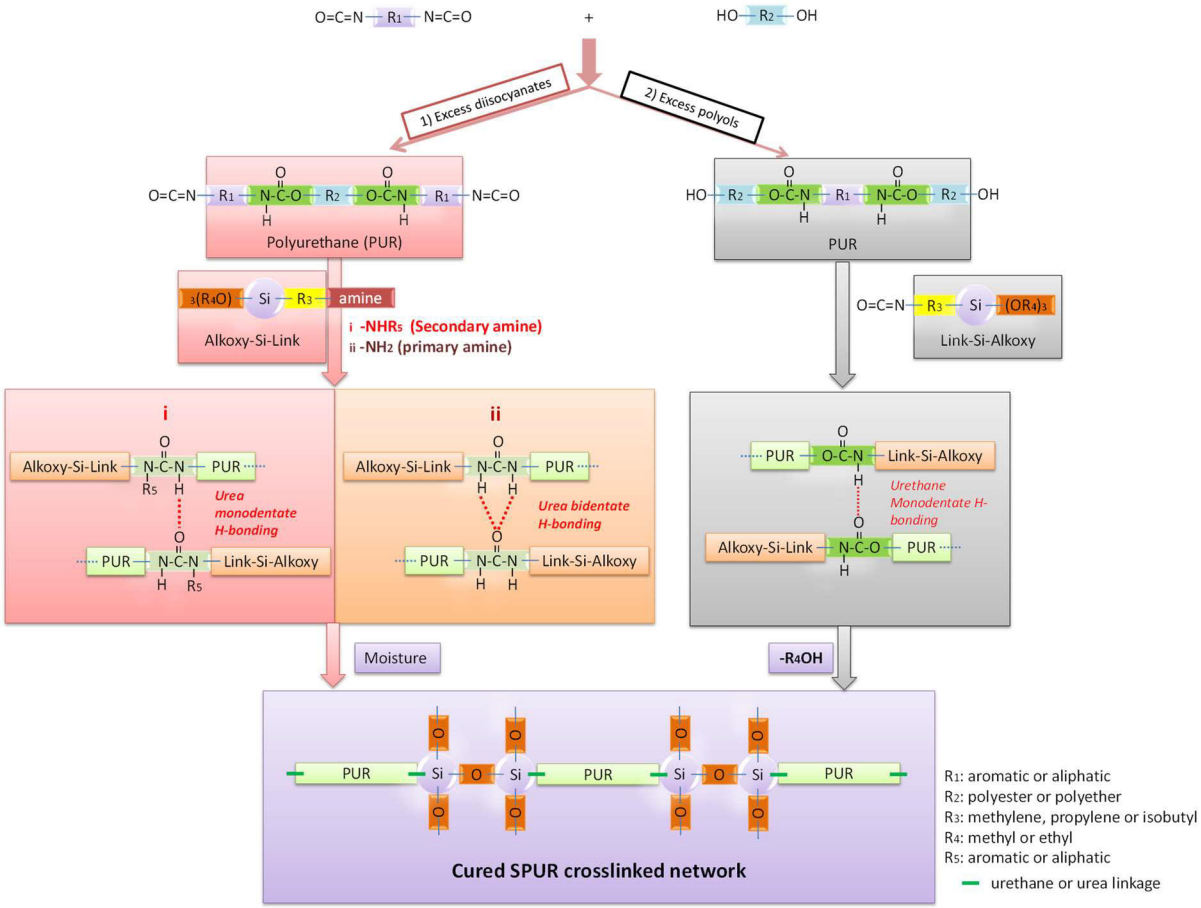

Figure 6. Two general routes for SPUR synthesis.

4. Experimental

This chapter is a summary of the experimental part of Papers I – III. Thus, it describes the chemicals and experimental setup for the preparation of core-shell structured poly (styrene-co-butyl acrylate) emulsions and characterization methods thereof, chemicals and synthetic procedure for synthesis of one-component moisture-curable polyurethane and characterization methods used and finally the chemicals and synthetic pathway to silane-terminated moisture-curable poly(urethane-urea) adhesives and characterization methods thereof.

4.1 Preparation of Core-Shell Structured Poly (Styrene-co-Butyl Acrylate) Emulsion

4.1.1 Chemicals and Materials

The following chemicals were used: Disponil FES32 (BASF, 31%), Disponil NG 3070 (BASF,70%), butyl acrylate (BuA) (Dow, 99.5%), styrene(St) (SigmaAldrich,99%), acrylic acid (AA) (Ecem, 99.5%), ethylene glycol dimethacrylate (EGDMA) (Sigma Aldrich, 98%), 1-dodecanethiol (Dm) (SigmaAldrich, 98%), potassium persulfate (KPS) (BASF,99%), tert-butyl hydroperoxide (TBHP) (AkzoNobel,70%inH2O), the reduction agent Bryggolit C (Brug- gemann Chemical, 40%), the preservative Proxel(Arch, 9.25%), sodium hydroxide solution (NaOH, 13.5%) (J.T.Baker,99.7%), tetra hydrofuran (THF) (Sigma Aldrich, 99%) and methanol (Sigma Aldrich, 99%). Distilled water was used in all polymerizations. All chemicals were of commercial grade and used as received.

4.1.2 Polymer Latex Preparation

The poly (styrene-co-butyl acrylate) latexes were synthesized via semi-batch emulsion polymerization, which were carried out in a 1L five-neck glass mantled reactor equipped with a thermo-stated water bath, a mechanical agitator with a perforated steel paddle, a flux condenser as well as two feeding inlets for pre-emulsion and initiator solutions, respectively (Figure 7). Peristaltic pumps were used to ensure even feeding of the solutions. Both core and shell pre-emulsions were prepared by mixing emulsifiers and monomers (i.e. BuA, St and AA) for 15 min at room temperature. Distilled water, Disponil FES 32, Disponil NG 3070 and KPS solution were charged into the reactor, while pre-heating to 80 °C under agitation (200rpm). Core pre-emulsion and the corresponding KPS solution were simultaneously fed into the reactor over 1h and subsequently post-polymerized for 30min. Then shell pre-emulsion and the corresponding KPS solution were simultaneously fed into the reactor for 1h 40 min. After finalizing the feed, the temperature was set to 65 °C and the agitation speed was adjusted to 300rpm. The system underwent post-polymerization for 2h before the redox agents (TBHP and Bryggolit C) were successively dropped into the reactor within 20min

in order to ensure the consumption of monomer residues. The system was left to react for an additional 30 min at 65 °C before being cooled down to 20 °C and then the preservative was added. To enhance the colloidal stability, 1 wt % of Disponil NG 3070 was post added. Then the pH was adjusted by 13.5% NaOH solution to 6. The obtained milky latex was weighed, and vacuum filtered through a pre-weighed 125 μm filter screen in order to measure the amount of coagulum in the latex. The basic formulation of the sample 0 is shown in Table 4.

Based on the basic formulation (Table 4), other samples were synthesized by changing the following variables: the incorporation of the crosslinker EGDMA in the core, different concentration of CTA in the shell and varying the ratio of core to shell (1:1.5 and 1:1). The samples were labeled, for example, sample 0-O-0-1:1.5 (sample code-O (without crosslinker) /X (0.45% crosslinker EGDMA)-CTA amount-ratio of core to shell). The general information on different samples and their particle sizes are shown in Table 5.

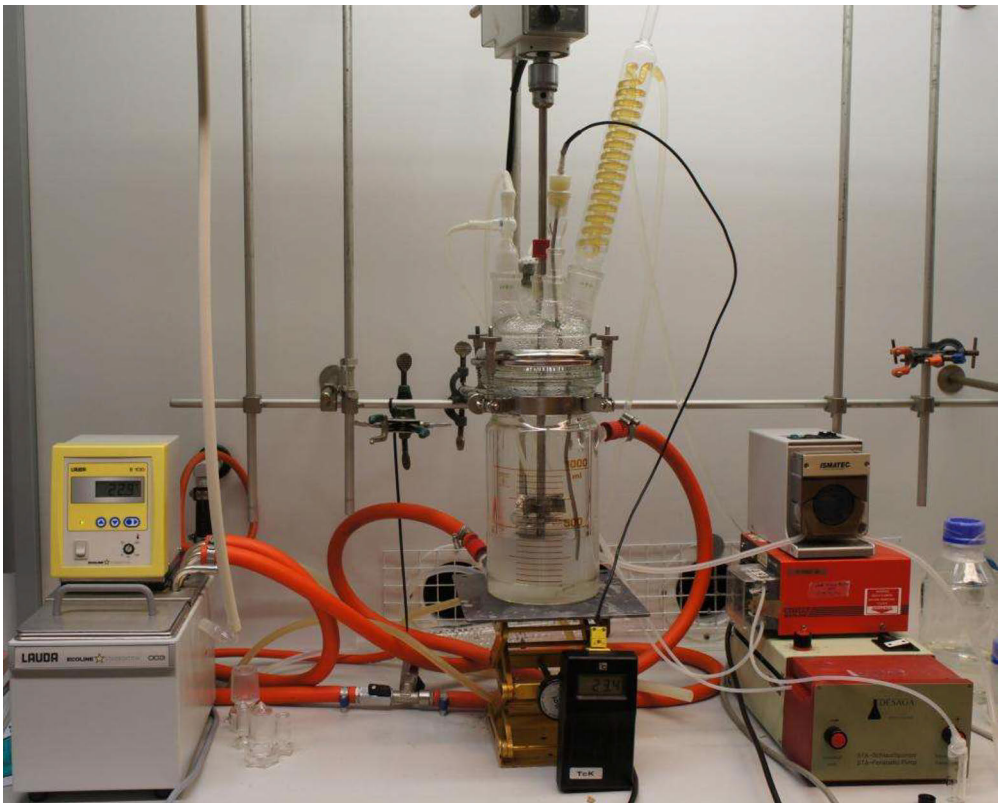

Figure 7. The experimental batch setup.

Table 4 The basic formulation of sample 0-O-**0**-*1:1.5*.

Stages	Ingredient	Amount/g
Pre-charge	Water	200
	Disponil FES 32	0.2
	Disponil NG 3070	2
	4.1% KPS solution	36.5
Core polymerization	BuA	117
	Sty	78
	AA	3
	4.1% KPS solution	36.5
Shell polymerization	BuA	233
	Sty	58
	AA	2.5
	4.1% KPS solution	40
Redox agents	33.3% TBHP solution	4.5
	6.1% Bryggolit C solution	21.3
Preservative	39.3% Proxel solution	3.3
Total		835.8

Table 5 Results of particle size measurements by the laser diffraction technique for the different samples.

Sample code	Variables			Particle size (nm)	
	EGDMA in core (100%)	Dm in shell (100%)	Ratio of core to shell	Mean	Mean/ Median
0-O-**0**-*1:1.5*	0	0	1:1.5	389	1.01
1-X-**0**-*1:1.5*	0.45	0	1:1.5	372	1.01
2-X-**0.1**-*1:1.5*	0.45	0.1	1:1.5	390	1.01
3-X-**0.3**-*1:1.5*	0.45	0.3	1:1.5	365	1.01
4-X-**0.5**-*1:1.5*	0.45	0.5	1:1.5	386	1.01
5-X-**0**-*1:1*	0.45	0	1:1	385	1.01

4.1.3 Characterization Methods

4.1.3.1 Characterization of the emulsion polymer and films

Coagulum and solid content

The coagulum amount and solid content were determined gravimetrically. The coagulum amounts of all samples were determined to be less than 0.1%. The solid contents of all samples were 49.4% (+/- 0.4%).

DLS

Latex particle sizes were measured using a laser diffraction instrument (LS 13 320 Particle Size Analyzer, Beckman Coulter), and the results are shown in Table 10. The average particle sizes of all samples were within a range of 365-390 nm, and the ratios of mean/median were one, which indicates a narrow particle size distribution without secondary nucleation. (Ferguson CJ, 2002)

CryoTEM

The particle morphology was investigated by JEM-3200FSC field emission cryoTEM spectrometer operated at an acceleration voltage of 200 kV. (Ballauff M, 2007; Crassous JJ, 2009; Friedrich H, 2010; Wan Q, 2011) A 3μL drop was applied on the carrier grid (plasma treated graphene), which was subsequently blotted with filter paper and plunge frozen at -175˚C using a Vitrobot. Three samples (sample 0, 1 and 4) were analyzed. Samples were diluted to 1-5% solutions by deionized water or tap water (pH 7.3) or standard buffer solution (pH=7).

Soxhlet extraction

The gel content of the fresh latex and dried film samples was determined via soxhlet extraction with THF under 24 h. (Kajtna J, 2009; Alarcia F, 2006; do Amaral M, 2005; Zhou C, 2011) Sample 1 was prepared in both forms to compare the difference, whereas the other samples were tested in the form of fresh latex. The gel content was calculated according to Equation (1) as follows:

$$Gel\% = \frac{W_{gel}}{W_{dry}} \times 100\% \qquad Wdry = Wfresh \times solid\ content \qquad (1)$$

where W_{gel} refers to the weight of a dried gel after soxhlet extraction; W_{dry} refers to the weight of a dried sample.

SEC

Prior to SEC measurements, the polymer was precipitated out by adding methanol to the sample emulsion. The solid residue was filtered off and dissolved in THF. This procedure was used instead of drying the latex in order to maximize the solubility of sample in THF. (Foster AB, 2009) The molecular weight of sol polymers was measured using a SEC instrument (Shimadzu) with a LT-ELSD (low temperature evaporative light scattering detector, Sedere sedex 85 LT),

equipped with AM gel guard column-100×7.8 mm and AM GPC gel linear 10 µ-100×7.8 mm column (Ohio, USA). The number-average molecular weight (Mn), weight-average molecular weight (Mw) and polydispersity index (PDI = Mw/Mn) were calculated relative to polystyrene standards (PSS polymer standards service GmbH), ranging from 374-2,570,000 g/mol (Mp). THF was used as the eluent at the flow rate of 1 ml/min.

DSC

The DSC analyses of the dried polymer films were performed using Q1000 equipment from TA Instruments over the temperature range of -90 to 80°C at a heating/cooling rate of 10 °C/min. The second heating curve was analyzed, and the middle point of the glass transition range was taken as T_g.

Rheology

Viscoelasticity of the dried polymer discs (25 mm*4 mm) was analyzed by a RA 1000ex rheometer (TA instruments) equipped with a 25 mm parallel plate geometry. Frequency sweep measurements from 0.01–100 rad/s were performed at 23°C. Temperature ramp measurements from 25–200°C were carried out at a heating rate of 2 °C/min and a frequency of 10 rad/s. For each sample, three parallel specimens were prepared and each one was measured twice on frequency sweep, but only once for temperature ramp measurement, due to heat-induced irreversible destruction of the polymer structure.

4.1.3.2 Testing of mechanical strength

Mechanical strength measurement methods for pressure-sensitive adhesives (PSAs) were utilized (due to the similarity of composition and application of PSA and the prepared latexes), including tensile strength (T-peel testing), tack (Q-stick testing) and shear strength. The sample strips were prepared by applying 60 g/m^2 emulsions onto a Mylar-film with subsequent drying for one day. T-peel and Q-stick tests were conducted using Tensile Testing equipment Instron 3366, and shear resistance testing was conducted on a Shear Tester.

T-peel tensile strength

The t-peel test was done according to the European standard prEN 1372. The force needed to release the glued films from each other by pulling them at 180° with a speed of 100 mm/min under constant conditions was measured. The sample strips were cut to a size of 2.5 cm × 40 cm. The peel strength is expressed as the average value of three parallel measurements in Newtons (N).

Tack

The tack was measured by the Quick stick (loop tack) test, in which the force needed to release a 25 mm wide adhesive film from a glass surface at a drawing speed of 300 mm/min is measured. The sample strips were cut into a size of 2.5 cm × 20 cm. The Q-stick value is expressed as an average value of at least three parallel measurements, in Newtons per 25 mm width (N/25 mm).

Shear strength

The shear strength was determined according to the European standard prEN 1373. A load of 1 kg was applied, and the time the adhesive joint could tolerate the static stress was measured. The sample strips were cut into a size of 2.5 cm × 15 cm, and the adhesion area was (2.5 × 2.5) cm^2. Shear resistance is expressed as the average time to failure for three parallel samples, in unit min.

4.2 Preparation of One-Component Moisture-Curable Polyurethane Adhesives

4.2.1 Chemicals and Materials

Polymeric methyl diisocyanate (pMDI) (NCO% = 32.2, functionality=2.3), polypropylene glycol 2000 (PPG 2000) (OH value = 56 mg KOH/g), di-propylene glycol (di-PPG), tri-propylene glycol (tri-PPG), butanediol, pentanediol and mono isocyanate were all obtained from Sigma-Aldrich, Finland. The polyols and chain extenders were pre-dried at 60 °C using reduced pressure.

4.2.2 Synthesis of One-Component Moisture-Curable Polyurethane

NCO-terminated chain extended urethane prepolymers were synthesized by poly-addition reactions of difunctional polyols and difunctional chain extenders with excess isocyanates. The synthesis reactions were carried out in a three-neck round bottom flask equipped with a mechanical stirrer, a dropping funnel and a water condenser connected to nitrogen inlet. Attenuated total reflectance-fourier transform infrared spectroscopy (ATR-FTIR) was used to monitor the formation of urethane prepolymers.

One shot process

Initially excess pMDI, PPG 2000 and chain extender were added into the reactor and the system was flushed with nitrogen. Inert atmosphere was maintained throughout the whole process. The mixture was then heated to 80 °C and stirred vigorously at 800-1000 rpm. When the reaction had been completed (monitored by ATR-FTIR), the mixture was cooled down to below 40 °C and an excess of pMDI was added in order to reach a constant theoretical isocyanate content of 15 wt% (Clauß, et al., 2011). Eventually, mono isocyanate was added to enhance storage stability. (Master, 2013)

Two stage process

Excess pMDI was poured into the reactor and the system was preheated to 60 °C, and simultaneously, the reactor was flushed with nitrogen and inert atmosphere was maintained throughout the duration of the reaction. In the first stage, PPG 2000 was dropped into the reactor at 60 °C under vigorous stirring of 800-1100 rpm. The temperature was raised to 80 °C. When the reaction between pMDI and PPG 2000 had been completed (determined by ATR-FTIR), the reactor was cooled down to 60 °C. In the second stage, chain extender was dropped in at 60 °C. When the reaction was completed, the mixture was cooled down. At a temperature below 40 °C, additional pMDI was added in order to reach a constant theoretical isocyanate content of 15 wt%. Eventually, mono isocyanate was added to enhance storage stability. (Master, 2013)

The composition of urethane prepolymers is shown in Table 5. These urethane prepolymers were labeled as UP**X-***CE*-***Y***: UP refers to urethane prepolymer; **X** refers to synthesis processes (**1** refers to one-shot process, **2** refers to two-stage process); *CE* refers to the different types of chain extenders (*O* refers to no chain extender; *DI* is the abbreviation for di-PPG; *TRI* is the abbreviation for tri-PPG; *PEN* is the abbreviation for pentanediol, *BUT* is the abbreviation for butanediol); ***Y*** refers to the molar ratio between chain extender and PPG 2000.

The final NCO-content of all samples (NCO-wt%), measured by titration with N,N'-dibutylamine, was 15 ± 0.5 wt%, which is in good agreement with the theoretical value. The theoretical NCO-wt%, the ratio of NCO and OH (NCO/OH) and the ratio of hard segment (HS) and soft segment (SS) (HS/SS) were calculated according to equations (2), (3) and (4), respectively. As can been seen in Table 6, at a constant NCO content of 15 wt%, the hard segment content increased and NCO/OH molar ratio decreased as a function of chain extender amount.

$$NCO\% = \frac{n\,(excess\ NCO) * M\,(NCO) * 100\%}{mtot} \tag{2}$$

$$\frac{NCO}{OH} = \frac{n(pMDI) * functionality}{n(polyols) * functionalit \quad (diol) * 2} \tag{3}$$

$$\frac{HS}{SS} = \frac{(weight\ of\ CE + weigh\ \ of\ pMDI) * 100\%}{weight\ of\ polyols} \tag{4}$$

Table 6 The compositions of urethane prepolymers

Sample (UPX-*CE-Y*) *	pMDI:PPG2000:CE molar ratio	NCO/OH molar ratio	HS/SS
UP1-*O-0*	7.44:1:0	8.57	1.12
UP2-*O-0*			
UP1-*DI-0.34*	8.08:1:0.34	6.94	1.23
UP2-*DI-0.34*			
UP1-*DI-0.54*	8.46:1:0.54	6.33	1.29
UP2-*DI-0.54*			
UP1-*DI-0.74*	8.84:1:0.74	5.85	1.36
UP2-*DI-0.74*			
UP1-*DI-0.94*	9.22:1:0.94	5.47	1.42
UP2-*DI-0.94*			
UP1-*PEN-0.34*	8.08:1:0.34	6.94	1.23
UP2-*PEN-0.34*			
UP1-*PEN-0.54*	8.46:1:0.54	6.33	1.29
UP2-*PEN-0.54*			
UP1-*PEN-0.74*	8.84:1:0.74	5.85	1.36
UP2-*PEN-0.74*			
UP1-*PEN-0.94*	9.22:1:0.94	5.47	1.42
UP2-*PEN-0.94*			
UP1-*TRI-0.74*	8.84:1:0.74	5.85	1.36
UP2-*TRI-0.74*			
UP1-*BUT-0.74*	8.84:1:0.74	5.85	1.36
UP2-*BUT-0.74*			

* **X**: synthesis processes: 1- one-shot process, 2- two-stage process; *CE*: chain extender: *DI* -di-PPG, *TRI* -tri-PPG, *PEN* - pentanediol, *BUT* - butanediol; ***Y***: the molar ratio of chain extender to PPG 2000.

4.2.3 Characterization methods

ATR-FTIR

ATR-FTIR spectroscopy (IS50 ATR-FTIR instrument from Thermo Scientific) was utilized to monitor the reaction progress and to characterize the final urethane prepolymers. Absorbance spectra were collected between 400 and 4000 cm^{-1} at a resolution of 4 cm^{-1}.

NMR

The chemical structure of urethane prepolymers was examined by proton nuclear magnetic resonance (^{1}H-NMR) spectroscopy, using a Bruker NMR 600 MHz spectrometer. $CDCl_3$ was used as a solvent.

DSC

Thermal transitions of urethane prepolymers were measured by differential scanning calorimetry (DSC) (Q1000 DSC instrument from TA Instrument), over a temperature range of -90 to 80 °C at a heating/cooling rate of 10 °C/min. The first heating curve was analyzed.

SEC

Prior to size exclusion chromatography (SEC) measurement, the urethane prepolymers were first treated with excess methanol to end-cap the free NCO groups. (Clauß, et al., 2011) Then excess methanol was removed by rotary evaporator and dried. Then the samples were dissolved in THF for SEC measurements. The molecular weight of sol polymers was measured using a SEC instrument (Shimadzu) with an LT-ELSD (low temperature evaporative light scattering detector, Sedere sedex 85LT), equipped with an AM gel guard column (8×50 mm) and AM GPC gel columns (500 Å: 8×300 mm; 10e5 Å: 8×300 mm) (Ohio, USA). The number-average molecular weight (Mn), weight-average molecular weight (Mw) and polydispersity index (PDI = Mw/Mn) were calculated relative to polystyrene standards (PSS polymer standards service GmbH), ranging from 374-2,570,000 g/mol (Mp). THF was used as the eluent at a flow rate of 0.8 ml/min.

Viscosity

Brookfield viscometer was utilized to measure the viscosity of urethane prepolymers at 20 °C. The ratio of spindle to speed was 5/20.

Mechanical strength of adhesive bonding

The samples were cured under standardized conditions for 7d. The bond strength of cured samples was measured by using a tensile shear strength instrument (Instron 3366), according to the standard DIN EN 1465.

4.3 Preparation of Silane-Terminated Polyurethane Adhesives

4.3.1 Chemicals and materials

Materials for the synthesis of SPUR polymers

Polypropylene glycols PPG 2000 (OH value = 56 mg KOH/g, molecular weight (Mw) = 2000 g/mol, 98 %), PPG 4000 (OH value = 26.5-29.5 mg KOH/g, Mw = 4000 g/mol, 98 %), PPG 8200 (OH value = 13.5-15.5 mg KOH/g, Mw = 8200 g/mol, 98 %), isophorone diisocyanate (IPDI, 98 %), and vinyl trimethoxysilane (VTMO,98 %) were obtained from Sigma-Aldrich, Finland. Metal catalysts dioctyltin dilaurate (DOTL) (metal content = 15.5–17.0 %), bismuth carboxylates Bi1 (metal content = 15.0–16.5 %) and Bi2 (metal content = 19.0–21.0 %) were obtained from ABCR, Germany. The general information of secondary aminoalkoxysilanes is shown in Table 7. Prior to use, polyols and glassware were dried at 60 °C overnight using reduced pressure.

Table 7 General information of secondary aminoalkoxysilanes (All supplied by ABCR Germany, purity 98%).

Silane code	Chemical name	Chemical structure
S1	N-ethyl-aminoisobutyl-trimethoxysilane	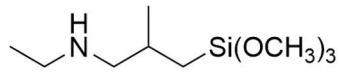
S2	N-phenyl-aminopropyl-trimethoxysilane	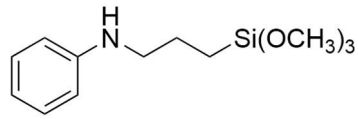
S3	Bis((3-trimethoxysilyl)-propyl)amine	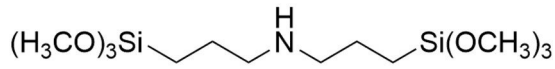
S4	N-butyl-aminopropyl-trimethoxysilane	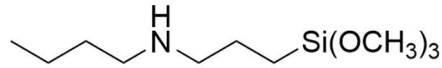
S5	N-cyclohexyl-aminomethyl-triethyoxysilane	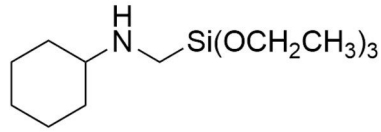

Materials for SPUR adhesive formulations

Surface coated and precipitated calcium carbonate (Sigma-aldrich, Finland, ≥99.9%), alkyl sulphonic ester of phenol (Sigma-Aldrich, Finland), vinyl trimethoxysilane (Sigma-Aldrich, Finland, 98 %) and 3-aminopropyltrimethoxysilane (Sigma-aldrich, Finland, 97 %) were utilized as additives in SPUR formulations.

4.3.2 Synthesis of SPUR prepolymer

The SPUR prepolymers were prepared via a two-stage process; the synthesis of NCO-terminated urethane prepolymers was followed by silane end-capping. The synthesis reactions were carried out in a three-neck round bottom flask equipped with a mechanical stirrer, a dropping funnel and a water condenser connected to nitrogen inlet. Inert atmosphere was maintained throughout the whole process to ensure absence of moisture.

Synthesis of NCO-terminated urethane prepolymer

NCO-terminated PUR was prepared in a one-shot process. Diisocyanate, polyol and catalyst were added into the reactor under nitrogen gas blanketing. The mixture was then heated up to 70 °C under a vigorous stirring of 800–1000 rpm. Temperature in the flask was kept constantly below 80 °C to avoid undesirable side reactions.

The reaction conversion was followed by attenuated total reflectance-Fourier transform infrared spectroscopy (ATR-FTIR). During the reaction progress, the relative intensity of urethane C=O band at 1680-1750 cm-1 increased, whereas the N=C=O stretching band at 2270 cm-1 decreased. The reaction was judged completed, when no relative changes in intensities were recorded.

Silane end-capping

After cooling down the reaction flask below 60 °C, the secondary amino alkoxysilane was added dropwise into the obtained PUR prepolymer under vigorous stirring. The silane end-capping reaction was monitored by following the increase in the intensity of the urea C=O vibration at 1600-1680 cm^{-1} and the decrease in intensity of the N=C=O stretching band at 2270 cm^{-1} in ATR-FTIR spectra. An absence of absorbance band at 2270 cm^{-1} indicated that free isocyanate had been completely end-capped. Subsequently, VTMO was added as a moisture scavenger to enhance the pot life of the products. SPUR prepolymers were obtained as viscous liquids.

The compositions of different SPUR prepolymers are shown in Table 8. The molar ratio of diisocyanate to polyol (NCO/OH) and the weight ratio of hard segment to soft segment (HS/SS) were calculated according to the methods presented in our previous work. (Tan, Tirri, & Wilen, 2017)

Table 8 The sample codes and compositions of the synthesized SPUR prepolymers.

SPUR sample code	Polyol molecular weight (g/mol)	Diiso-cyanate	NCO/ OH	Catalyst (0.1 wt%)	Secondary amino-silane	HS/SS (wt%)
SPUR 1	PPG 4000	IPDI	1.5	Bi2	S4	8.35
SPUR 2	PPG 4000	IPDI	2.0	Bi2	S4	11.10
SPUR 3	PPG 4000	IPDI	2.8	Bi2	S4	15.56
SPUR 4	PPG 2000	IPDI	2.0	Bi2	S4	22.20
SPUR 5	PPG 8200	IPDI	2.0	Bi2	S4	5.42
SPUR 6	PPG 4000	IPDI	2.0	Bi2	S1	11.10
SPUR 7	PPG 4000	IPDI	2.0	Bi1	S4	11.10
SPUR 8	PPG 4000	IPDI	2.0	DOTL	S4	11.10
SPUR 9	PPG 4000	IPDI	2.0	Bi2	S2	11.10
SPUR 10	PPG 4000	IPDI	2.0	Bi2	S5	11.10
SPUR 11	PPG 4000	IPDI	2.0	Bi2	S3	11.10

SPUR adhesive formulation

The composition of SPUR adhesive formulation is shown in Table 9. The filler, moisture scavenger, plasticizer and adhesion promoter were added to the synthesized SPUR polymer by rapid mixing (2 min). The formulated SPUR prepolymers are coded as SPUR-F.

Table 9 The composition of SPUR adhesive formulation.

Type	Details	Parts by weight
Polymer	SPUR prepolymer	20.00
Filler	Surface coated and precipitated calcium carbonate	62.00
Plasticizer	Alkyl sulphonic ester of phenol	15.00
Moisture scavenger	Vinyltrimethoxysilane	2.00
Adhesion promoter	3-aminopropyltrimethoxysilane	1.00
Total		100

The formulated SPUR adhesives were set to cure in dumbbell-shaped PTFE (polytetrafluoroethylene) molds at 23 °C and at the relative humidity of 50 %. The cure rates of these samples were monitored for 7 days (7d), and the tack-free time was noted. The same specimens were used for mechanical tests.

4.3.3 Characterization methods

NMR

Nuclear magnetic spectroscopy of SPUR prepolymers was carried out using Bruker 500 MHz spectrometer. $CDCl_3$ was used as the solvent.

ATR-FTIR

Attenuated total reflectance-Fourier transform infrared spectroscopy (IS50 ATR-FTIR instrument from Thermo Scientific) was utilized to analyze both SPUR prepolymers and cured SPUR films. Absorbance spectra were collected between 400 and 4000 cm^{-1} at a resolution of 4 cm^{-1}.

TGA

Thermal stability of SPUR prepolymers and cured SPUR films was investigated by thermogravimetric analysis (TGA) (TA Instrument SDT Q600). Samples were analyzed under nitrogen atmosphere (flow rate 100 ml/min), over a temperature range of 25 to 800 °C at a heating rate of 10 °C/min.

Rheology

The viscosity of SPUR prepolymers was evaluated by using a rotational rheometer Physica MCR 301 (Anton Paar GmbH). A cone-plate geometry (CP25-1) was used having a diameter of 25 mm and cone angle of 1 degree. Measurements were done at 23 °C, at shear rates ranging from 1–100 s^{-1}.

The viscosities of SPUR-F were measured using a Brookfield viscometer with a spindle to speed ratio of 7/20. Viscosity measurements were performed the same day as the formulations were prepared.

Mechanical strength of the cured adhesives

7d bond strength of the cured adhesives was measured using a tensile testing instrument (Instron 3345), according to the standard DIN 53504/ ASTM D412/ ISO 37. The crosshead speed was set to 50 mm/min. The average tensile results for every sample were based on measurements of at least five specimens.

5. Results and Discussion

5.1 Core-Shell Structured Poly(Styrene-co-Butyl) Emulsion Polymers

5.1.1 Influence on Tg

In general, it is known that the T_g value has a strong correlation with the thermomechanical properties of emulsion polymers. Adhesive tack decreases with increasing T_g, whereas shear strength and cohesive strength follow the opposite trend and increase with T_g. Peel strength increases with T_g up to a limit and after that it decreases dramatically. To find an optimal balance between tack, peel and shear strength, the T_g of latex polymer should be tuned to meet the desired performance level of a construction adhesive. As a consequence, polymer emulsions with different chemical compositions were prepared in order to provide polymer emulsions with various T_g values and thus also thermomechanical properties. The T_g values obtained from DSC measurements of the various latexes are shown in Table 10.

Table 10 Glass transition temperatures (T_gs) measured by DSC.

Sample	**T_g/°C**	
	Core	**Shell**
0-O-0-*1:1.5*	-17.3	
1-X-0-*1:1.5*	-5.9	-19.8
2-X-0.1-*1:1.5*	-7.1	-21.8
3-X-0.3-*1:1.5*	-7.3	-21.6
4-X-0.5-*1:1.5*	-7.2	-22.7
5-X-0-*1:1*	-4.0	-17.6

Only the step changes due to glass transition were observed in the DSC curves over the used temperature range from -90 to 80°C, which indicates that the latex polymers were completely amorphous. The *Fox-Florry equation* (do Amaral M, 2005) predicted, the theoretical T_gs of the core and the shell copolymers (1:1.5 core to shell ratio) to be -11°C and -35°C, respectively. The results depicted in

Table 3 revealed that the T_gs determined by the DSC measurements were higher than the predicted ones.

The DSC thermograms of samples with a crosslinked core and a non-crosslinked core were compared and results shown in Figure 8. For sample 0 with a non-crosslinked core, a T_g with a narrow onset/end interval (ΔT_g~20°C) was detected in the DSC curve, which indicates a homogeneous copolymer structure. This can be attributed to the similarity in the composition of core and shell structures of the polymer particles. During film formation, the coalescence of particles enabled the miscibility of core and shell parts whereby a uniform film was obtained. No different core and shell domains were observed or detected by the DSC measurement. However, when the core part was crosslinked, the increasing heterogeneity promoted immiscibility between the core and the shell polymers in the sample film. Indeed, two T_gs and a broader onset/end interval (ΔT_g~34°C) for sample 1 were observed due to its crosslinked core. In fact, the similarity in the shell copolymer composition led to no significant differences in the onset point of T_g, but the end point of T_g range for sample 1 extended to a much higher temperature than that of sample 0.

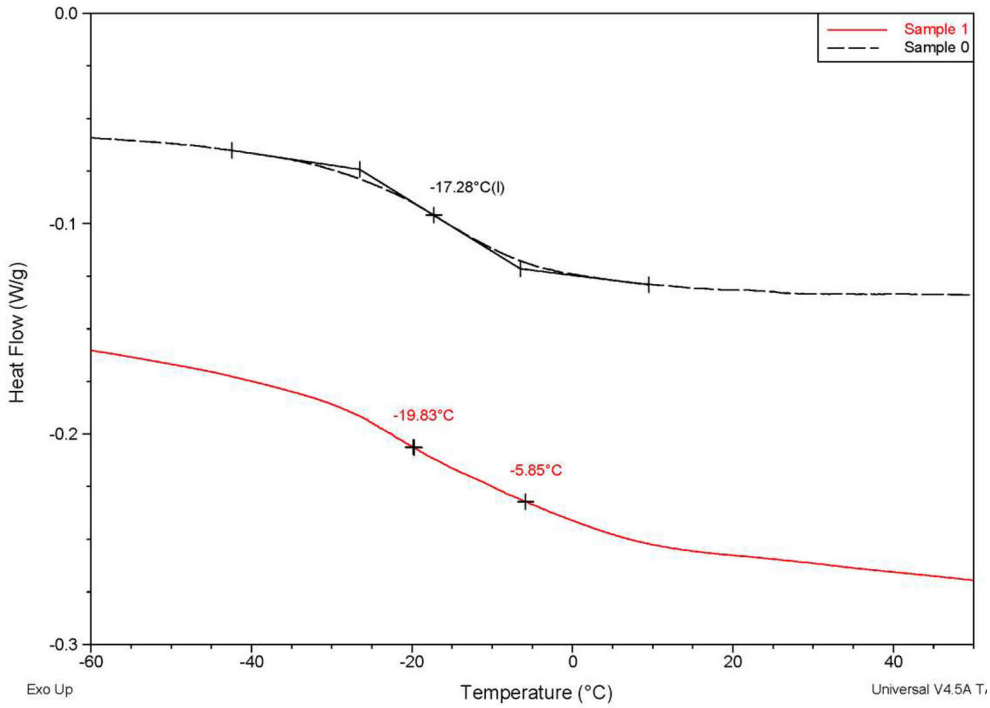

Figure 8. DSC curves of samples with non-crosslinked core (sample 0-O-**0**-*1:1.5*) and crosslinked core (sample 1-X-**0**-*1:1.5*).

To study the influence of CTA on the T_g values, three experiments were carried out. The results are shown in Table 3. As could be anticipated the samples prepared in the presence of CTA exhibited slightly lower T_g values compared to

sample 1. Not surprisingly, sample 5 with a higher core to shell ratio (1:1) had 2°C higher T_gs for both the core and the shell than sample 1 with lower core to shell ratio (1:1.5).

5.1.2 Influence of gel content and polymer molecular weight of sol on mechanical properties

A previous report (Roberge S, 2006) has shown that both the Mw and gel content have a significant influence on the adhesive´s mechanical properties. Therefore, it was meaningful to adjust these parameters by addition of CTA and crosslinker in order to study their impacts on adhesion properties. The polymer molecular weights of soluble fraction and gel contents are summarized in Table 11, and the combined SEC chromatograms are illustrated in Figure 9.

Table 11 Polymer molecular weight of sol and gel content of all samples.

Sample Code	Mn	Mw	PDI	Gel content (wt-%)
0-O-0-*1:1.5*	75808	211598	2.79	1.3/50*
1-X-0-*1:1.5*	55254	166957	3.02	59.5
2-X-0.1-*1:1.5*	42768	145175	3.39	54.2
3-X-0.3-*1:1.5*	35398	102997	2.91	51.5
4-X-0.5-*1:1.5*	32370	90416	2.79	43.0
5-X-0-*1:1*	56077	165562	2.95	72.3

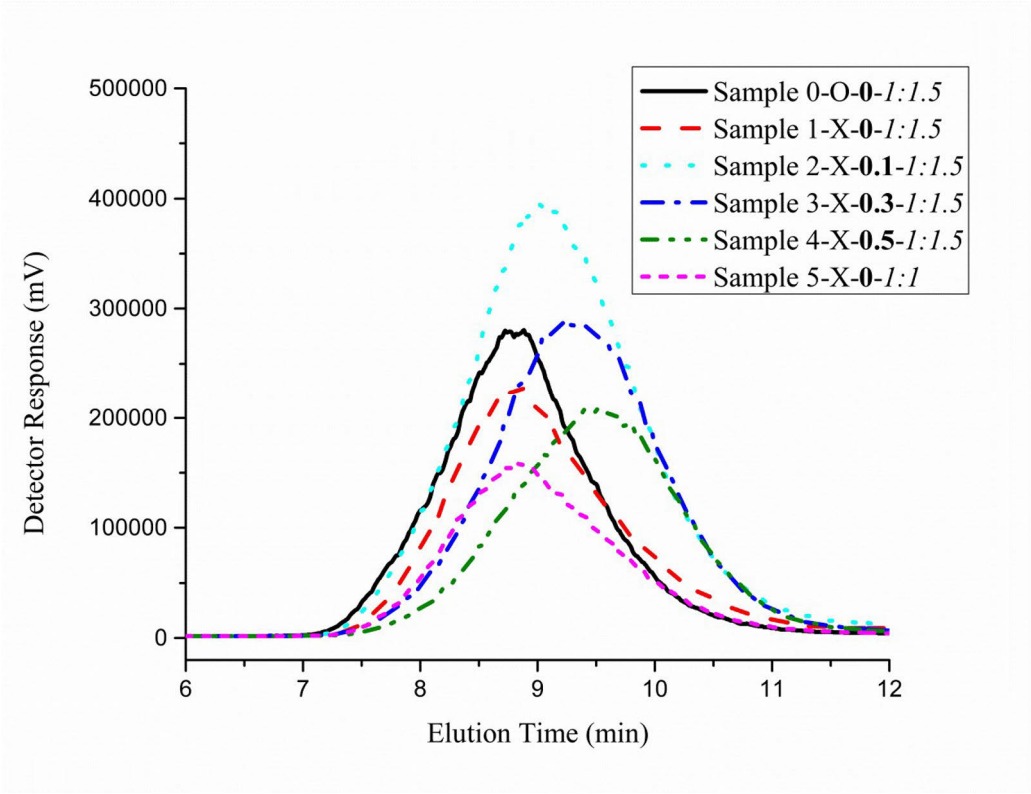

Figure 9. SEC chromatogram of the sol polymer fractions of emulsion polymers.

It is well known that gel is formed either by long-chain branches via intermolecular chain transfer followed by termination via recombination, or by the network formation via propagation to pendant double bonds. (JM., 2004; Chauvet J, 2005) In theory, chain growth of butyl acrylate is realized by a combination of intermolecular and intramolecular transfer to polymer, yielding branches and gel due to the presence of labile hydrogen in the units. However, incorporation of relatively small amount of styrene can dramatically decrease the gel content of poly(butyl acrylate) by reducing the level of branching. (JM., 2004; Kajtna J, 2009; Chauvet J, 2005; Qie L, Manipulation of chain transfer agent and cross-linker concentration to modify latex micro-structure for pressure-sensitive adhesives, 2010; Qie L, The influence of butyl acrylate/methyl methacrylate/2-Hydroxyethyl methacrylate/acrylic acid latex properties on pressure sensitive Adhesive performance, 2010) This theory is supported by the low gel content of 1.3 wt% recorded for the non-crosslinked sample 0. However, it must be noted that gel content of the virgin latex and its dry film may be totally different. Thus, the gel content of sample 0 was measured both before and after drying of the latex, and the obtained values were 1.3% and 50%, respectively. The surprisingly high gel content of the film may be attributed to the occurrence of physical crosslinking during the film formation process. Therefore, gel content

and molecular weight measurements of the fresh latexes gave more meaningful and representative results than those obtained for the dried films. The gel content of Sample 1 with a crosslinked core was considerably higher than that of sample 0, but the Mw and Mn were lower than those of sample 0. This is in agreement with the finding that Mw of sol polymer fraction decreases with an increase in gel content, as long polymer chains readily incorporate into gels especially in the presence of crosslinkers with pendant double bonds. (Qie L, Manipulation of chain transfer agent and cross-linker concentration to modify latex micro-structure for pressure-sensitive adhesives, 2010; Chauvet J, 2005; Qie L, The influence of butyl acrylate/methyl methacrylate/2-Hydroxyethyl methacrylate/acrylic acid latex properties on pressure sensitive Adhesive performance, 2010) In addition, highly crosslinked core copolymers were excluded from SEC measurements and thereby leaving a larger portion of soluble fractions with relatively low Mw for analysis.

When comparing samples with different ratios of core to shell (sample 1 and sample 5), there was no notable difference in the values of Mn, Mw and PDI, as the recipe and reaction time were recalculated according to the core-shell ratio in order to keep all the other factors unchanged. Whereas it is not a surprising result that sample 5 had higher gel content than the other samples because of its higher portion of crosslinked core copolymer.

The amount of CTA had only a minor influence on the gel content, especially at low concentration of CTA. The gel content decreased slightly when CTA amount increased from 0.1% to 0.3% but the effect became more apparent when 0.5% of CTA was added. This is probably because the crosslinked networks were formed at the core polymerization stage (1st stage) prior to the addition of CTA. Thus, gel formation was not influenced by the chain transfer processes induced by the addition of CTA at later stage (2nd stage). Nevertheless, the addition of CTA decreased molecular weight of the soluble polymer fractions that mainly derive from the shell polymers. The decrease of molecular weight was pronounced for samples 2 and 3, whereas for sample 4 with 0.5% of CTA the effect started to level off. These findings are in-line with previous research reports. (Chauvet J, 2005; Qie L, Manipulation of chain transfer agent and cross-linker concentration to modify latex micro-structure for pressure-sensitive adhesives, 2010)

5.1.3 Influence on particle morphology

In Figure 10, cryoTEM images of the samples 0, 1, 3 and 4 are presented. Not only the polymer composition but also the diluent of the TEM samples had an influence on the recorded particle morphologies. Deionized water caused significant swelling of the particles (Figure 10 (a1) and (b1)) and around the dark particle cores, a corona was observed. This phenomenon has been mentioned in some previous research papers, and it has been attributed to osmotic pressure. (Ballauff M, 2007; Crassous JJ, 2009; Friedrich H, 2010) The emulsion particles are rich in internal and interfacial ions originating from the anionic surfactants and from the acrylic acid, which has been neutralized by NaOH. To balance the osmotic pressure, deionized water readily penetrates into the ion-rich particles during the interval time between the dilution and the plunge freezing of the cryoTEM samples. Because the particle morphology is fixed after freezing, the extent of swelling is likely to be dependent on the time between these procedures. The particles also had a tendency to vanish from the sample holder during the blotting stage or gather on the plasma treated graphene grid when deionized water was used as diluent. In some cases, only vesicles were found in the vitrified ice. In order to minimize the aforementioned problems, both buffer solution (pH 7) and tap water (pH 7.3) were tested as alternative diluents. Interestingly, the best micrographs in terms of e.g. ice thickness were obtained using tap water.

Due to the similarity in chemical composition between the core and the shell parts, no clear boundary could be observed in the cryoTEM micrographs. It is noteworthy that osmotic pressure has different impact on the non-crosslinked (Figure 10 (a1)) and crosslinked (Figure 10 (b1)) samples, which can be helpful when studying the morphological differences. The crosslinked particles of sample 1 diluted in deionized water (Figure 10 (b1)) did not swell equally much as the sample 0 with the non-crosslinked core (Figure 10 (a1). In both cases, the boundary between the particle and ice was blurred. The average diameter of the expanded particles in sample 0 (Figure 10 (a1)) was more than 600 nm, whereas the one measured by laser diffraction instrument was 389 nm. The effective particle size of the crosslinked particles in sample 1 (Figure 10 (b1)) was estimated to be in average 500 nm, which is also larger than the one measured by the light diffraction (372 nm). The difference may be attributed to the fact that the densely packed core effectively inhibits the penetration of water. However, when tap water was used as diluent, the boundary between the particles and the matrix was sharp, and the effective particle sizes observed in the cryoTEM images (Figure 10 (a2) and Figure 10 (b2)) were in accordance with the ones measured by light diffraction. It can be observed from the Figure 10 (b2), (c) and (d) that the particles had a tendency to aggregate. Logically, the particles produced in the presence of 0.5 wt % of CTA (Figure 10 (d)) deformed the most in this series of experiments under the external pressure due to an increased softness of the shell.

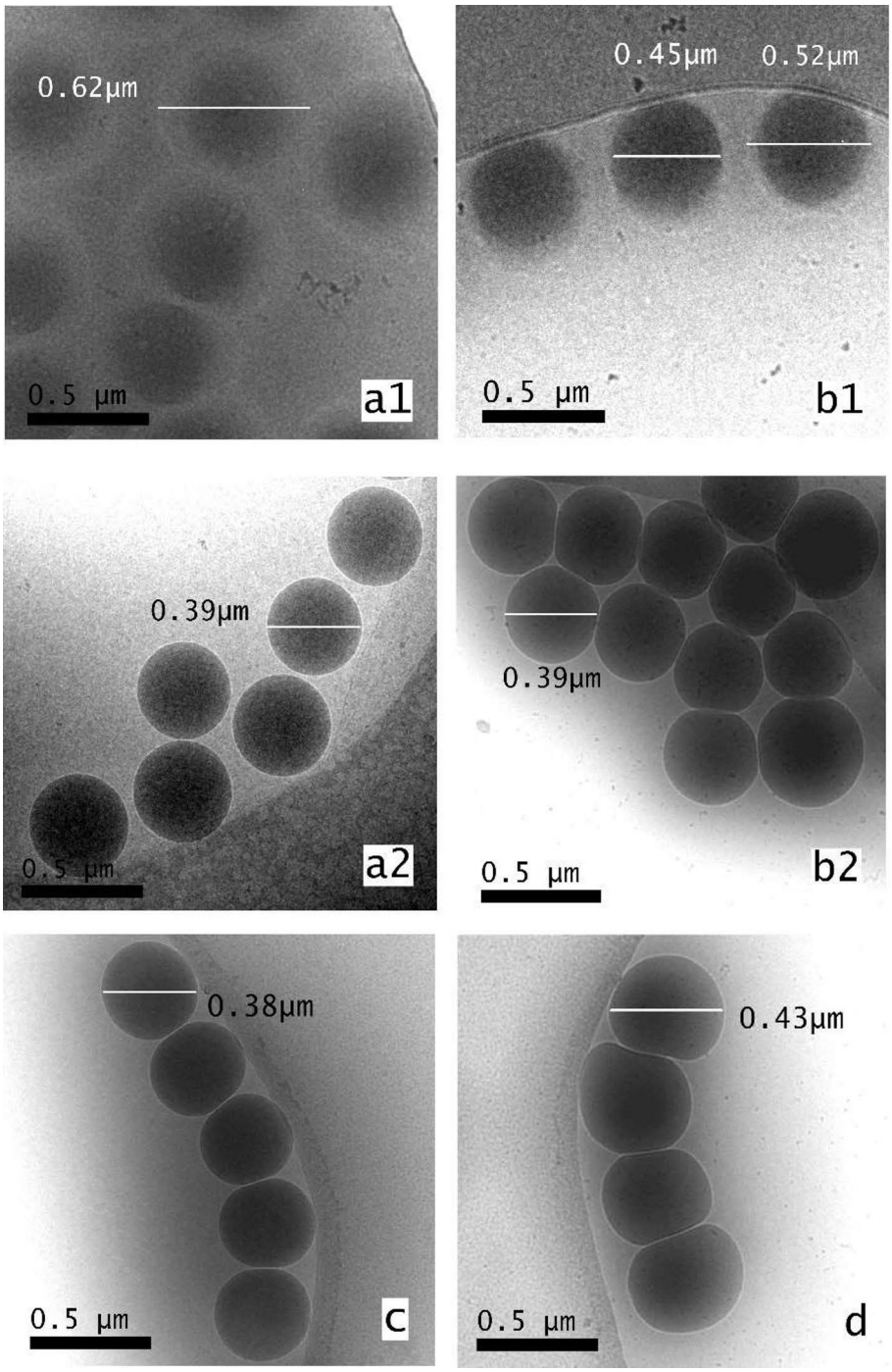

Figure 10. CryoTEM images of the non-crosslinked sample 0 in deionized water (a1) and in tap water (a2); crosslinked sample 1 in deionized water (b1) and in tap water (b2); sample 3 with 0.3 % CTA (c) and sample 4 with 0.5 % CTA (d) in tap water.

5.1.4 Influence on viscoelasticity

The adhesive properties have a close relationship with the rheological and viscoelastic properties of polymers. Therefore, DMA rheometer provides an effective way to explore the structure-property relationship of polymers. In this work, two types of DMA measurements were performed, i.e. frequency and temperature dependent testing.

Frequency sweep measurement

The frequency sweep curves of all samples are shown in Figure 11. According to the Dahlquist theory, an adhesive adheres to a substrate when the creep compliance at the application temperature is greater than 10^{-7} cm^2/dyne after one second of compression. Preferably as high value as 10^{-6} cm^2/dyne is needed for a good performance in a Quick-tack test. In terms of DMA data, the simplified variation of Dahlquist's theory specifies that G' (storage modulus) should be less than $1*10^5$ Pa at a frequency of 1 rad/s. According to the Figure 11 (a), G' of all samples were less than $1*10^5$ Pa at a frequency of 1 rad/s, which indicates that all samples fulfilled the Dahlquist criterion and possessed enough flow to wet a substrate. In addition, tan (delta) curves in Figure 11(c) illustrate the rubbery nature of these samples, since G' is greater than G'' throughout a broad range of frequencies (ca. 0.01-10 rad/s).

As seen in Figure 11 (a), the G' curves of the samples are scattered at the low frequency range, while they are concentrated at high frequency range. This can be explained by the theory of packing states of polymer chains in particles, which was proposed by Qie and his coworkers. (Qie L, The influence of butyl acrylate/methyl methacrylate/2-Hydroxyethyl methacrylate/acrylic acid latex properties on pressure sensitive Adhesive performance, 2010) The G' curves of the samples with CTA (sample 2, 3 and 4) exhibit a steeper slope than for other samples, and the degree of the slope is increasing with the amount of CTA. At low frequency range, samples with CTA have relatively low G', which was attributed to a relatively low gel content and loosely packed polymer chains particularly in the shell part. On the contrary, in samples 1 and 5 with higher gel contents, the polymer chains tend to be densely packed. At the high frequency range, the curves start to overlap irrespective of low or high gel content of the samples. Although the sample 0 had a low amount of chemical crosslinks, it still possessed high G' at low frequency range (densely packed polymer chains) due to the physical crosslinking existing in the film form as discussed earlier. In Figure 11 (b), it can be noticed that the G'' curves of the samples containing CTA (sample 2, 3 and 4) show a sharper slope than the samples without CTA (sample 0, 1 and 5), and the latter samples seem to have a more pronounced G'' valley due to their relatively high molecular weights. The samples with CTA (sample 2, 3 and 4) perform more likely as pressure sensitive adhesive (PSA) than the others, as a good PSA possesses a higher storage modulus at high frequencies than at low frequencies. (Sun S, 2013) However, in order to develop an optimal construction adhesive with high creep resistance, a higher cohesive strength is pivotal especially at low frequency.

Creep resistance is a measure of low frequency deformation, which is an effective reflection of shear resistance over long run time. (Foster AB, 2009) It is favored by a high storage modulus G' and a low tan (delta) at low frequency range. Therefore, in the frequency dependent curves, the low frequency region is the most important and interesting part. In Figure 11 (a), samples 0, 1 and 5 show a high storage modulus at a low frequency of 0.01-0.1 rad/s. In the same region, the samples with CTA have relatively low storage modulus, and it is notable that the modulus G' decreases with an increase in CTA amount. Figure 11 (c) reveals that samples 1 and 5 exhibit the lowest tan (delta) values at low frequency region (0.01-1 rad/s). At the same frequency region, it is observed that samples 2, 3 and 4 with CTA have higher tan (delta) values that increase with the concentration of CTA. This corresponds well to the observation that good shear resistance is associated with emulsion polymers having a crosslinked core and a soft shell of relatively high molecular weight. (Roberge S, 2006; Kajtna J, 2009)

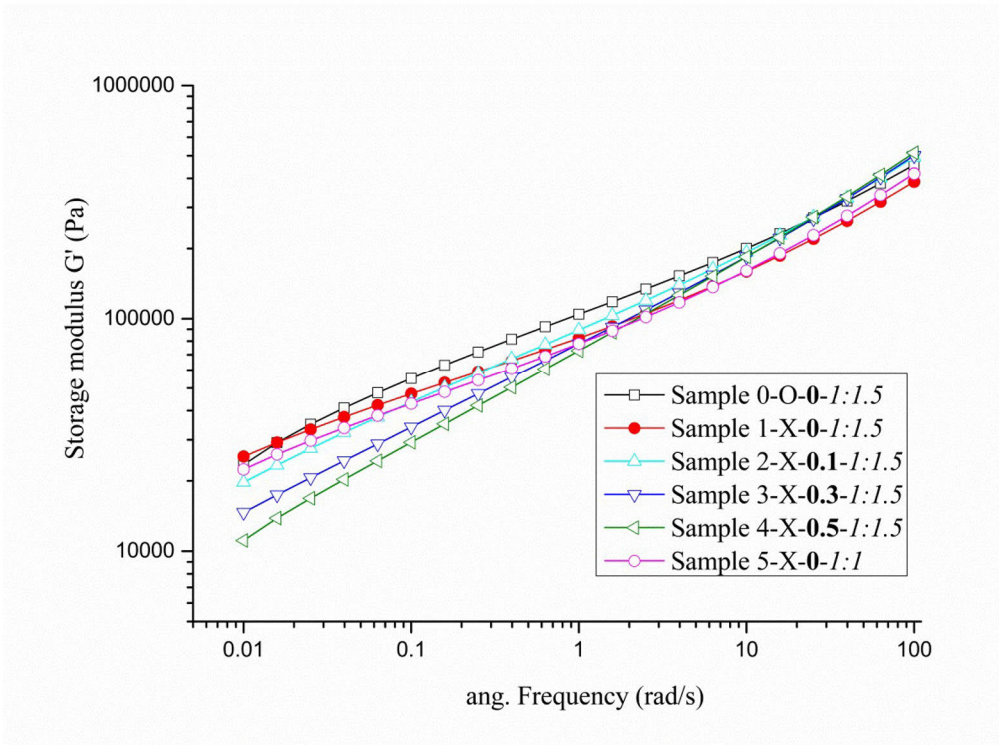

Figure 11 (a). Storage modulus (G') versus frequency at 23°C.

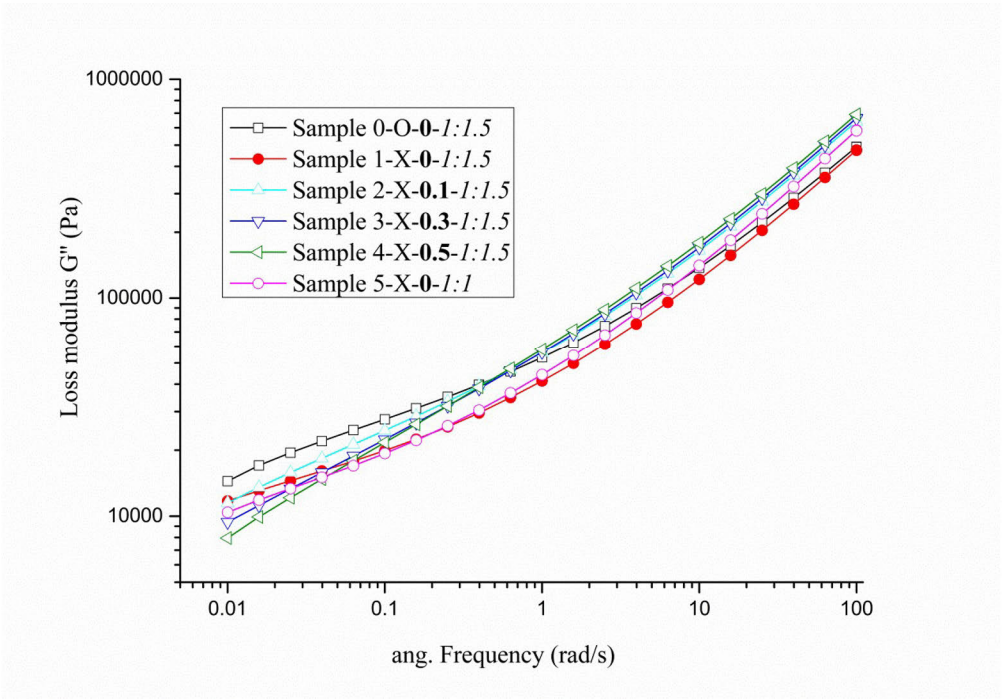

Figure 11 (b). Loss modulus (G'') versus frequency at 23°C.

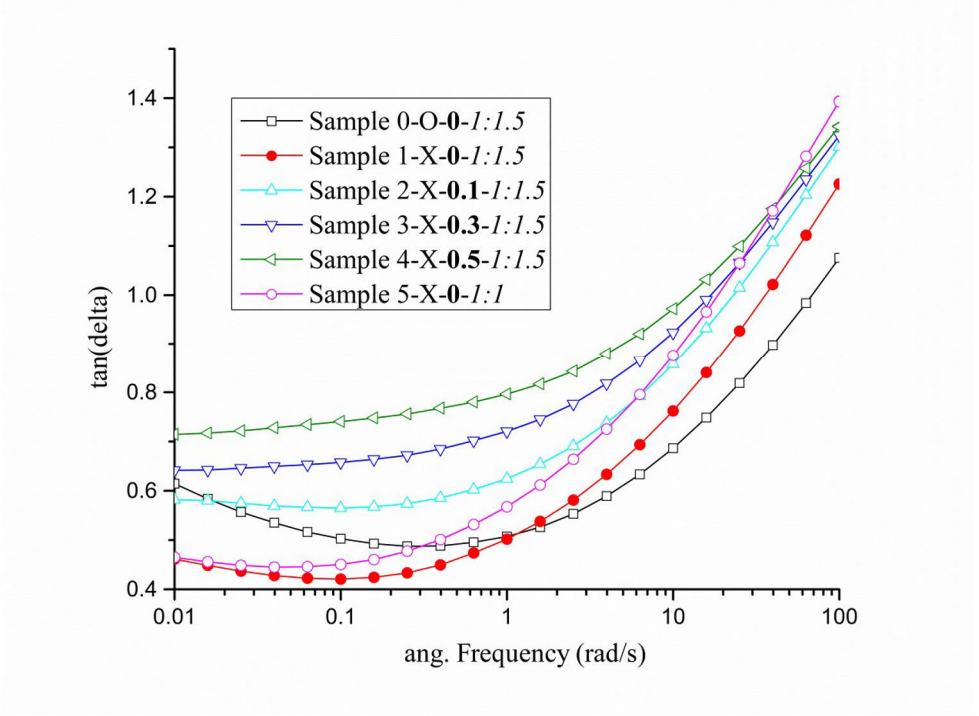

Figure 11 (c). Tan (delta) versus frequency at 23°C.

Temperature ramp measurement

Temperature ramp measurements provide an insight into the structures of viscoelastic polymers over a wide temperature range. In this case, we wanted to study how phase transitions and rheology changes are impacted by the crosslinker and the added CTA. The G' and tan (delta) changes over a temperature range from 25°C to 200°C are shown in Figure 12. The testing temperature range also covers the rubbery plateau region.

From Figure 12 (a) and Figure 12 (b), it is seen that the crosslinked samples 1 and 5 show relatively high G' and low tan (delta) at the low temperature range due to their high gel content, which is indicative of good elastic strength. On the contrary, the samples with CTA which possess relatively low gel content have low G' and high tan (delta) values that decline with the amount of CTA. This is because CTA decreases the chain length and gives rise to polymers with high chain flexibility that in turn promotes the viscous property, and thus enhances the energy dissipation. At low temperature range, the non-crosslinked sample 0 possesses relatively high G' and low tan (delta) which can be compared with crosslinked samples 1 and 5, because it exhibits high gel content in the film form as discussed earlier. As temperature increases, a strong and abrupt change occurs in the non-crosslinked sample 0, i.e. a continuously steep decrease in G' and increase in tan (delta) was seen until the polymer started to melt and flow at a high temperature of 120°C. However, the crosslinked samples behave quite differently. As the temperature increases, the crosslinked samples go through a milder decrease in G' and increase in tan (delta) when the polymer chains become more mobile, and then G' curves gradually level out. In contrary to the non-crosslinked sample 0, the crosslinked samples do not melt but just soften at very high temperatures. In addition, the crosslinked network enables the predominant role of elastic property, that is manifested by the fact that G' is higher than G'' (tan (delta) <1), over the whole temperature range. This behavior is not observed for the non-crosslinked sample 0. These observations prove that crosslinking markedly enhances the elastic strength and heat resistance of the polymer.

Generally, the tan (delta) curves of the tested samples have a trough at low temperature range and a peak at high temperature range. However, there are distinct differences in tan (delta) changes between the crosslinked samples without CTA (sample 1 and 5) and the samples with CTA (sample 2, 3 and 4), which are shown in Figure 12 (b). For the crosslinked samples without CTA, a tan (delta) peak is observed at the high temperature range, especially for sample 1. Sample 1 undergoes a noticeable increase in tan (delta) until a peak value of 0.8 is obtained at 175°C and then starts to decrease at the levelling out stage of G' curve (Figure 12 (a)), in other words, the difference between G' and G'' is diminished from 50°C to 175°C. Tan (delta) of sample 5 with a higher ratio of core to shell perform in a similar way as sample 1, but the peak value is reduced by 0.2. This is attributed to the higher gel content of sample 5, which exerts a higher contribution to energy storage that counterbalances the energy dissipation. It is interesting to see that in the samples with CTA (sample 2, 3 and

4), the increase in tan (delta) is much reduced and the peak of tan (delta) appears earlier (<175°C), especially for sample 4 with the highest amount of CTA. A rough generalization can be made: at low temperatures, the extremely soft shell of samples with CTA play a dominant role in the determination of the viscoelastic behavior exhibiting relatively high tan (delta) (Figure 12 (b)) and low G' (Figure 12 (a)); as the temperature increases, the crosslinked core starts to act and the competition between the energy storage and loss maintains the tan (delta) steady, until finally the crosslinked hard domains predominate at high temperature range. The change in the tan (delta) of the crosslinked samples (1 and 5) can be explained in a similar way: at low temperature range, the crosslinked core predominates as the shell is not flexible enough; as the temperature increases, the shell softens and shows an incremental effect with a significant increase in tan (delta) (Figure 12 (b)), and lastly the crosslinked core supports the main structure and prevents the polymer from completely losing its elastic property.

The rubbery plateau region is of great importance, as it relates to the chain length between the crosslinks or entanglements. According to the rubbery elasticity theory, a vital parameter for a rubber-like polymer is the crosslink density, which is expressed as Mc (the average molecular weight between crosslinks), and can be determined as following Equation (5) (Chattopadhyay DK, 2005; El-Sabbagh S, 2007):

$$Mc = \frac{\rho RT}{G'} \quad (T \gg Tg) \tag{5}$$

where G'- elastic modulus at rubbery plateau region, R-the universal gas constant, T- the absolute temperature, ρ- material density (g/cm^3).

The rubbery plateau region is commonly defined as the region between transition region and terminal region. For the non-crosslinked sample 0, the case is rather simple, as the polymer film is close to a homogeneous structure according to the findings presented in the DSC section. Sample 0 has a very short rubbery plateau region and the crosslink density is so low that the polymer melts at terminal region. For the crosslinked samples, the situation is more complex, as the polymer consists of two parts: the crosslinked core and the non-crosslinked shell. At low temperature range, the non-crosslinked soft shell is more apt to soften and substantially contributes to the decrease in G' and increase in tan (delta), until a tan (delta) peak is obtained. When the tan (delta) starts to decrease at high temperature range, the crosslinked core starts to soften. Thus, it is assumed that the crosslinked samples have a prolonged rubbery plateau region, but the actual region concerning the determination of the crosslinking density lies in the softening temperature of the crosslinked core, which situates above 160°C.

According to Equation (5), the Mc is inversely proportional to G' at the rubbery plateau region. In Figure 12 (c), it is observed that sample 1 and 5 have

highest G' at rubbery plateau region, which means that they have the lowest Mc and the highest crosslink density. Out of the crosslinked samples, the ones containing CTA (samples 2, 3 and 4) have the lowest G' at the rubbery plateau region, which indicates that they have lower crosslink density. Additionally, crosslink density decreases with an increase in the CTA amount.

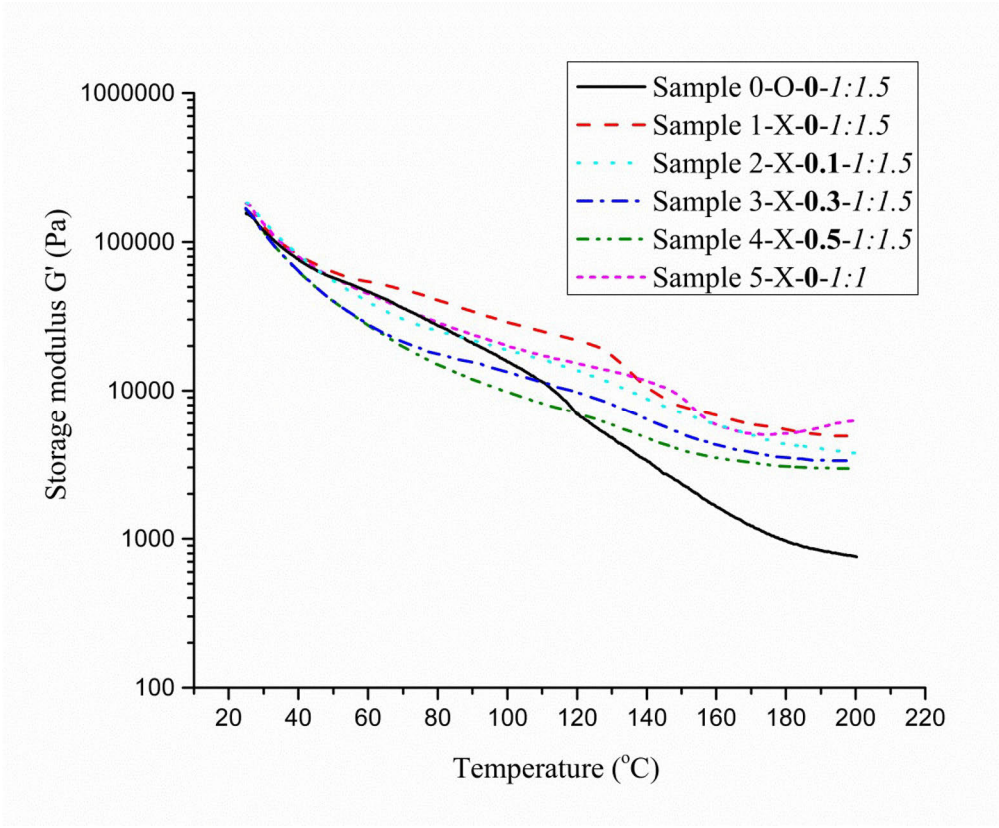

Figure 12 (a). G' versus temperature at a frequency of 10 rad/s.

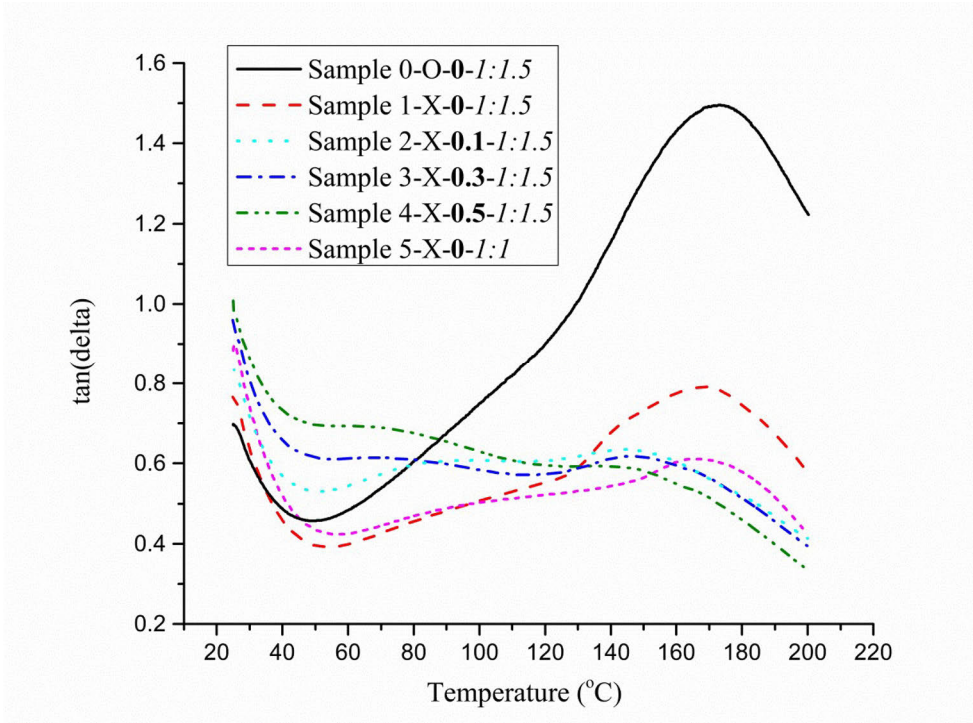

Figure 12 (b). Tan(delta) versus temperature at a frequency of 10 rad/s.

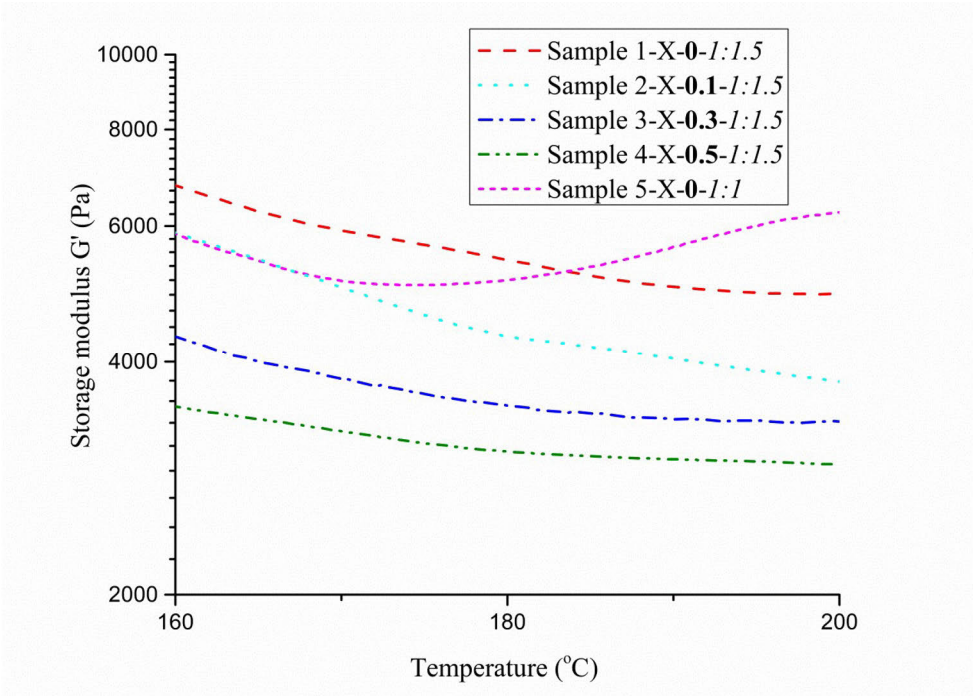

Figure 12 (c). G' versus temperature in the rubbery plateau region of all crosslinked samples.

5.1.5 Influence on adhesive properties

The results of mechanical strength measurements in terms of tack, peel and shear strength properties are graphically shown in Figure 13. In order to be qualified as high-performance construction adhesive, our target was to design an adhesive emulsion which simultaneously exceeds a Q-stick value of 5 N/25 mm, a T-peel value of 2 N and a shear resistance of 20000 min.

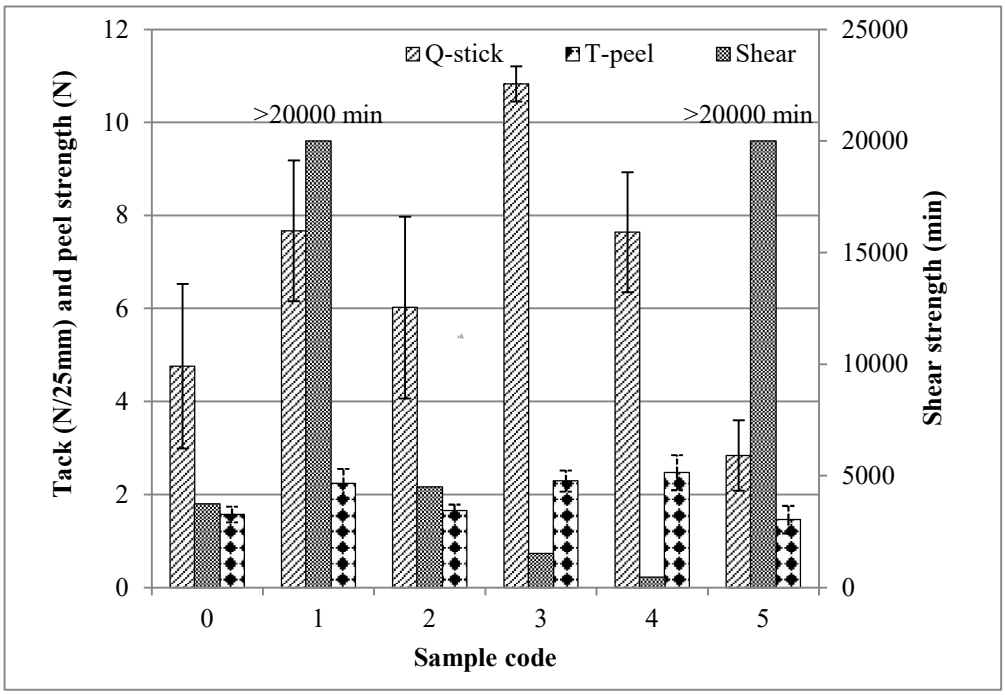

Figure 13. The mechanical strength results.

Tack

Tack refers to the ability of an adhesive to wet a surface and instantaneously bind to a substrate. The measurement (loop tack test) involves two stages: bonding and debonding. During debonding process, either adhesive or cohesive failure is expected to separate the adhesive from the substrate and the energy of debonding is utilized to evaluate the tack. (Aymonier A, 2003) The results of tack are expressed as Q-stick values and they are shown in Figure 13. Tack primarily depends on the deformability and flow ability of low T_g polymers as has been reported in the case of poly(butyl acrylate). As could be anticipated already based on fulfilling Dahlquist´s criterion (see DMA part), the obtained Q-stick values confirm the good level of tack of all samples. By comparison of samples 0 and 1, the crosslinker has no negative influence on the tack, because the crosslinked networks are encapsulated inside the core and therefore impart insignificant influence on the flow ability and deformability of the polymer particles. In other words, the tack performance mainly relates to the shell part. The addition of CTA in the shell gives rise to shorter polymer chains that promote

the deformability and flow ability, and thus higher Q-stick values were recorded for the samples 2, 3 and 4. Sample 5 with a higher ratio of core to shell (1:1) exhibited significantly reduced Q-stick value, which is reasonable as it contains lower amount of the shell copolymers in comparison to the other samples having a lower ratio of core to shell (1:1.5). In conclusion, small addition of CTA during the shell polymer synthesis can further help to improve tack. However, when optimizing tack via CTA addition one should also simultaneously consider its effect on the other factors such as peel and shear strength.

T-peel strength

Peel strength is a complex property that is influenced by several factors such as T_g, gel content and molecular weight. Similar with tack, T-peel strength is a reflection of the adhesive strength of a polymer material to a substrate surface and the testing involves bonding and debonding processes. (Roberge S, 2006) However, the main difference lies in the bonding process that the peel strength test features a much longer bonding time than tack test, which determines that the deformability and flow ability have a smaller influence on peel strength than on tack. (Qie L, The influence of butyl acrylate/methyl methacrylate/2-Hydroxyethyl methacrylate/acrylic acid latex properties on pressure sensitive Adhesive performance, 2010) Moreover, to some extent, peel strength increases with T_g and gel content, but peel strength will dramatically decreases when the gel content is very high (> 60 wt%). (Qie L, The influence of butyl acrylate/methyl methacrylate/2-Hydroxyethyl methacrylate/acrylic acid latex properties on pressure sensitive Adhesive performance, 2010) From Figure 13, it can be seen that there are no big differences in the peel strength values of different samples, but still some trends can be found. The crosslinked sample 1 possesses slightly higher peel strength than the non-crosslinked sample 0, because of its higher T_g and gel content. As it could be anticipated based on the former reasoning, the peel strength of sample 2 (lower T_g and gel content than sample 1) is lower than that of sample 1. However, it is interesting to notice that the peel strength increases with the CTA amount (compare samples 2, 3 and 4). The possible explanation is that an increasing amount of CTA significantly increases the deformability and flow ability of polymers, which counterbalances the slightly decreased gel content of samples 3 and 4. Not surprisingly, sample 5 exhibited the lowest peel strength among the samples, because of its high amount of hard core copolymer and very high gel content (> 60 wt%).

Shear strength

Shear strength is an evaluation of cohesive strength of a material. High shear strength is normally recorded for samples with high gel content and crosslink density, while high gel content simultaneously has a deleterious effect on tack and peel strength. (Qie L, The influence of butyl acrylate/methyl methacrylate/2-Hydroxyethyl methacrylate/acrylic acid latex properties on pressure sensitive Adhesive performance, 2010) In addition, shear strength, as the intrinsic or cohesive strength of the adhesive itself, increases as the amount of high T_g component increases. (Roberge S, 2006) When comparing the non-crosslinked

sample 0 with the crosslinked samples 1 and 5 (see Figure 13), it can be noticed that the crosslinked core dramatically enhanced the shear strength. It is worth mentioning that the measurement was ceased when the shear strength exceeded 20000 min, which means that the absolute values for samples 1 and 5 are higher than that. However, the samples with CTA exhibited considerably lower shear strengths than the other samples. This could not be ascribed simply to the decrease in gel content or crosslink density, as they were not low enough to trigger such a change. A speculative reason is related to the chemical heterogeneity of the polymer morphology, which was proposed in the work by A. Aymonier and coworkers. (Aymonier A, 2003) The crosslinking of core increases the difference between core and shell, which was already confirmed by detection of two T_gs (see DSC section). The incorporation of CTA in the shell further promotes the difference between the core and the shell morphology, leading to an adhesive film structure with the hard core domains distributed in the soft shell matrix. Consequently, the boundary between hard core and extremely soft shell readily undergoes cohesive failure, resulting in the low shear strength for the samples in which CTA was used. The shear strength results are in agreement with the temperature ramp measurements at low temperature range, i.e. samples with added CTA (sample 2, 3 and 4) exhibit low storage modulus and high tan (delta), which indicates poor cohesive strength. Crosslinked samples without CTA (sample 1 and 5) exhibit relatively high storage modulus and low tan (delta) at the same temperature range, which is associated with the good cohesive strength.

5.2 One-Component Moisture-Curable Polyurethane Adhesive

5.2.1 Characterization and Properties of Urethane Prepolymers

NMR

The chemical structure of urethane prepolymers was examined by NMR spectroscopy. The ^{1}H-NMR spectra of the blank sample UP**2**-*O*-***0*** and chain extended samples containing the same amount of chain extenders (0.74 molar ratio) are shown in Figure 14(a) and Figure 14(b), respectively. The proton chemical shifts for the blank sample and chain extended samples are additionally listed in Tables 12(a) and Table 12(b). (Šebenik & Krajnc, 2007; Pegoraro, Galbiati, & Ricca, 2003; Daniel da Silva, Martín-Martínez, & Bordado, 2006; Heintz, et al., Effects of reaction temperature on the formation of polyurethane prepolymer structures, 2003; Lapprand, Boisson, Delolme, Méchin, & Pascault, 2005)

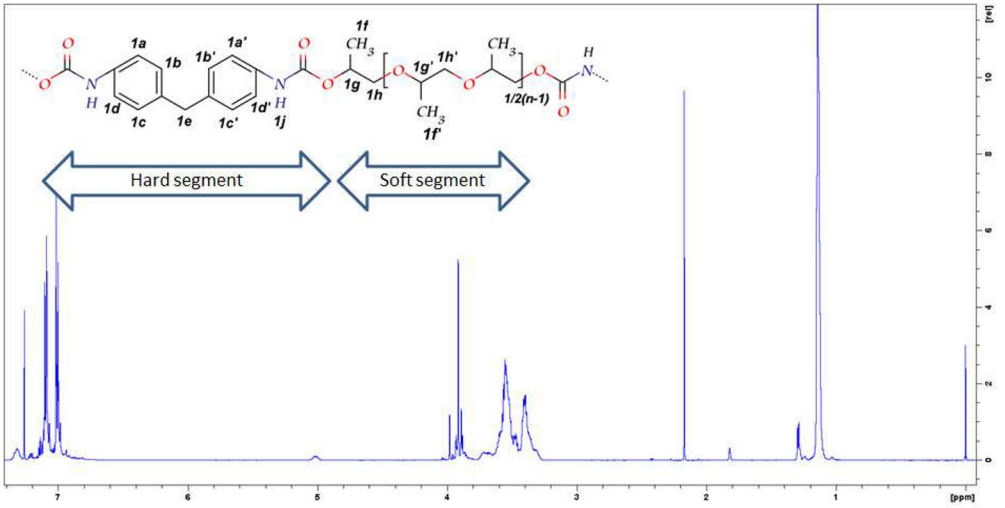

Figure 14(a). ^{1}H-NMR spectra of the blank sample UP**2**-*O*-***0***.

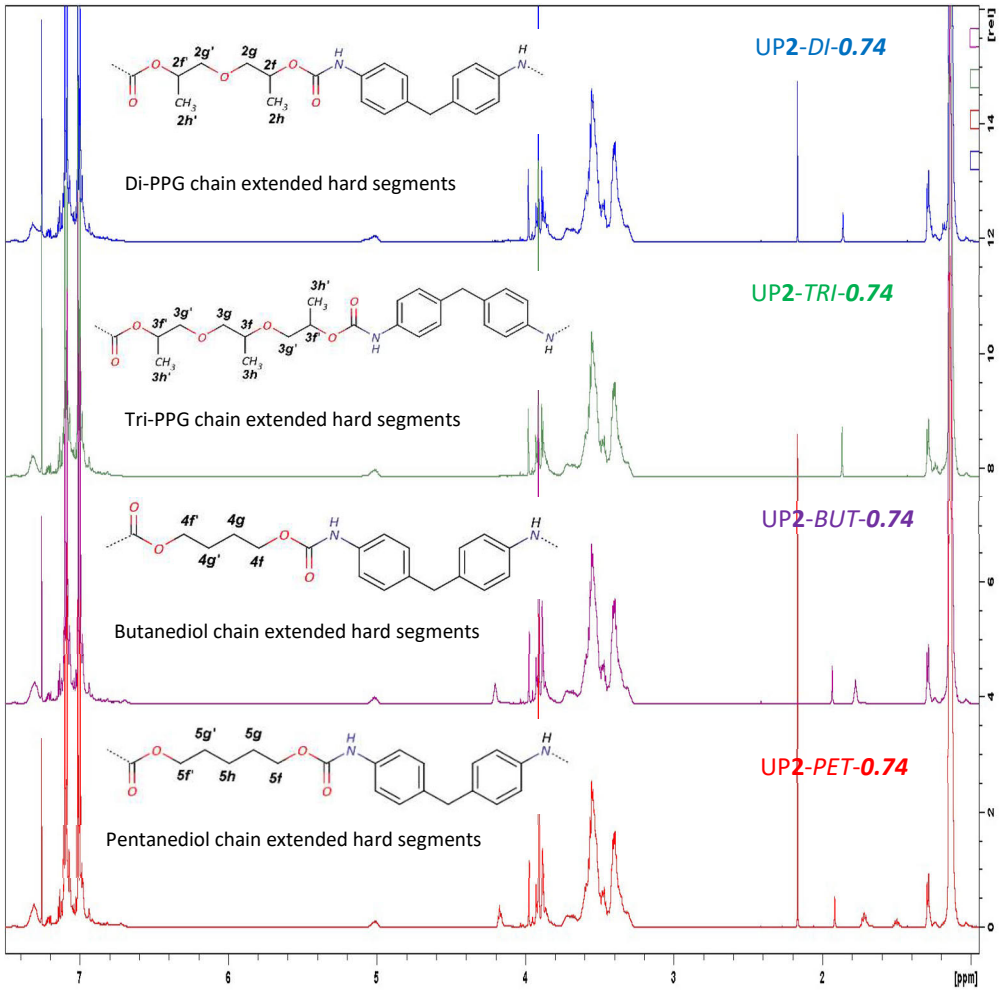

Figure 14(b). ^{1}H-NMR spectra of the chain extended samples UP**2**-*DI*-***0.74***, UP**2**-*TRI*-***0.74***, UP**2**-*PEN*-***0.74*** and UP**2**-*BUT*-***0.74***. The chemical structure for the chain extended hard segments is sketched in the figure.

Table 12(a). Proton chemical shifts for the blank sample UP**1**-*O*-***0***.

Segment	Assignment of protons	Shift (δ, ppm)
Hard	1a-1d and 1a'-1d'	6.9-7.1
	1e	3.9-4.0
	1j	7.3
Soft	1f'	1.1-1.2
	1f	1.3
	1g	5.0
	1g', 1h, 1h'	3.2-3.8

Table 12(b). Proton chemical shifts for the chain extended hard segments of samples UP**2**-*DI*-***0.74***, UP**2**-*TRI*-***0.74***, UP**2**-*PEN*-***0.74*** and UP**2**-*BUT*-***0.74.***

Sample code	Assignment of protons	Shift (δ, ppm)
UP**2**-*DI*-***0.74***	2h, 2h'	1.3
	2f, 2f'	5.0
	2g, 2g'	3.2-3.8
UP**2**-*TRI*-***0.74***	3h, 3h'	1.3
	3f'	5.0
	3f, 3g, 3g'	3.2-3.8
UP**2**-*BUT*-***0.74***	4f, 4f'	4.2
	4g, 4g'	1.8
UP**2**-*PEN*-***0.74***	5h	1.5
	5g, 5g'	1.7
	5f, 5f'	4.2

No significant differences between the ^{1}H NMR spectra of samples prepared by one or two stage processes could be observed (not shown here).

ATR-FTIR

ATR-FTIR is a powerful and convenient method to study polyurethanes. In this work, both intermediate and final polymers were analyzed by ATR-FTIR in order to monitor the reaction progress and to study the hydrogen bonding in the prepolymers. The ATR-FTIR spectrum of blank sample UP**2**-*O*-***0*** is shown in Figure 15 and the assignments of its characteristic peaks are given in Table 13. (Delpech & Miranda, 2011)

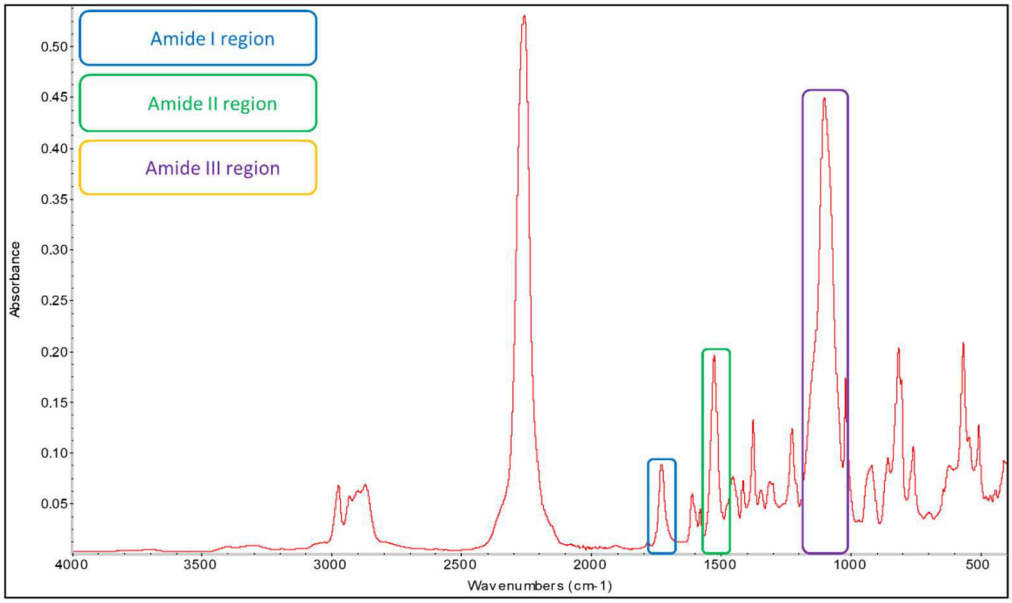

Figure 15. ATR-FTIR spectrum of blank sample UP**2**-*O*-***0***.

Table 13. ATR-FTIR characteristic peak assignments for UP**2**-*O*-***0***.

	Functional group	**Wavenumber /cm-1**
	pMDI N=C=O stretching	2270
	pMDI aromatic C=C stretching	1611, 1578
	Urethane prepolymer (UP)urethane N-H stretching	3200-3400
Amide-I region	UP urethane C=O stretching	1680-1760
Amide-II region	UP urethane N-H bending and C-N stretching	1524-1527
Amide-III region	UP urethane C-O stretching	1220-1222
	UP aromatic C=C stretching	1598
	PPG 2000 C-O-C stretching	1100
	PPG 2000 CH2 stretching vibration (symmetric and asymmetric)	2857-2940

Since the driving force for the formation of dual phase structure in polyurethanes is related to hydrogen bonding interactions within or between the HS and SS, the organization of urethane prepolymer chains and the extent of phase separation can be investigated through analyzing the patterns of hydrogen bonding interactions. Thus, the extent of hydrogen bonding with the carbonyl group can be correlated with a shift in its stretching signals as follows: non-hydrogen bonded carbonyl in free urethane group is assigned to 1730-1760 cm^{-1}; hydrogen bonded carbonyl group in disordered (amorphous) conformation is assigned to 1700-1730 cm^{-1}, which represents the hydrogen bonding between SS and HS; whereas hydrogen bonded carbonyl group in ordered (crystalline) conformation is assigned to 1680-1700 cm^{-1}, representing hydrogen bonding within HS. (Saralegi, et al., 2013; Ren & Frazier, 2013; He, Xie, & Zhang, 2014) Likewise, the free N-H stretching absorbance (non-hydrogen bonded) appeared at 3330 cm^{-1} and the hydrogen bonded N-H stretching absorbance band can be assigned to 3340 cm^{-1}. (Yoon & Han, 2000; He, Xie, & Zhang, 2014) As a consequence, the characteristic absorbance peaks at the wavenumber regions of 1760-1680 cm^{-1} and 3200-3400 cm^{-1} were chosen for the subsequent morphological studies of prepolymers by ATR-FTIR. (Chattopadhyay DK, 2005; Delpech & Miranda, 2011)

In addition, in order to study the effect of aging on formation of hydrogen bonding, ATR spectra were also recorded at different time periods within 1 month. It was found that most samples did not show significant changes in ATR-FTIR spectra upon aging, except for UP**1/2**-*PEN*-***0.74***, UP**1/2**-*PEN*-***0.94*** and UP**1/2**-*BUT*-***0.74***. All of the samples showed a shift of carbonyl peaks to lower wavenumbers with an increasing intensity of peaks at 1680-1700 cm^{-1} and 3300 cm^{-1} within 1-2 days after production, which is closely related to their tendency of forming hydrogen bonding interactions within HS. In particular, UP**1/2**-*BUT*-***0.74*** presented a strong shoulder peak at 1680-1700 cm^{-1} and sharp peak at 3300 cm-1 after 1 day of aging, which indicated a higher content of highly ordered structure via substantial hydrogen bonding interactions within hard segments. These changes are not only time dependent but also thermally reversible. A test was made with a 1 month old sample, i.e. UP**2**-*BUT*-***0.74*** was reheated to 70 °C, and then ATR-FTIR spectrum was immediately recorded (labeled as UP**2**-*BUT*-***0.74*** aged 70 °C). The ATR-FTIR spectra of UP**2**-*BUT*-***0.74*** at different stages (instant, aged and aged 70 °C) are compared in Figure 16, at carbonyl stretching absorbance ranging 1680-1760 cm^{-1} (left) and N-H absorbance ranging 3200-3450 cm^{-1} (right). It is clearly observed, that after the thermal treatment ATR-FTIR spectrum of UP**2**-*BUT*-***0.74*** aged 70 °C showed significantly decreased intensity of peaks at 1680-1700 cm^{-1} and 3300 cm^{-1}, which was almost identical to the initial UP**2**-*BUT*-***0.74*** spectra. This is because increasing temperature weakened hydrogen bonding within HS domains and instead improved phase mixing of HS and SS. (He, Xie, & Zhang, 2014; Yoon & Han, 2000)

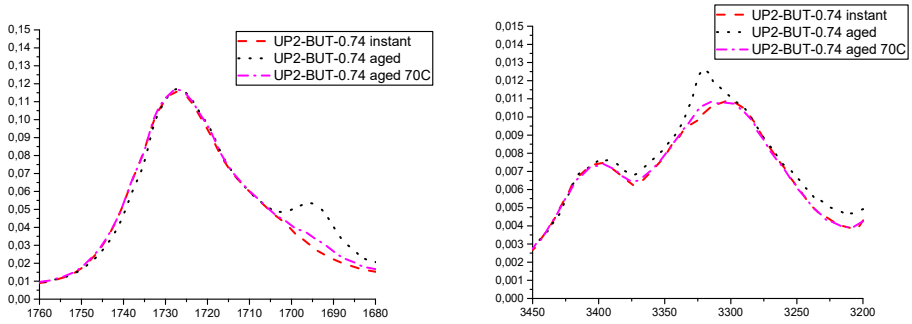

Figure 16. ATR-FTIR spectra at the carbonyl stretching absorbance region ranging from 1680–1760cm^{-1} (left) and N-H absorbance ranging from 3200–3450 cm^{-1} (right): UP**2**-*BUT*-***0.74*** instant was measured soon after production; UP**2**-*BUT*-***0.74*** aged was measured after 1 month; UP**2**-*BUT*-***0.74*** aged 70 °C was measured after UP**2**-*BUT*-***0.74*** aged was reheated to 70 °C.

Further ATR-FTIR spectra (carbonyl stretching absorbance ranging 1680–1760 cm^{-1} and N-H absorbance ranging 3200-3450 cm^{-1}) of 1 month aged samples are compared in Figure 17.

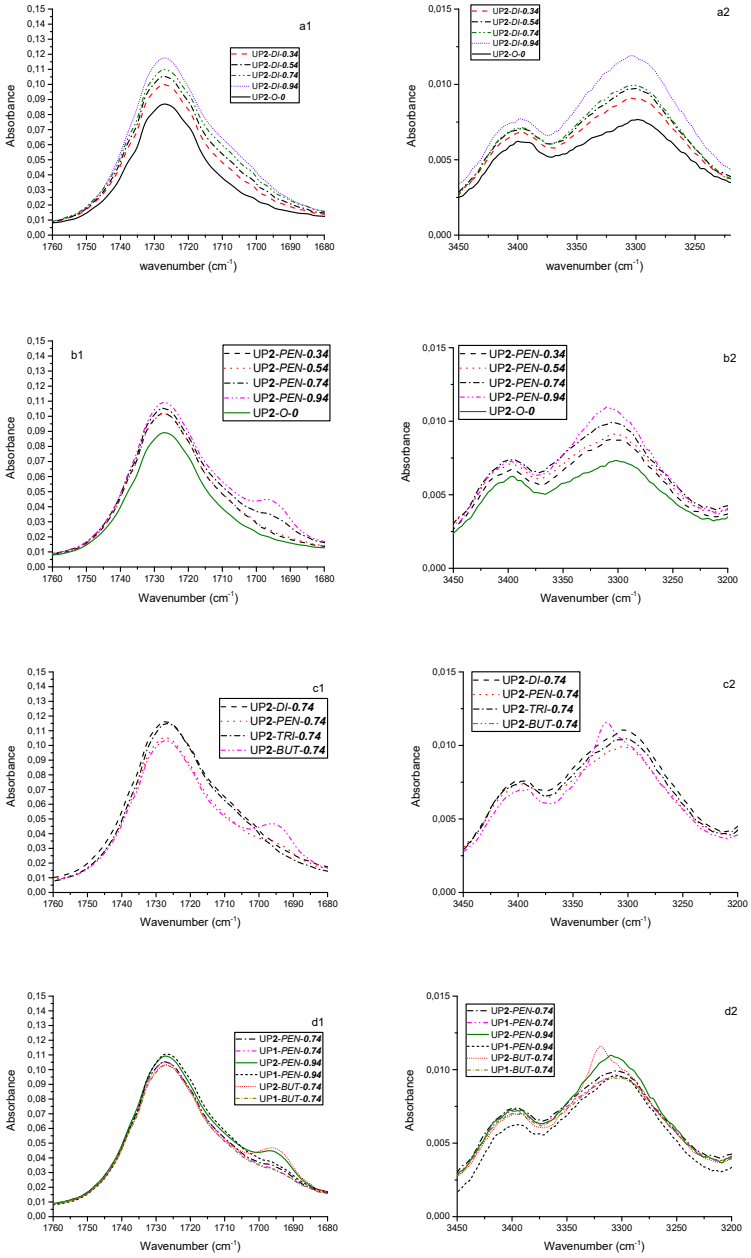

Figure 17. Comparison of ATR-FTIR spectra at the carbonyl stretching absorbance region ranging from 1680–1760cm^{-1} (left) and N-H absorbance region ranging from 3200–3450 cm^{-1} (right): (a1,a2) samples prepared by the two stage process with varying di-PPG amount compared with blank sample UP**1**-*O*-***0***; (b1,b2) samples prepared by the two stage process with varying pentanediol amount compared with blank sample UP**1**-*O*-***0***; (c1,c2) samples prepared by two stage process with 0.74 molar ratio of different chain extenders; (d1,d2) selected samples made by the two different synthesis processes.

In order to quantify the contributions of chain extenders, the intensity ratios of the peak at 3300 cm^{-1} (P3300 represents hydrogen bonded N-H) and the peak at 3400 cm^{-1} (P3400 represents free/non-hydrogen bonded N-H) were calculated and they are shown in Figure 18.

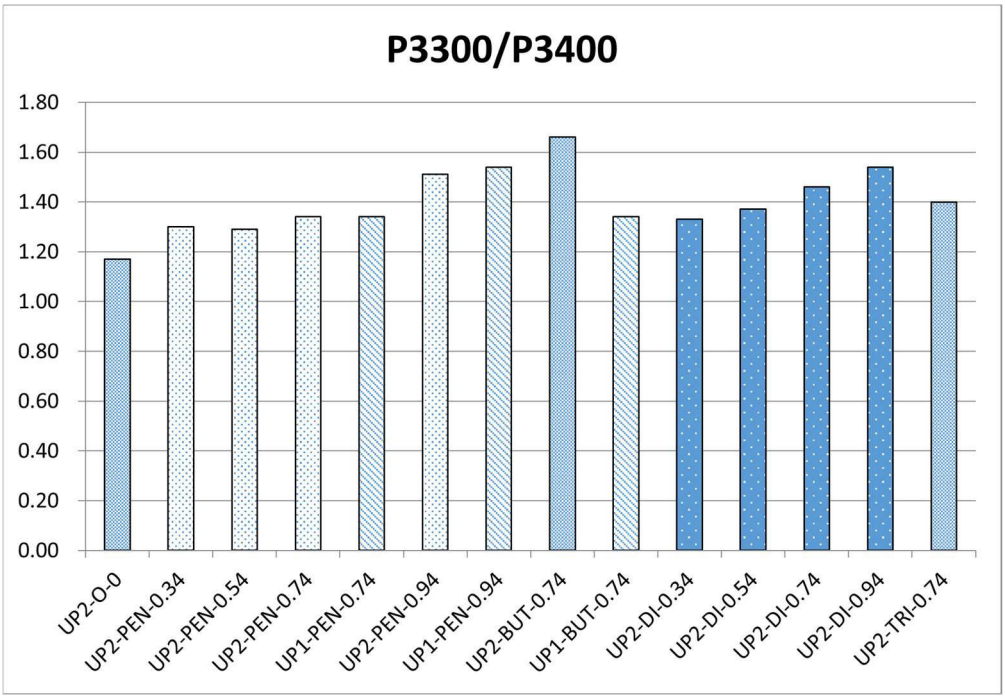

Figure 18. The intensity ratios of P3300 and P3400 of selected samples.

According to Figures 17(a1, a2) and 18, the intensity of peaks ranging between 1690–1720 cm^{-1} and the ratio of P3300/P3400 increased as di-PPG amount increased. Particularly, the major change in carbonyl stretching absorbance regions was observed at 1700–1720 cm^{-1}, which reveals that the majority of HSs has formed disordered (amorphous) hydrogen bonding with SSs. This is because the di-PPG contains branches that are capable of hindering the formation of highly ordered hydrogen bonding within HS. Furthermore, the structural similarity between branched chain extenders of di-PPG in HS with PPG 2000 in SS enables the formation of hydrogen bonding between HS and SS. (Saralegi, et al., 2013) Both could explain why di-PPG readily promotes the formation of hydrogen bonding interactions between HS and SS, and thus improves phase mixing between HSs and SSs.

As can be seen from Figure 18, the addition of pentanediol had generally a similar effect as di-PPG on hydrogen bond formation. The hydrogen bond formation was more pronounced at higher dosages of 0.74 and 0.94. However, it was observed that due to different type of hydrogen bonding interactions the absorbance peak patterns on carbonyl region (Figure 17(b1)) were different in pentanediol and di-PPG chain extended samples. At a low dosage of pentanediol (0.34 to 0.54 molar ratio), the overall extent and type of hydrogen bonding were

almost the same (Figure 18) as in the case of di-PPG, where hydrogen bonding was primarily formed between HSs and SSs (Figure 17(b1)). Whereas, at a high dosage of pentanediol (0.74 to 0.94), a shoulder peak corresponding to hydrogen bonded carbonyl absorbance in ordered conformation (crystalline) gradually appeared at 1680–1700 cm^{-1} and increased as a function of pentanediol amount, which reveals that the HSs associated into hard domains via hydrogen bonding interactions.

The influence of chain extender structure on the formation of hydrogen bonding was investigated by comparing samples containing different chain extenders in a molar ratio of 0.74, as shown in Figures 17(c1, c2) and 18. In general, the overall hydrogen bond formation was similar for all of these samples, except for UP**2**-*BUT*-***0.74*** which showed a sharp peak shift to higher wavenumber (~3320 cm^{-1}) and an extremely high ratio of P3300/P3400. According to Figure 17(c1), UP**2**-*DI*-***0.74*** and UP**2**-*TRI*-***0.74*** have tendency to disordered hydrogen bonding interactions (1700-1720 cm^{-1}), whereas UP**2**-*PEN*-***0.74*** and UP**2**-*BUT*-***0.74*** exhibit more pronounced highly ordered hydrogen bonding interactions, as evidenced by the appearance of shoulder peaks at 1680-1700 cm^{-1}. This peak is most intensive for the sample UP**2**-*BUT*-***0.74***. Combined with the findings in the N-H stretching absorbance region (Figures 17(c2) and 18), UP**2**-*BUT*-***0.74*** contained substantial amount of highly ordered hydrogen bonded structure. It has been earlier reported that linear chain extenders with even number of CH_2 (like butandiol) readily promote HS association into hard domains via hydrogen bonding and hence enhance phase separation in comparison to the one with odd number of CH_2 (e.g. pentanediol). (Corcuera, et al., 2010; He, Xie, & Zhang, 2014)

The synthesis process has more influence on those samples, that also otherwise tend to phase separate easily (UP**1/2**-*PEN*-***0.74***, UP**1/2**-*PEN*-***0.94*** and UP**1/2**-*BUT*-***0.74***). Thus, ATR spectra of these samples were compared in Figures 17(d1), (d2) and 18. Based on Figure 18, butanediol chain extended samples UP**1/2**-*BUT*-***0.74*** were the most susceptible to the influence of synthesis process, the one-shot sample being much less hydrogen bonded than the two-stage sample. Figure 17(d1) gives additional support that both UP**1**-*BUT*-***0.74*** and UP**1**-*PEN*-***0.94*** (one-shot) showed less pronounced shoulder peak compared to their counterparts (two-stage), revealing that they have greater phase mixing between HS and SS. This finding confirms the statement that one-shot process produces a urethane prepolymer with more randomly distributed polymer chains and more dispersed HSs that eventually enhance phase mixing between HS and SS. (Lee, Tsai, Tsai, & Chen, 2007; He, Xie, & Zhang, 2014)

Appearance

The appearance of urethane prepolymers in terms of colour, transparency and viscosity can be correlated with the architecture and morphology of the prepolymers. For instance, phase separation can render light scattering and thereby the miscibility between SSs and HSs can have influence on the transparency. The viscosity was measured by a Brookfield viscometer and the results are shown in Table 14. (Lee, Tsai, Tsai, & Chen, 2007)

The blank samples PU**1/2**-*O*-***0*** containing no chain extenders were clear, brownish liquids and least viscous (Table 14), and the appearance did not change during storage. The brownish colour was attributed to the effect of pMDI. When chain extenders were added, the viscosity of urethane prepolymers dramatically increased as the amount of chain extender increased, because the increasing hard segments intermolecularly associate via hydrogen bonding and form physical cross-linking that restricts the mobility of soft segments and results in a decreased miscibility between HS and SS. (Clauß, et al., 2011; Ren & Frazier, 2013)

The type and amount of chain extenders had a significant influence on the appearance of samples. The appearance of two-stage prepared urethane prepolymers are shown in Figure 19. Similarly, as blank samples, di-PPG chain extended urethane prepolymers were brownish and transparent (see Figure 19(a)). As the di-PPG amount increased, the colour of urethane prepolymers became deeper and the viscosity increased. The increased viscosity was attributed to increasing pMDI addition and HS content. On the contrary, urethane prepolymers containing linear chain extenders (butanediol and pentanediol) showed quite different behavior. As can be seen in Figure 19(b), pentanediol chain extended urethane prepolymers showed a tendency towards lighter colours, increasing non-translucent appearance (invisible marks) and viscosity as pentanediol amount increased. In particular, UP**1/2**-*BUT*-***0.74*** presented completely opaque, yellow and waxy behavior (not flowing) (Figure 19(c)). These findings are consistent with the ATR-FTIR results: the incorporation of di-PPG and tri-PPG greatly contributed to phase mixing between HS and SS. In contrast, the incorporation of pentanediol and butanediol readily promoted the immiscibility between HS and SS, whereupon at higher chain extender ratios (≥ 0.74) prepolymers exhibited opaque yellow appearance and extremely high viscosities. According to the viscosity results in Table 13, it is generally noticed that the effect of synthesis processes is more clear for the samples with high amount of chain extenders (molar ratio no less than 0.74). Most samples prepared via the one-stage process had lower viscosity than their two-stage counterparts due to their less pronounced phase separation.

Figure 19. The appearance of samples made in two-stage: (a) di-PPG chain extended samples compared with the blank sample UP**1**-*O*-***0***; (b) pentanediol chain extended samples compared with the blank sample UP**1**-*O*-***0***; (c) samples with 0.74 molar ratio of different chain extenders.

DSC

Table 14 The DSC result and viscosity of urethane prepolymers

Sample (UPX -*CE-Y*) *	DSC results			Viscosity
	Tg_1 of 1st heating	Tm of 1st heating	Melting enthalpy	
UP1-*O-0*	-48,58	--	--	3640
UP2-*O-0*	-50,01	--	--	3640
UP1-*DI-0.34*	-45,98	--	--	6500
UP2-*DI-0.34*	-46,27	--	--	6060
UP1-*DI-0.54*	-44,68	--	--	6150
UP2-*DI-0.54*	-43,67	--	--	7740
UP1-*DI-0.74*	-43,82	--	--	8600
UP2-*DI-0.74*	-42.93	--	--	11080
UP1-*DI-0.94*	-39,63	--	--	22400
UP2-*DI-0.94*	-39,05	--	--	12000
UP1-*PEN-0.34*	-48,15	--	--	6920
UP2-*PEN-0.34*	-47.43	--	--	5100
UP1-*PEN-0.54*	-44,83	--	--	9220
UP2-*PEN-0.54*	-44.54	--	--	6820
UP1-*PEN-0.74*	-43,10	59,98	2,176	17500
UP2-*PEN-0.74*	-45,41	53,25	1,688	45600
UP1-*PEN-0.94*	-43,82	58,28	2,138	50880
UP2-*PEN-0.94*	-42.52	56,52	2,304	52600
UP1-*TRI-0.74*	-38,91	--	--	9950
UP2-*TRI-0.74*	-40.35	--	--	9600
UP1-*BUT-0.74*	-43,10	83,58	3,016	36200
UP2-*BUT-0.74*	-43.53	81,41	3,229	44000

* **X**: synthesis processes: 1- one-shot process, 2- two-stage process; *CE*: chain extender: *DI* -di-PPG, *TRI* -tri-PPG, *PEN* - pentanediol, *BUT* - butanediol; ***Y***: the molar ratio of chain extender to PPG 2000.

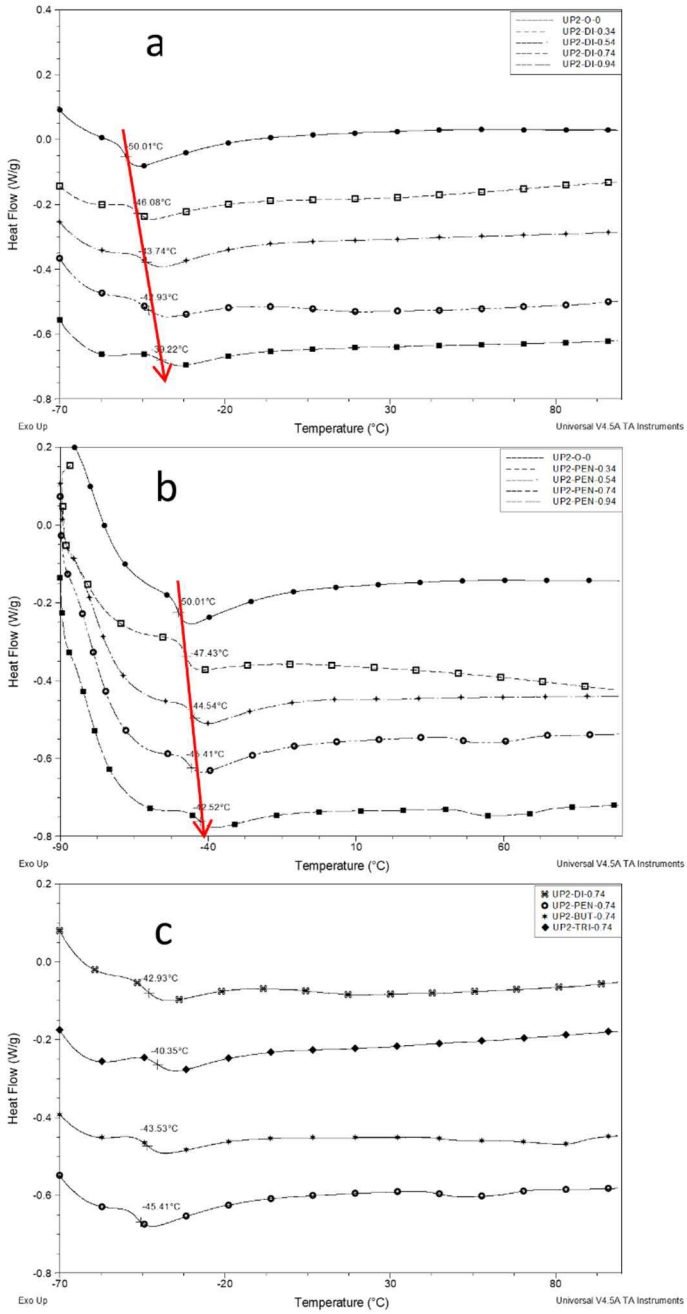

Figure 20. DSC thermograms: (a) two-stage samples with varying di-PPG amount compared with blank sample UP**2**-*O*-; (b) two-stage samples with varying pentanediol amount compared with blank sample UP**2**-*O*-***0***; (c) two-stage made samples of 0.74 molar ratio of different chain extenders.

The DSC thermograms of different urethane prepolymers are presented in Figure 20. The thermal transitions of all the urethane prepolymers are presented in Table 14. Since the chemical composition of SS is kept constant in all samples, the changes in thermal transitions of urethane prepolymers are closely linked to the HS chain length and the degree of phase separation (miscibility of HS and SS).

The transparent samples (UP**1/2**-*O*-***0***, di-PPG series (UP**1/2**-*DI*-***0.34-0.94***), UP**1/2**-*TRI*-***0.74*** and UP**1/2**-*PEN*-***0.34***/***0.54***) showed only one distinct Tg that is higher than that of neat PPG 2000 (-70°C), indicating extensive phase mixing of HS and SS. Tg of urethane prepolymers are primarily determined by the SS derived from long chain polyol, especially for the ones with low HS content. For instance, blank samples UP**1/2**-*O*-***0*** have the lowest and narrowest Tg. The chain extended urethane prepolymers follow the expected trend that Tg increases and becomes broader as chain extender amount increases (Figures 20(a) and (b)), due to greater interactions of increasing HSs that limit the movements of SSs.

The translucent and opaque samples UP**1/2**-*PEN*-***0.74***/***0.94*** and UP**1/2**-*BUT*-***0.74*** exhibited both Tg and a melting peak within the analyzed temperature range, which further indicated a greater phase separation. The Tgs were mainly attributed to a phase of mixed HS and SS, while the melting peak derived from highly ordered hard domains. By comparing UP**1/2**-*PEN*-***0.74*** and UP**1/2**-*PEN*-***0.94***, it was generally noticed that Tg, Tm and enthalpy all slightly increased as pentandiol amount increased, indicating that the increasing formation of HS contributes to both disordered and highly ordered structure. UP**1/2**-*BUT*-***0.74*** showed highest Tm and enthalpy, which confirmed that they have the most highly organized structure among these samples. These findings are in accordance with the previous results. The influence of synthesis processes is not clearly detected in the Tg results ($\Delta Tg \leq \pm 2°C$).

SEC

Molecular weight measurement helps to gain an insight into the formation of urethane polymer chains and particularly whether the chain extenders has been incorporated via reacting with the isocyanate terminals of the urethane polymer chains or with the free pMDI.

SEC chromatograms of the two-stage samples are shown in Figure 21. SEC curves of chain extended samples showed overlapping peaks in a range of elution times from 21 to 29 min. The five peaks denoted P1-P5 had manly the following consistency: the peak P5 at the longest elution time (27 min) corresponded to the unreacted pMDI; the peaks P3 and P4 appearing at ca. 25.4 and 26 min have been assigned to the hard segments consisting of pMDI reacted with chain extenders. Whereas, the major peak P2 at 23 min and the peak P1 at ca. 21.9 min represented the NCO-terminated urethane polymers.

Molecular weights of the prepolymers were calculated from the combined peaks of P1 and P2. The obtained values for Mn, Mw and Mw/Mn are summarized in Table 15. The molecular weight and its distribution slightly increased as the chain extender amount increased. This trend is more evident for the samples with pentanediol than for the samples with di-PPG. As can be seen from the Figure 21, the chain extender mainly affected the low molecular weight part of

the SEC chromatogram (elution time 25.4–26 min). The intensity of peaks P3 and P4 steadily grow as the chain extender amount increases.

The ratio of peak intensities was compared in Figure 22. Firstly, the majority of chain extenders contributed to P3 and the relative intensity of P3 increased with the chain extender amount, as chain extenders readily reacted to low molecular weight fractions like free pMDI. A minority of chain extenders contributed to P1 and P2 by reacting with the isocyanate terminals of polyurethane.

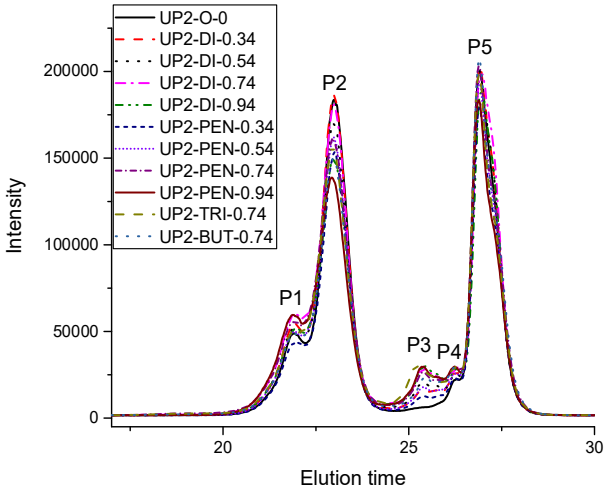

Figure 21. SEC chromatograms of the samples made via the two-stage process.

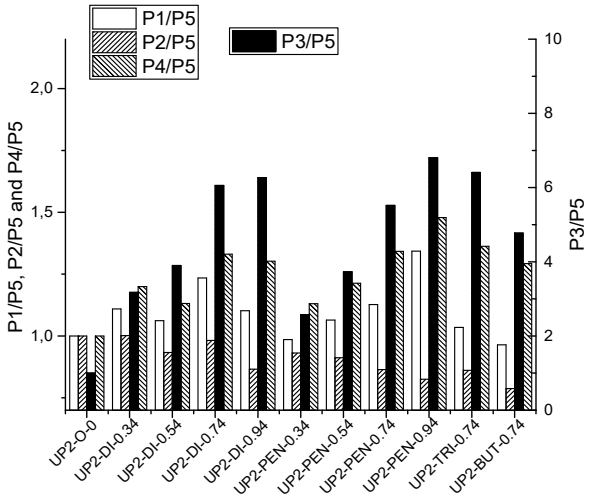

Figure 22. The relative intensities of peaks P1/P5, P2/P5, P3/P5 and P4/P5 compared to the blank sample UP**2**-*O*-***0***.

Table 15 The integrated molecular weight and distribution for P1 and P2.

Sample (UPX -*CE-Y*)*	Total average of P1 and P2		
	Mn	Mw	Mw/Mn
UP2-*O-0*	4329	5247	1.21
UP2-*DI-0.34*	4436	5450	1.23
UP2-*DI-0.54*	4508	5567	1.24
UP2-*DI-0.74*	4565	5712	1.25
UP2-*DI-0.94*	4538	5634	1.24
UP2-*PEN-0.34*	4377	5326	1.22
UP2-*PEN-0.54*	4481	5599	1.25
UP2-*PEN-0.74*	4540	5745	1.27
UP2-*PEN-0.94*	4763	6091	1.28
UP2-*TRI-0.74*	4483	5586	1.25
UP2-*BUT-0.74*	4458	5497	1.23

* **X**: synthesis processes: 2- two-stage process; *CE*: chain extender: *DI* -di-PPG, *TRI* - tri-PPG, *PEN* - pentanediol, *BUT* - butanediol; ***Y***: the molar ratio of chain extender to PPG 2000.

5.2.2 Properties of Cured Polyurethane-Urea Films

Bond strength

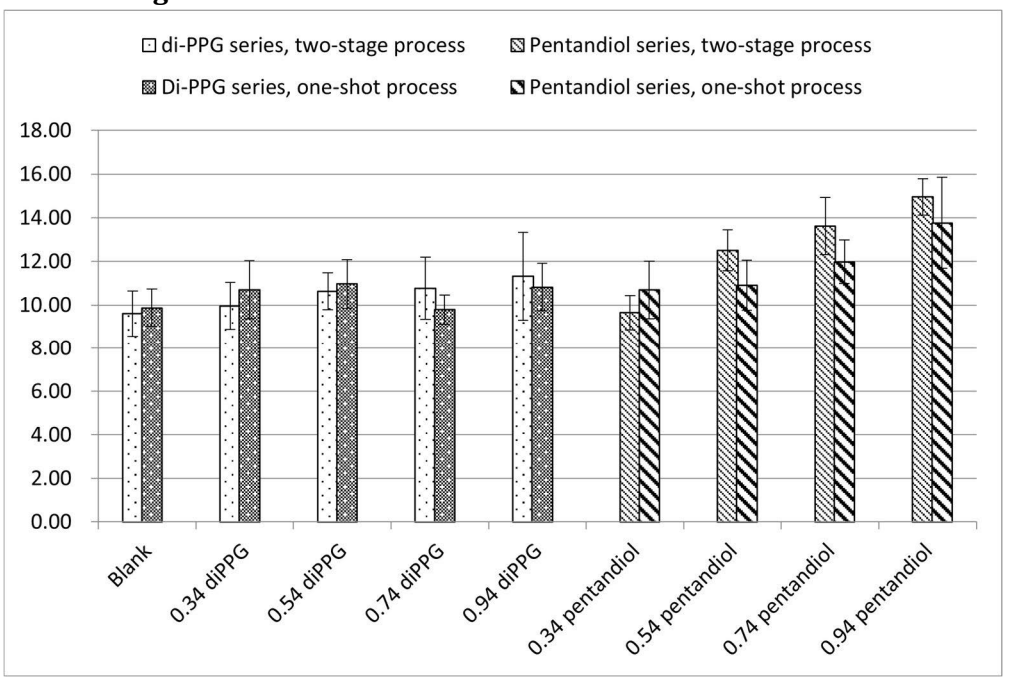

Figure 23(a). The bond strength of cured samples containing different amounts of di-PPG and pentanediol, prepared both by one-shot and two-stage process.

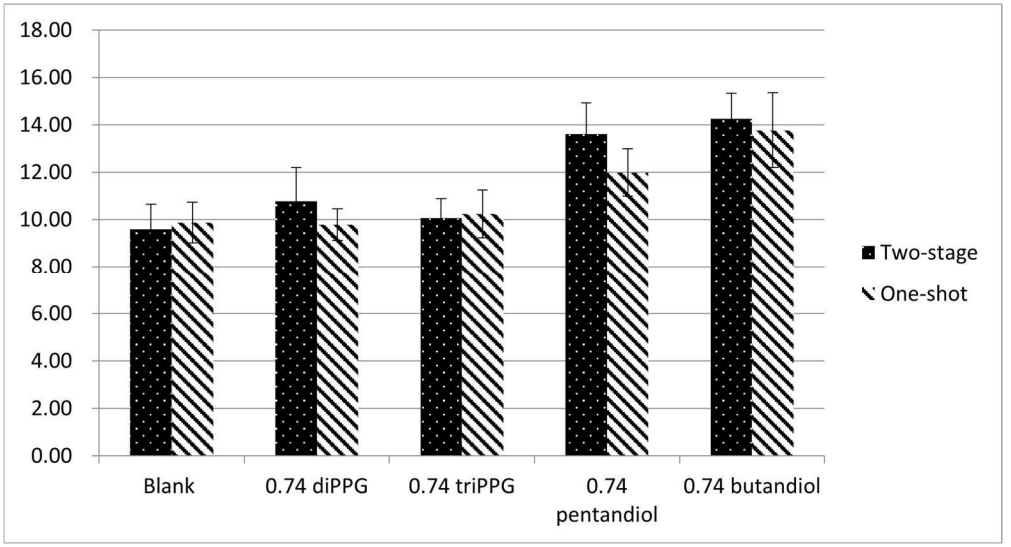

Figure 23(b). The bond strength of cured samples with 0.74 molar ratio of different chain extenders, prepared in one-shot and two-stage processes.

Figure 23(a) shows the bond strength results of cured samples containing different amounts of di-PPG and pentanediol, prepared according to the one-shot and two-stage processes. The trend was clearly towards higher bond strengths with the increasing amounts of chain extender. As the amount of free NCO is constant, the increase in bond strength is only attributed to increasing HS content and hydrogen bonding interactions. This trend is more obvious for the cured samples containing pentanediol, as pentanediol chain extended samples readily form highly ordered physically crosslinked regions within HS that reinforce the material. The cured samples prepared by two-stage process showed higher strength than their one-shot counterparts.

Figure 23(b) exhibits the influence of different chain extenders on bond strength of the cured samples at a constant molar ratio of 0.74. Not surprisingly, the cured samples containing butanediol or pentanediol exhibited the highest bond strength, due to strong hydrogen bonding interactions and a higher extent of phase separation. However, as these prepolymers also show high viscosities and turn wax-like after a couple of days of storage, they do not fulfill the initial goal of high strength combined with industrially acceptable flow properties. In case of tri-PPG and di-PPG, in turn, the enhancement in strength is relatively low compared to the blank sample.

Finally, in this series of samples the optimal combination of properties was achieved using pentanediol chain extender at a molar ratio of 0.54. For the UP**2**-*PEN*-***0.54***, over 12 MPa's lap shear strength accompanied by low viscosity was obtained (Table 14). Clearly enhanced lap shear strength was also reached using di-PPG at a CE molar ratio of 0.94.

5.3 Silane-Terminated Polyurethane Adhesives

5.3.1. NMR

NMR is a sensitive and powerful tool to study the chemical structure of SPUR prepolymers and the reactivity of primary and secondary isocyanates in IPDI, as well as to predict number-average molecular weight of SPUR prepolymers. (Nomura, Sato, Sato, Mori, & Endo, 2007; Prabhakar, Chattopadhyay, Jagadeesh, & Raju, 2005; Sardon, Irusta, & Fernández-Berridi, Synthesis of isophorone diisocyanate (IPDI) based waterborne polyurethanes: Comparison between zirconium and tin catalysts in the polymerization process, 2009)

As an example, the ^{1}H and ^{13}C NMR spectra of SPUR 6 are shown in Figures 24 and 25. The assignments of its characteristic resonance signals were based on the 2D-specta of proton-proton correlation (^{1}H-^{1}H COSY) and proton-carbon single and multiple bond correlation (^{1}H-^{13}C HSQC and HMBC). The protons of α-methylenes next to alkoxysilanes (H21) show a resonance signal at around 0.5-0.6 ppm, except for SPUR 10 (S5), which have a higher chemical shift of around 2.5 ppm due to the effect of nearby nitrogen atom. The methine (H1') of PPG close to urethane shows a characteristic chemical shift at 4.9 ppm, which was used for the estimation of number-average molecular weight (M_n) of SPUR prepolymers. M_n calculation was accomplished by calibrating the integral of H21 to be 4, which

refers to a SPUR prepolymer chain with two alkoxysilane terminals. Thus, the integral of H1' indicates the amount of urethane units in a SPUR prepolymer chain. By this way, it was deduced that there are in average 5.0 urethane units per chain in SPUR 1 (1.5:1), 1.2 urethane units in SPUR 2 (2:1) and 0.6 urethane units in SPUR 3 (2.8:1). The polymer chain length increases as the NCO/OH decreases, which is in accordance with the previous findings. (Ionescu, 2005)

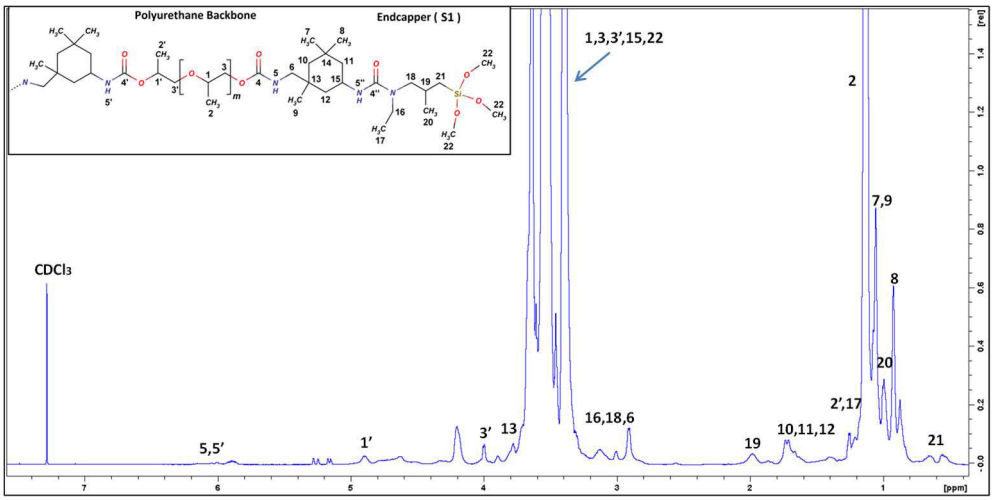

Figure 24. ^{1}H-NMR spectrum of SPUR 6.

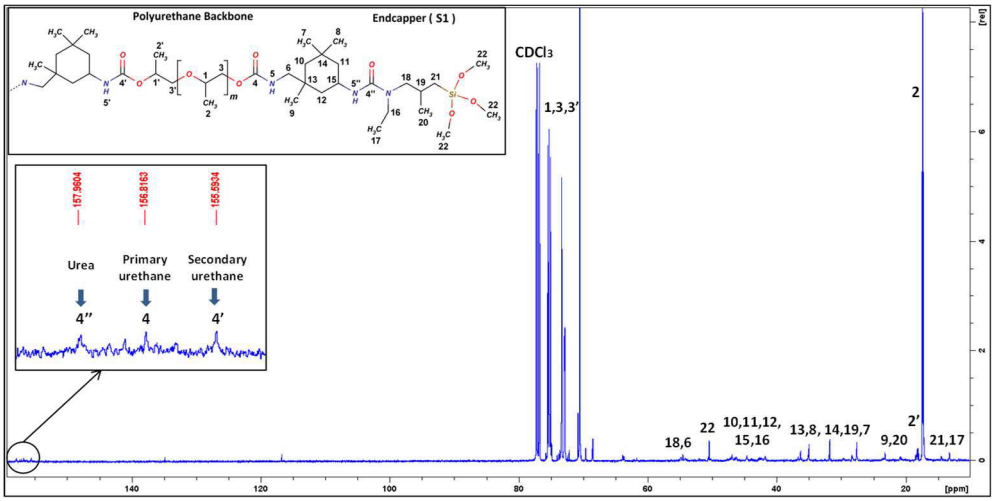

Figure 25. ^{13}C-NMR spectrum of SPUR 6.

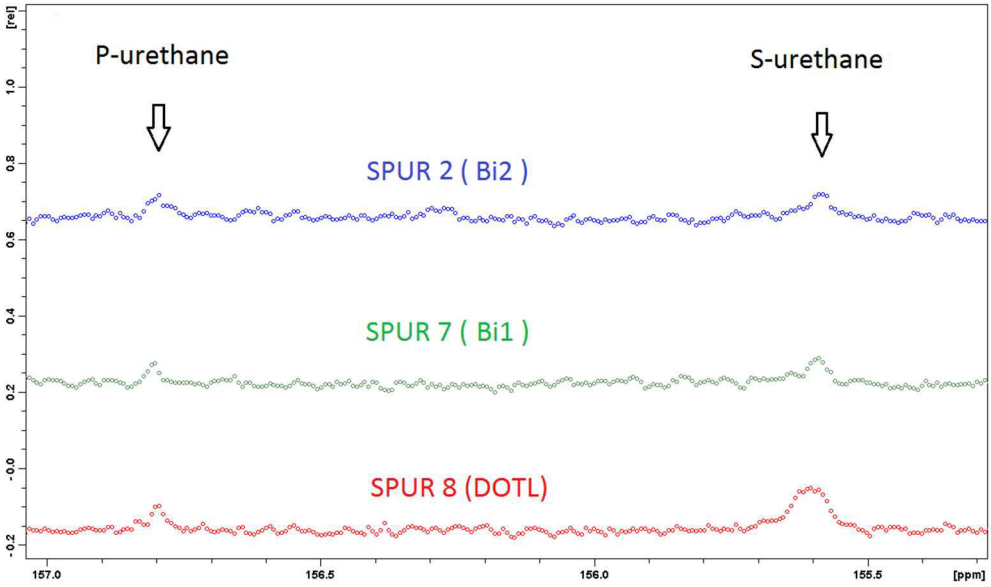

Figure 26. The expanded ^{13}C-NMR spectra (155-157 ppm) for samples with different catalysts.

IPDI is an asymmetric cycloaliphatic diisocyanate, containing primary isocyanate (p-NCO) (bonded through a primary carbon) and secondary isocyanate (s-NCO) (bonded directly to the cycloaliphatic ring) which may exhibit different reactivity towards active hydrogen compounds. Reactivity differences in the presence of catalysts can be studied by investigating the carbon resonances in the urethane region from 155 to 157 ppm, as the primary urethane (P-UR) and secondary urethane (S-UR) have clearly different resonance frequencies in the ^{13}C-NMR spectroscopy. (Sardon, Irusta, González, & Fernández-Berridi, 2013; Prabhakar, Chattopadhyay, Jagadeesh, & Raju, 2005; Sardon, Irusta, & Fernández-Berridi, Synthesis of isophorone diisocyanate (IPDI) based waterborne polyurethanes: Comparison between zirconium and tin catalysts in the polymerization process, 2009) The two peaks at 155.6 and 156.8 ppm in Figures 25 and 26 were assigned to the carbonyls in S-UR and P-UR, respectively. SPUR 8 catalyzed by DOTL has higher relative peak intensity at S-UR (155.6 ppm) than the one at P-UR (156.8 ppm), which indicates that DOTL is more selective towards the secondary isocyanate. In comparison, the samples with bismuth catalysts show similar relative intensities of peaks at the S-UR and P-UR regions.

5.3.2 ATR-FTIR characterization

ATR-FTIR measurements were used to monitor the progress of synthetic reactions and to characterize the structure of SPUR prepolymers as well as curing of SPUR films. (Huber, Kelch, & Berke, 2016; Gurunathan & Chung, 2016; Allauddin, Narayan, & Raju, 2013; Sardon, Irusta, Fernández-Berridi, Lansalot, & Bourgeat-Lami, Synthesis of room temperature self-curable waterborne hybrid

polyurethanes functionalized with (3-aminopropyl)triethoxysilane (APTES), 2010) In particular, it provides a convenient and effective way to characterize the organization and association of polymer chains, in terms of the types and extent of hydrogen bonding interactions. Meanwhile, the catalyst activity and silane reactivity can be evaluated. In addition, the relative reactivity of the primary isocyanate (p-NCO) and secondary isocyanate (s-NCO) in IPDI for different catalysts can be studied. (Sardon, Irusta, & Fernández-Berridi, Synthesis of isophorone diisocyanate (IPDI) based waterborne polyurethanes: Comparison between zirconium and tin catalysts in the polymerization process, 2009)

Reaction progress

The ATR-FTIR spectra of SPUR 8 taken at different reaction stages are compared in Figure 27. The characteristic functional groups are assigned in Table 16. During the 1st stage reaction between PPG (OH) and IPDI (NCO), the intensity of the NCO absorbance peak at 2260 cm^{-1} decreased and the intensity of the absorbance peak of carboxyl in the urethane linkage at 1750-1700 cm^{-1} increased. No changes of these peak ratios marked the end of the 1st stage reaction. In the 2nd stage, the reaction between secondary aminosilane and isocyanate end groups resulted in new absorbance peaks at 1680-1600 cm^{-1} (carboxyl in urea linkages) and 817-774 cm^{-1} (methoxysilane Si-OMe). The intensity of NCO absorbance peak continuously decreased as the 2nd stage reaction proceeded. The disappearance of NCO absorbance peak indicated the end of the 2nd stage reaction.

Table 16. The assignments of functional groups of SPUR 8.

	Functional groups	Wavenumber (cm^{-1})
	Urethane N-H stretching	3300-3400
Amide I	Urethane C=O	1750-1700
	Urea C=O	1680-1600
Amide II	N–H in-plane bending, C–N stretching	1500-1600
Amide III	C–N stretching, N-H bending	1200-1400
	PPG C-O-C	1100
	Si-OMe rocking	1194
	Si-OMe	2840, 1085, 863, 817, 774

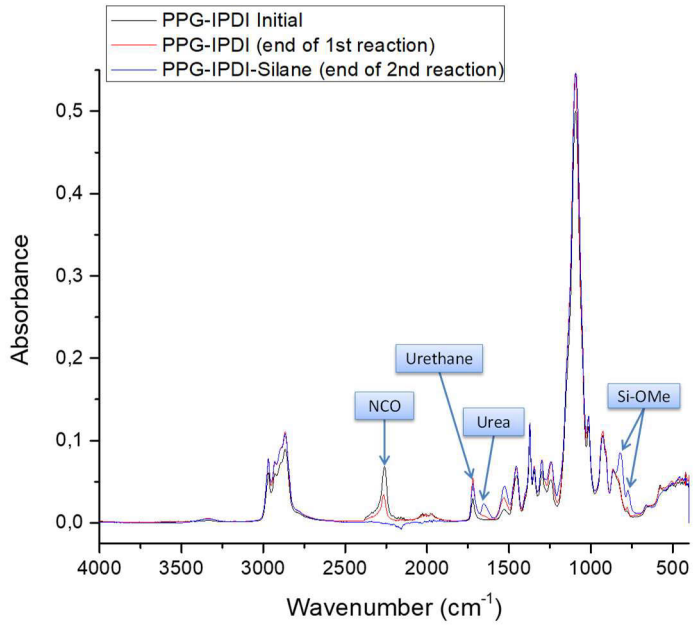

Figure 27. The comparison of ATR-FTIR spectra of SPUR 8 taken at different reaction stages.

The progress of curing

The ATR-FTIR spectra of SPUR 8 before and after cure are compared in Figure 28. The curing process results in decreased intensities of Si-OMe absorbance peaks, which are clearly observed at 774 and 817 cm^{-1}, and the appearance of siloxane Si-O-Si absorbance peaks (single siloxane bond at 1040-1060 cm^{-1} and multiple siloxane bonds at 1120-1140 cm^{-1}). (He, Xie, & Zhang, 2014; Gurunathan & Chung, 2016; Sardon, Irusta, Fernández-Berridi, Lansalot, & Bourgeat-Lami, Synthesis of room temperature self-curable waterborne hybrid polyurethanes functionalized with (3-aminopropyl)triethoxysilane (APTES), 2010) However, the siloxane absorbance peaks are barely noticed, as they overlap with strong signals of C-O-C in polyurethane backbone at 1100 cm^{-1}. Another significant finding is that the absorbance peak of carboxyl in urea linkages (1680-1600 cm^{-1}) shifts to a lower wavenumber upon curing, which indicates that, irrespective of the crosslinking reactions, the hydrogen bonding ability of urea linkages increases upon siloxane formation.

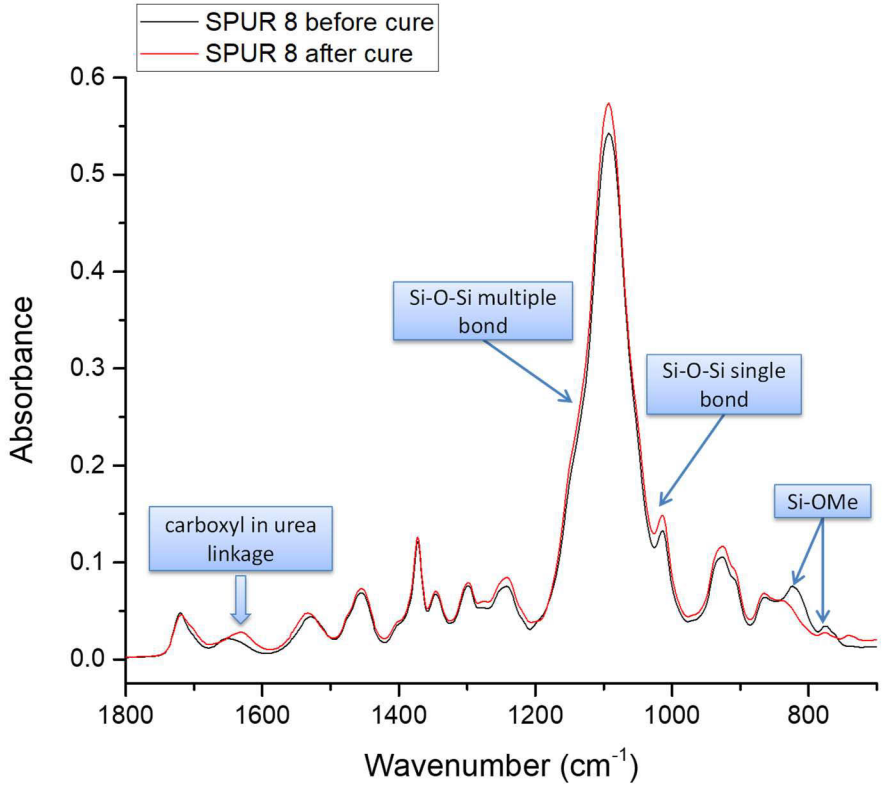

Figure 28. The comparison of ATR-FTIR spectra of SPUR 8 before and after cure.

The reactivities of NCOs in IPDI

The effect of catalyst on the reactivity of isocyanates in IPDI can be investigated using FTIR. Generally, isocyanate vibrations give rise to a single broad band centered at around 2260-2255 cm^{-1}, which is a combined signal from p-NCO and s-NCO difficult to be distinguished. However, the shape of the peak can change, if the p- and s-NCO have different reactivity. According to Figure 29, isocyanate peaks of SPUR 2 (Bi2) and SPUR 7 (Bi1) had no significant change in peak position during the reaction progress, which indicates that the reactivity of p- and s-NCO was similar in catalyst systems based on bismuth carboxylates (Bi1 and Bi2). On the contrary, in the DOTL system, it was obvious that isocyanate peak shifted to a higher wavenumber. This strongly indicates that the reactivity of p- and s-NCO was different in DOTL system. Since the p-NCO band has been reported to appear at a slightly higher wavenumber than the s-NCO in FTIR spectrum (Sardon, Irusta, & Fernández-Berridi, Synthesis of isophorone diisocyanate (IPDI) based waterborne polyurethanes: Comparison between zirconium and tin catalysts in the polymerization process, 2009), it is suggested that the reactivity of s-NCO is higher than that of p-NCO in the DOTL catalyzed system. This finding confirms the NMR results, and it is also in line with the previous findings suggesting a higher reactivity of s-NCO towards hydroxyls in tin catalyzed reactions. (Sardon, Irusta, González, & Fernández-Berridi, 2013; Sardon, Irusta, & Fernández-Berridi, Synthesis of isophorone diisocyanate (IPDI) based waterborne polyurethanes: Comparison between zirconium and tin catalysts in the polymerization process, 2009; Delebecq, Pascault, Boutevin, & Ganachaud, 2013) Thus, based on this observation, we can conclude that the reactivity of p- and s-NCO towards hydroxyl groups is highly dependent on the catalyst system.

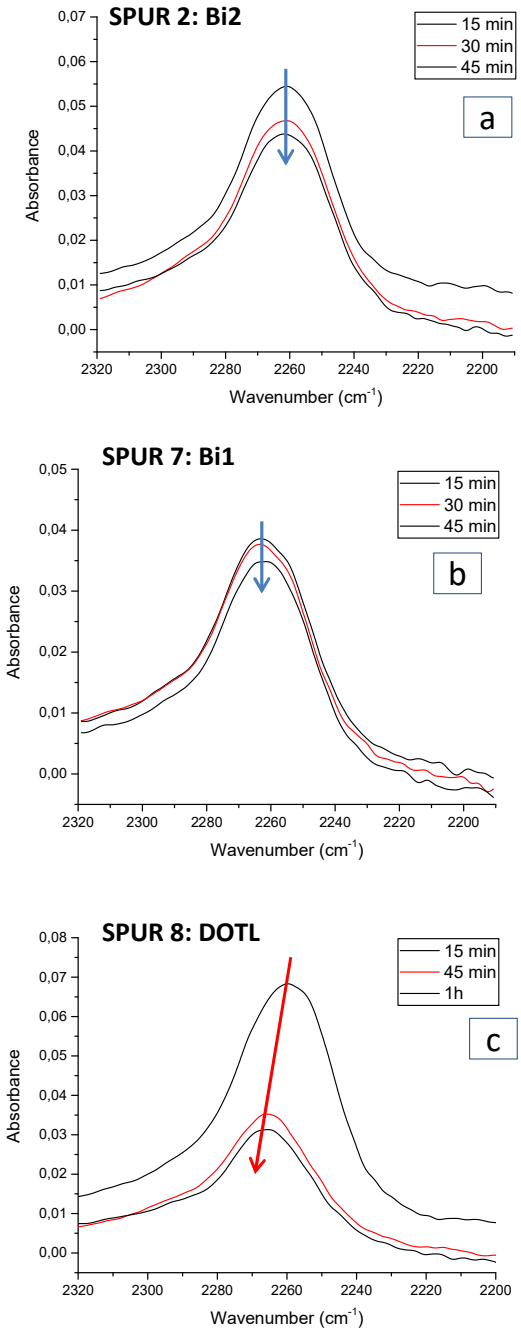

Figure 29. ATR-FTIR spectra in the isocyanate stretching region of samples taken at different reaction times during 1st stage reaction for different catalyst systems: a. SPUR 2 (Bi2); b. SPUR 7 (Bi1); c. SPUR 8 (DOTL).

Catalyst activity

Catalysts play a dominate role in accelerating the isocyanate-hydroxyl reaction (PUR prepolymer formation), particularly in the presence of IPDI with a low reactivity. The activities of different organometallic catalysts were evaluated by simply monitoring the time required for reaction to reach completion by ATR-FTIR.

Comparing samples prepared under similar conditions in the presence of 0.1 wt% of different types of catalysts, time for their urethane prepolymer formation is shown in Table 17.

Table 17. The evaluation of different catalyst activities.

SPUR sample code	Catalyst (metal content)	Time for urethane prepolymer formation (min)	Amount of silane
SPUR 2	Bi2 (19.0–21.0 %)	45	S[a]
SPUR 7	Bi1 (15.0–16.5 %)	45	S
SPUR 8	DOTL (15.5–17.0 %)	60	S

[a] S refers to stoichiometric.

Irrespective of the catalyst type, substantial urethane formation was detected after 15 min of mixing at 70 °C. According to ATR-FTIR results, no significant differences in urethane signals of SPUR 2 (catalyzed by Bi2) and SPUR 7 (catalyzed by Bi1) could be observed after 45 min of reaction, which indicated that these two bismuth carboxylates have similar activities, while for sample SPUR 8 catalyzed by DOTL it took 60 minutes to complete the reaction. This suggests that bismuth carboxylates have initially higher catalysis activity than DOTL. (Guhl D. , Alternatives to DBTL catalysts in polyurethanes A comparative study, 2015; Guhl D. , Replacing a veritable workhorse, 2008; Guhl D. , 2008) Previous studies have shown that tin-catalyst (DBTDL) can form complexes with both isocyanate and hydroxyl moieties that in turn serve as intermediates which convert into urethane in the subsequent rate-determining step. Consequently, the catalyst efficacy is also dependent on whether a one-shot or two-stage process is utilized. (Luo, et al., 1997; Niyogi, Sarkar, & Adhikari, 2002) DBTDL addition in a mixture of polyol and isocyanates (one shot process) results in a more rapid formation of polyurethane than when adding DBTDL catalyst in a two-stage process. (Niyogi, Sarkar, & Adhikari, 2002) This is one reason why we synthesized PUR prepolymers in a one-shot process. DOTL has a similar chemical structure as DBTDL, and thus a similar catalytic mechanism is to be expected.

Silane reactivity

The effect of chemical structure of silanes, in terms of substitution pattern (alicyclic, cyclic or aromatic), spacer (α or γ) and alkoxyl (methoxy or ethoxy)

groups, on their reactivity in 2nd stage reaction was studied. By virtue of the convenience of ATR-FTIR method, the reactivity of different silanes was evaluated by recording the time required for completing the reaction. The reaction was considered to be completed when –NCO signal could not be detected in ATR-FTIR spectra.

Five samples denoted SPUR 2, 6, 9, 10 and 11 were synthesized using different types of silanes and the end-capping time for the formulations is shown in Table 18.

Table 18. The evaluation of reactivity of different silanes.

SPUR sample code	Silane	Observed endcapping time (min)
SPUR 2	**S4**	**5**
SPUR 6	**S1**	**5**
SPUR 9	**S2**	**>120**
SPUR 10	**S5**	**5**
SPUR 11	**S3**	**5**

Aminosilanes S1, S3, S4 and S5 were effective endcappers, as they were able to completely endcap the NCO-terminated prepolymers in five minutes. S2 had considerably lower reactivity. Free isocyanate groups were still detectable in SPUR 9 after two hours of reaction. The reason for this remains unclear.

Polymer structure

The mechanical and physical properties of polyurethanes are largely controlled by their dual-phase structure which stems from the extent and patterns of hydrogen bonding interactions. The extent of hydrogen bonding can be investigated by studying the urethane N–H stretching region (3450-3200 cm^{-1}) and C=O stretching regions (amide I: 1760-1600 cm^{-1}) in ATR-FTIR spectrum. As the polymer structure is primarily influenced by NCO/OH ratio and PPG chain length, their impacts were elaborated by comparing ATR-FTIR spectra of relevant SPUR prepolymers in these stretching regions, as shown in Figure 30.

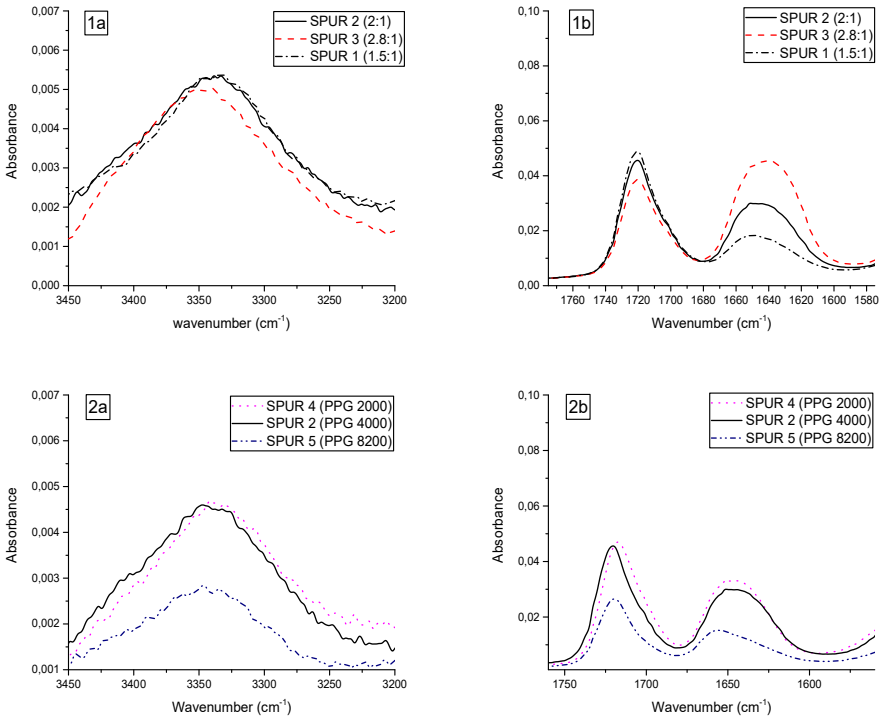

Figure 30. The ATR-FTIR spectral comparison of relevant samples with different variables in N–H stretching region (3450-3200 cm^{-1}) (left) and C=O stretching region (1760-1600 cm^{-1}) (right). Figures 1a and 1b: Impact of NCO/OH ratio; Figures 2a and 2b: Impact of PPG chain length.

Molar ratio of NCO/OH

According to Figure 30 (1a and 1b), NCO/OH ratio had little impact on the N-H (3450-3200 cm^{-1}) and urethane C=O (1760-1680 cm^{-1}) absorbance peaks. Whereas, the recorded slight decrease in the intensity of urethane absorbance peaks as the NCO/OH ratio increases can be attributed to the decrease in PUR chain length. Not surprisingly, it was observed that urea C=O (1680-1600 cm^{-1}) absorbance increased as the NCO/OH ratio increased. Besides, the N-H peak of SPUR 3 (NCO/OH=2.8:1) slightly shifted to a higher wavenumber, which also indicates a higher urea content. (Delebecq, Pascault, Boutevin, & Ganachaud, 2013)

PPG molecular weight

In Figure 30 (2a and 2b), it can be observed that N-H (3450-3200 cm^{-1}) and urethane C=O (1760-1680 cm^{-1}) absorbance peaks slightly shifted to a higher wavenumber as PPG molecular weight increased. Especially, SPUR 5 (PPG 8200) with a low content of hard segments (HS/SS ratio in Table 5) contained less hydrogen bonding interactions (urea C=O shifted to a higher wavenumber).

5.3.3 Rheology of SPUR prepolymers

The rheology of SPUR prepolymers was investigated at low and high shear rates in order to simulate the deformation processes to which the prepolymers are subjected to during storage and application processes. The low shear rate condition ($\dot{\gamma}$=1 s^{-1}) simulates samples at steady state, giving important information closely related to the average molecular weight and polymer chain interactions. On the other hand, the high shear rate simulates application conditions of SPUR polymers.

The SPUR prepolymers showed considerable shear-thinning behavior (see Table 19), and the decrease in viscosities at higher shear rates have been attributed to gradual breakdown of secondary intramolecular forces. (Poljanšek, Fabjan, Moderc, & Kukanja, 2014) By comparing SPUR 2 (PPG 4000), SPUR 4 (PPG 2000) and SPUR 5 (PPG 8200), it can be noted that viscosities of SPUR prepolymers increased with PPG chain length at a shear rate of 1 s^{-1}, which indicates that PPG chain length plays a dominant role in the evolution of viscosity at steady state. As could be anticipated, shear thinning was more pronounced for SPUR 5 (PPG 8200) than for the other samples, as the weaker secondary intermolecular forces (less hydrogen bonding interactions) in SPUR 5 (PPG 8200) sample are insufficient to hold polymer chains together at a high shear rate. In contrast, SPUR 2 (PPG 2000) exhibited only a moderate shear thinning behavior, as the relatively high content of hydrogen bonding interactions contribute to the ability to withstand increasing shear rates.

The viscosities of SPUR prepolymers SPUR 1 (1.5:1), SPUR 2 (2:1) and SPUR 3 (2.8:1) decreased as the NCO/OH ratios increased, which is attributed to a decreasing polyurethane chain length. This is in line with earlier studies. The shear thinning is less pronounced for SPUR 3 with the highest NCO/OH ratio, because of its substantial hard segment content (urea) effectively reducing chain mobility via hydrogen bonding. Among the samples containing different silanes, SPUR-11 (S3) exhibited considerably higher viscosity than other samples, which could be attributed to the bis-(trimethoxysilylpropyl) amine structure. (For, Curing, Adhesives, By, & Schindler, 2005; Chemmie, 2012) Comparing samples with different catalysts, samples with DOTL and Bi2 exhibited considerably lower viscosities.

Table 19. Viscosities of SPUR prepolymers and formulated adhesives at various shear rates.

Sample code	Viscosity of SPUR prepolymers (mPa·s) at different shear rates		Viscosity of formulated SPUR adhesives / mPa·s
	$\dot{\gamma}$=1 s^{-1}	$\dot{\gamma}$=100 s^{-1}	
SPUR-1	119 000	38 500	83 000
SPUR-2	45 900	20 000	59 300
SPUR-3	21 900	12 900	49 800
SPUR-4	33 000	32 800	52 400
SPUR-5	150 000	48 800	86 800
SPUR-6	30 300	12 000	58 700
SPUR-7	187 000	65 800	62 800
SPUR-8	56 400	20 700	44 800
SPUR-9	35 800	16 500	73 000
SPUR-10	96 000	37 400	59 000
SPUR-11	217 000	64 000	79 000

The viscosities of formulated SPUR adhesives were measured by a Brookfield viscometer, in order to evaluate their open time and viability as a SPUR adhesive in practice. When compared with their prepolymer counterparts, it was generally observed that by appropriate formulation design one could adjust viscosities of SPUR polymers to a reasonably low level by the addition of plasticizers.

5.3.4 Thermal stability

Thermal stability of cured SPUR films was investigated by TGA. It has been earlier established that the decomposition of a (silane-modified) polyurethane occurs at three distinct stages: the first weight loss takes place at the temperature range of 25–250 °C resulting from water evaporation, decomposition of oligomers and by-products; the second significant decomposition occurs at the temperature range of 250–350 °C, attributed to the

degradation of HSs (urethane and urea); the third stage begins at 350 °C, where SSs and silane segments start to decompose.

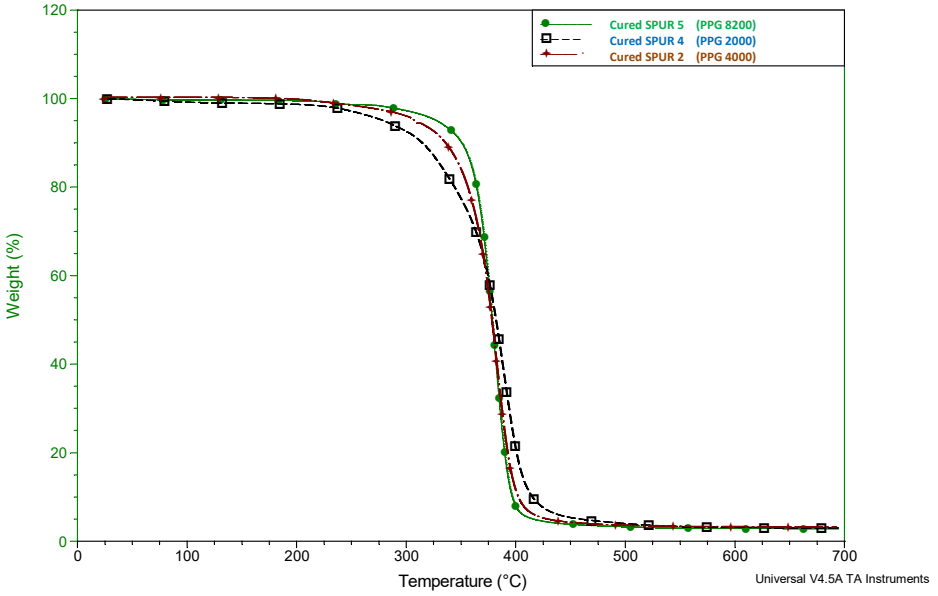

Figure 31. TGA curves comparison of cured SPUR 5 (PPG 8200), SPUR 4 (PPG 2000) and SPUR 2 (PPG 4000).

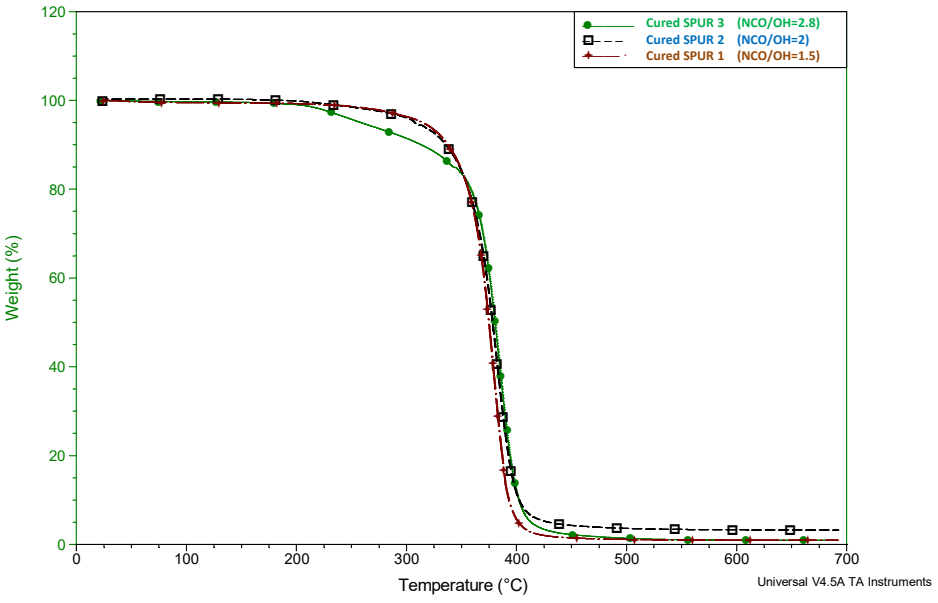

Figure 32. TGA curve comparison of cured SPUR 1 (1.5:1), SPUR 2 (2:1) and SPUR 3 (2.8:1).

TGA curves of the samples with different PPG chain lengths are presented in Figure 31. The onset of weight loss was delayed as the PPG molecular weight

increased. The cured SPUR 4 has high initial weight loss between 250 °C to 350 °C due to the HS decomposition. In contrast, cured SPUR 5 shows a rather small weight loss due to HS segment decomposition, but it undergoes an abrupt/steep weight loss due to SS segment decomposition at about 350 °C. The thermal stability above 350 °C was enhanced when the PPG chain length decreased, which can be attributed to the increased content of siloxane crosslinks. Cured SPUR 5 exhibited a dominate character of SSs due to its low HS and silane content. Therefore, it seems that the thermal stability is enhanced with a low content of HSs and high content of SSs.

TGA curves of the samples with different NCO/OH ratios are compared in Figure 32. It is noticed that much more volatiles are formed between 200–250 °C for the cured SPUR 3 than for the other samples, which indicates that it, due to the higher NCO/OH ratio, contains lower molecular weight compounds. The cured SPUR 2 followed a similar weight loss trend as the cured SPUR 1.

5.3.5 Cure rate of formulated SPUR adhesives

Effect of catalyst

The cure times of formulated samples prepared with different types of catalysts are compared in Figure 33. The sample with bismuth carboxylate catalyst Bi1 had the longest cure time (3 days) which can partly depend on the lowest metal content (15-16.5 %) among all the samples. Bismuth carboxylate Bi2 with a high metal content (19-21 %) induced curing as fast as DOTL (15.5-17.0 %) (1 day) and it exhibited high catalytic activity also in the silanol-water reaction. These results can be explained by the fact that bismuth with a lower Lewis acidity in comparison to a tin catalyst has a tendency to lose activity during the curing process, and therefore an initially higher metal content is needed for a bismuth catalyst than for a tin catalyst. (Guhl D. , Alternatives to DBTL catalysts in polyurethanes A comparative study, 2015)

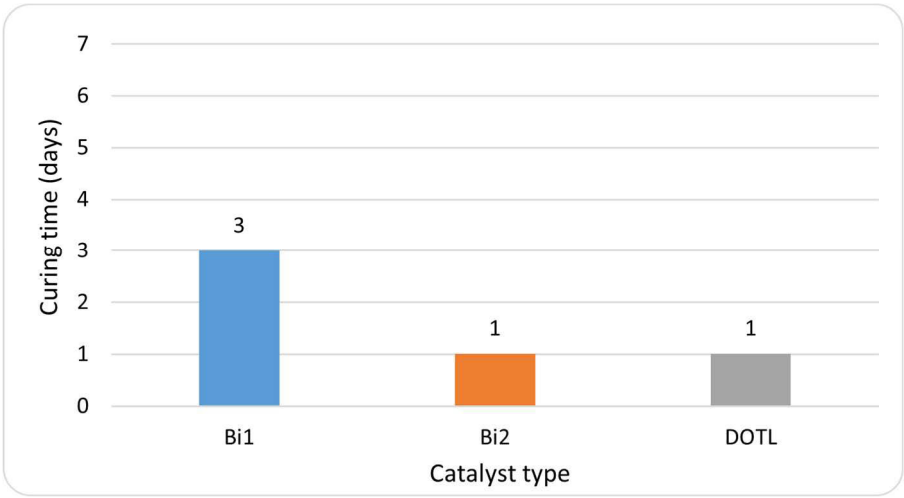

Figure 33. Effect of catalysts on cure time of formulated SPUR samples.

Effect of silane

In the presence of 0.1 % bismuth carboxylate Bi2, the cure times of formulated samples containing different types of silanes were compared (Figure 34). Formulated SPUR samples containing S1 and S4 showed the fastest cure (1 day). In comparison, slightly longer cure times (2d or 3d) were required for samples containing S3. Sample containing S5 had the slowest cure, and even after 7d bulk curing was incomplete. A soft skin formation was observed in the sample with S5, which indicates that the α-linked nitrogen in the silane induced such a fast cure on the film surface that a complete through-cure underneath was delayed.

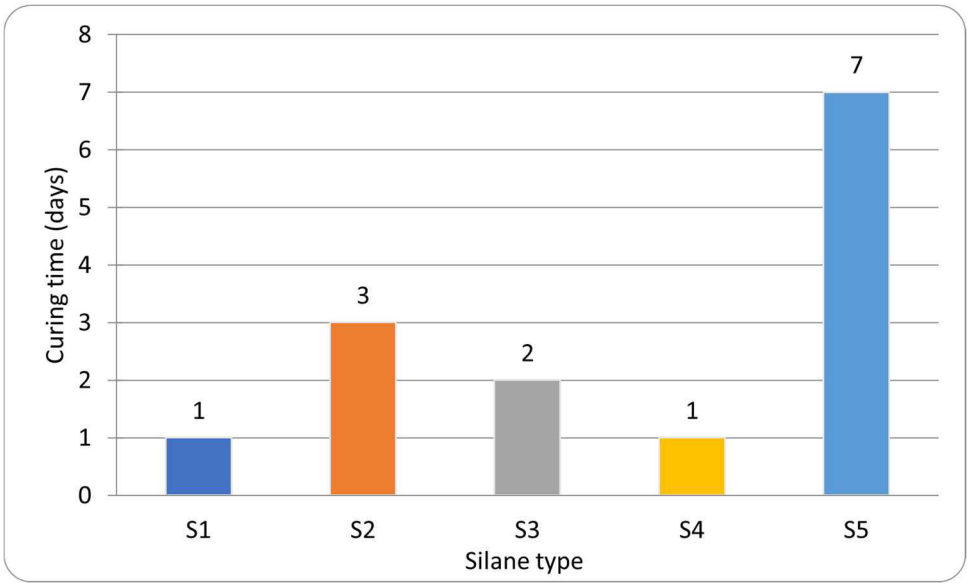

Figure 34. Effect of silanes on cure time of formulated SPUR samples

5.3.6 Mechanical properties of cured SPUR adhesives

Mechanical properties of cured SPUR adhesives, including tensile strength and elongation at break, are shown in Table 20.

Table 20. The mechanical test results of cured SPUR adhesives.

SPUR sample code*	Variables	Tensile strength (N/mm^2)	Elongation at break (%)
SPUR-4-F	PPG 2000	2.00	17.82
SPUR-2-F	PPG 4000	2.06	43.64
SPUR-5-F	PPG 8200	2.37	67.95
SPUR-1-F	NCO/OH=1.5	1.56	71.35
SPUR-2-F	NCO/OH=2	2.06	43.64
SPUR-3-F	NCO/OH=2.8	2.05	21.79
SPUR-2-F	Bi2	2.06	43.64
SPUR-7-F	Bi1	2.13	57.97
SPUR-8-F	DOTL	2.07	34.06
SPUR-2-F	S4	2.06	43.64
SPUR-11-F	S3	1.47	43,22
SPUR-6-F	S1	2.23	54.51

* Formulated SPUR samples X were abbreviated as SPUR-X-F: X refers to the code; F is the abbreviation for formulated.

By comparing the first three results SPUR-4-F (PPG 2000), SPUR-2-F (PPG 4000) and SPUR-5-F (PPG 8200), one can see that the elongation increased as PPG molecular weight increased due to enhanced flexibility of the polymer chains. However, it was surprisingly observed that also the tensile strength slightly increased with an increase in PPG molecular weight. Despite SPUR-5-F exhibited good mechanical strength, its high viscosity (Table 19) makes it less favorable. Therefore, PPG 4000 based SPUR was used in all the following comparisons (Table 20).

When mechanical test results of samples with different NCO/OH are compared, one can see that the tensile strength of SPUR-1-F (NCO/OH=1.5) was

significantly lower than that of SPUR-2-F (NCO/OH=2) and SPUR-3-F (NCO/OH=2.8), which indicates that low NCO/OH ratio gives a weak bondline. SPUR-2-F and SPUR-3-F have high NCO/OH ratio, and thereby an increased content of silane and urea linkages as well as greater hydrogen bonding interactions contribute to greater crosslink density and enhanced tensile strength. As expected, the elongation decreased as a function of NCO/OH, due to the increased stiffness and reduced flexibility.

Similar tensile strength results were observed for the samples catalyzed with Bi1, Bi2 or DOTL, whereas the sample prepared with the tin catalyst showed slightly lower elongation than the samples prepared with the bismuth-based catalysts.

The mechanical strength of samples containing different silanes S1, S3 and S4 were also compared. The best mechanical strength results were observed for SPUR-6-F with S1, exhibiting simultaneously high tensile strength and elongation. Comparable good results were obtained for SPUR-2-F with S4. The lowest tensile strength was observed for SPUR-11-F with S3.

6. Conclusions

In this thesis work, various adhesives were synthesized and developed in order to increase the knowledge of modifying adhesives to provide more sustainable adhesive solutions as well as adhesives exhibiting enhanced and tailor-made set of desired properties, including: 1) to design core-shell type of emulsion adhesives that exhibit simultaneously high cohesive and adhesive properties, 2) to prepare isocyanate terminated urethane prepolymers that exhibit high adhesive strength in combination with low viscosity by rational adjusting the length and type of chain extenders, and 3) to develop low viscous organotin-free high performance one-component silane-terminated polyurethane adhesives.

In publication I a series of environmentally friendly waterborne poly(styrene-co-butyl acrylate) latexes with a rigid core and soft shell structure have been successfully synthesized via semi-batch emulsion polymerization. The structure–property relationship has been examined by changing different factors such as crosslinking of the core, concentration of CTA in the shell part, and core to shell ratio, with the objective of optimizing the adhesive performance. The adhesion properties were characterized via measurements of tack, peel and shear strength and they were in conformity with the recorded DMA data. Hard core–soft shell structure was obtained by proper combinations of butyl acrylate and styrene in the particles core and shell, respectively, with the theoretically predicted Tg's of -11 °C for the core and -35 °C for the shell. The incorporation of crosslinker in the core part greatly increased the gel content and crosslink density, and subsequently significantly improved the cohesive strength (shear resistance). The addition of CTA in the shell part promoted polymer chain mobility and deformability, and thus enhanced tack and adhesion strength (peel strength) to a significant extent. However, CTA addition had a negative impact on the cohesive strength due to weakening of the boundary between the core domain and the shell matrix, thereby partially undermining the positive effects of CTA on the tack and the adhesion strength. The change in the ratio of core to shell from 1:1.5 to 1:1 increased the relative amount of the crosslinked core copolymer and subsequently the gel content, whereby high cohesive strength was obtained; on the other hand, the adhesive strength and particularly the tack decreased significantly. It was found that sample1, which consisted of a crosslinked core, a shell without CTA and a core–shell ratio of 1:1.5, possessed an optimal balance between tack, peel strength and shear strength. Thus, the goal of combining sufficient energy storage and energy dissipation properties within single latex particles has been achieved. The optimized environmentally friendly poly(styrene-co-butyl acrylate) latex with a crosslinked rigid core and soft shell can favorably be utilized as a new, low cost and high performance construction adhesive.

In publication II, a series of chain extended urethane prepolymers was synthesized, and the effects of different chain extenders, as well as the influence of the synthesis process were systematically investigated. As anticipated, the

incorporation of chain extenders enhanced the adhesive strength of MCPUs, and this enhancement was dependent on the structure of chain extenders and the synthesis process. The one-shot process produced urethane prepolymers with more randomly organized polymer chains than the two-stage process, leading to better phase mixing. Compared to the linear chain extenders, the branched chain extenders (di-PPG and tri-PPG) generated less phase segregation between HS and SS, enabling low viscosity. Compared to non-chain extended polyurethane, clearly enhanced lap shear strength was reached only when using di-PPG at a high molar ratio of 0.94. On the contrary, the incorporation of linear chain extenders readily promoted HS association into hard domains via hydrogen bonding interactions within HS. The degree of phase separation was particularly pronounced for butanediol, and/or when the linear chain extender molar ratio was no less than 0.74. However, phase separation significantly increased the viscosity, whereby at a high linear chain extender amount (0.74 molar ratio), the urethane prepolymers became wax-like (no flow) and were therefore not ideal for their intended use. Above all, polyurethane with a 0.54 molar ratio of pentanediol showed strong adhesive strength with simultaneously low viscosity. This work demonstrates that chain extenders can be used to prepare one-component polyurethane adhesives that exhibit simultaneously low viscosity and enhanced shear strength after curing. The type and the amount of CE, together with the synthesis manner determine the degree of HS hydrogen bonding, and thereby the degree of phase segregation. This in turn is the main contributing factor both for viscosity and shear strength build-up.

In publication III: a series of moisture-curable silane-terminated polyurethanes (SPUR) was prepared and the effects of polyol (PPG) molecular weight, NCO/OH ratio and the types of catalyst and aminosilane used in the synthesis of SPUR polymers were investigated. SPUR polymers of significantly lower viscosity were obtained by using PPG of molecular weight 2000 g/mol and 4000 g/mol in comparison to 8200 g/mol. Furthermore, increasing the NCO/OH ratio was found to lead to SPUR of favorably low viscosity. Bismuth carboxylates Bi1 and Bi2 were effective catalysts in the synthesis of SPUR prepolymers, even superior to the tin catalyst DOTL. Most of the tested secondary aminosilanes were found to be effective end-cappers for the NCO-terminated polyurethanes, since complete endcapping was achieved according to the FTIR studies. The curing behavior of SPUR adhesives was found to be dependent on the silane and catalyst type, and 1-day curing time was established to be sufficient for the SPUR adhesives catalyzed by the bismuth carboxylate of a high metal content (Bi2) and the tin catalyst DOTL when using either aminosilane S1 or S4. Mechanical properties of the cured SPUR adhesives, in terms of tensile strength and elongation, are closely related to the flexibility of polymer chains, the content of silane and hard segments as well as the extent of hydrogen bonding. An optimal performance with balanced flexibility and toughness was obtained with an adhesive formulation containing the bismuth carboxylate catalyst Bi2, the medium long polymer chains (PPG 4000 and NCO/OH=2) and the silane end-cappers S1 or S4. The presented results give an insight into the effects of bismuth

catalysts and the polymer composition on the performance of SPUR adhesives. It gives good guidelines for selecting raw materials for the synthesis of low viscous organotin-free high-performance moisture-curable silane-terminated polyurethane adhesives.

6.1 Outlook

The ever-shifting landscape of customer demand has a serious impact on adhesive producers that need to make adhesives and bonding processes more sustainable, and at the same time having a positive impact on saving time, material resources and energy. Over the past years we have seen a surge in activity towards waterborne adhesives and resource conservation by using bio-based raw materials in the development of new adhesive formulations. Virtually all modern adhesives are based on polymers. The contemporary development of adhesive science stems from the ability to create new polymeric materials with a corresponding set of special properties and with high adhesive bonding to various surfaces including high physico-mechanical, thermophysical, and selective-sorption properties.

In the future, polymer chemists will be able to further leverage an ever-growing array of high- performance adhesives due to enhancements in polymerization processes, catalysts and availability of monomers that provide a more precise control over all aspects of polymer chemistry and technology. Therefore, future polymer adhesives synthesized by industry may have improved tailor-made structures, molecular weight distributions, block architectures, topologies and functional groups at controlled locations allowing specific adhesive interaction and optimized mechanical and rheological properties.

The field of emulsion polymerization offers not only better environmental compliance due to dispersion in water, but also advantages such as a utilization of inexpensive raw materials including biobased monomers, high control of final product properties and morphologies which enable the reduction of both adhesive and cohesive failures, as also demonstrated in this doctoral thesis work. This combination of tailored performance, longevity, and environmental friendliness will become the future industry standard.

Overall solvent-free adhesives and utilization of greener chemicals for their production will be dominating the future adhesive markets. In line with this trend, adhesives based on polyurethane end capped with alkoxysilanes have grown commercially and this development is likely to continue. These silanized polyurethanes with moisture condensable terminal groups give raise to hybrid adhesives that exhibit synergistic effects due to the beneficial interaction between the organic and inorganic phases. Thus, these silane-modified polyurethanes combine the unique properties of elastic silicones and the toughness of polyurethane polymers. The use of silane-modified polyurethanes is expected to increase as their chemistries are further refined and optimized.

In general, environmentally benign adhesive solutions will stay in the focus of intense research efforts. Multi-functional adhesives triggerable by external stimuli such as ions, electrical current or UV light will gain increasing interest. Moreover, the development of reversible adhesives to ease the recycling of bonded components will become more important in the future.

Despite the great deal of publicity that different adhesive types have received in recent years, there still tends to be challenges in formulating optimal structural, thermoplastic and pressure sensitive adhesives. Notably, due to a more comprehensive integration and comparison of experimental, theoretical, and computational data in the field of polymer adhesives further progress is clearly foreseeable.

References

Alarcia F, D. C. (2006). Continuous production of specialty waterborne adhesives: tuning the adhesive performance. Chem Eng J, 122(3), 117–26.

Allauddin, S., Narayan, R., & Raju, K. (2013). Synthesis and properties of alkoxysilane castor oil and their polyurethane/urea-silica hybrid coating films. *ACS Sustain. Chem. Eng., 1*, 910–918.

(2004). *Assessment report on 2-ethylhexanol for developing ambient air quality objectives.* Toxico-Logic Consulting Inc. .

Aymonier A, P. E. (2003). Influence of surface and bulk structures of acrylic psa films on to their tack properties. *J Colloid Interface Sci, 268*(2), 341–7.

Ballauff M, L. (2007). "Smart" nanoparticles: preparation, characterization and applications. *Polymer, 48*(7), 1815–23.

Blank, W. J. (2002). New Developments in Catalysis. *Macromolecular Symposia* . Retrieved from Researchgate: http://www.wernerblank.com/pdfiles/paper32.pdf

Chattopadhyay DK, S. B. (2005). Effect of chain extender on phase mixing and coating properties of polyurethane ureas. *Ind Eng Chem Res, 44*(6), 1772–9.

Chattopadhyay, D., Sreedhar, B., & Raju, K. (2005). Effect of chain extender on phase mixing and coating properties of polyurethane ureas. *Ind. Eng. Chem. Res.*, 1772–1779.

Chauvet J, A. J. (2005). Independent control of sol molar mass and gel content in acrylate polymer/latexes. *Polymer, 46*(23), 9555–61.

Chemmie, W. (2012). *Silanes Oganofunctional for Powerful Connections.* München: Wacker Chemmie.

Chino S, K. S. (2013). Measurement of 2-ethyl-1-hexanol emitted from flooring materials and adhesives. *J Adhes Sci Technol*, 659–70.

Clauß, S. (2011). Influence of the adhesive formulation on the mechanical properties and bonding performance of polyurethane prepolymers. *Holzforschung*, 835–844.

Clauß, S., Dijkstra, D., Gabriel, J., Kläusler, O., Matner, M., Meckel, W., & Niemz, P. (2011). Influence of the chemical structure of PUR prepolymers on thermal stability. *Int. J. Adhes. Adhes.*, 513–523.

(2009). *COMMISSION REGULATION (EC) No 552/2009.* The European Parlament and the Council of the European.

(2010). *Commission Regulation (EU) No 276/2010.* Official Journal of the European Union.

Corcuera, M., Rueda, L., Fernandez d'Arlas, B., Arbelaiz, A., Marieta, C., Mondragon, I., & Eceiza, A. (2010). Microstructure and properties of polyurethanes derived from castor oil. *Polym. Degrad. Stab.*, 2175–2184.

Cornille, F. e. (2017). Environment Friendly Polyurethane : Nonisocyanate Synthesis. *Euro. Poly. J.*, 535-552.

Crassous JJ, R. C. (2009). Quantitative analysis of polymer colloids by cryo-transmission electron microscopy. *Langmuir, 25*(14), 7862–71.

CS, C. (2006). Emulsion polymerization mechanisms and kinetics. *Prog Polym Sci*, 443–86.

da Silva LF, Ö. A. (2011). *Handbook of adhesion technology.* Springer.

Daniel da Silva, A., Martín-Martínez, J., & Bordado, J. (2006). Influence of the free isocyanate content in the adhesive properties of reactive trifunctional polyether urethane quasi-prepolymers. *Int. J. Adhes. Adhes.*, 355–362.

Daniels, C. A. (2003). *Emulsion Polymerization and Latex Applications.* Rapra Review Reports.

Delebecq, E., Pascault, J., Boutevin, B., & Ganachaud, F. (2013). On the versatility of urethane/urea bonds: Reversibility, blocked isocyanate, and non-isocyanate polyurethane. *Chem. Rev., 113*, 80–118.

Delpech, M., & Miranda, G. (2011). Waterborne polyurethanes: Influence of chain extender in ftir spectra profiles. *Cent. Eur. J. Eng.*, 231–238.

Dennis G. Lay, P. C. (2018). Polyurethane Adhesives. In K. M. A. Pizzi, *Handbook of Adhesive Technology* (p. 321). NW: CRC Press.

Dennis G. Lay, P. C. (2018). Polyurethane Adhesives. In K. M. A. Pizzi, *Handbook of Adhesive Technology* (p. 321). CRC press.

do Amaral M, R. A. (2005). Assessing the effect of latex particle size and distribution on the rheological and adhesive properties of model waterborne acrylic pressure-sensitive adhesives films. *Colloid Interface Sci, 281*(2), 325–38.

Dubé, R. J. (2007). Emulsion-Based Pressure-Sensitive Adhesives: A Review. *Journal of Macromolecular Science, Part C: Polymer Reviews*, Vol. C44, No. 1, pp. 1–51.

El-Sabbagh S, Y. A. (2007). Detection of crosslink density by different methods for natural rubber blended with SBR and NBR. *Egypt J Solids, 30*(2), 157–73.

Engels, H.-W., Pirkl, H.-G., Albers, R., Albach, R., Krause, J., Hoffmann, A., . . . Dormish, J. (2013). Polyurethanes: Versatile materials and sustainable problem solvers for today's challenges. *Angew. Chem. Int. Ed. Engl.*, 9422–9441.

Ferguson CJ, R. G. (2002). Modelling secondary particle formation in emulsion polymerisation: application to making core–shell morphologies. *Polymer, 43*(17), 4557–70.

Fernandes, I. P. (2015). Water-based poly(urethane-urea) dispersions - meeting the European Union legislation. *Polimery*, 536–540.

For, B., Curing, F., Adhesives, E., By, P., & Schindler, W. (2005). *Alpha-Silane-Terminated Polymers as Novel Binders for Fast Curing Elastic Adhesives.* München: Wolfram Schindler at the European Coatings Show.

Foster AB, L. P. (2009). Control of adhesive properties through structured particle design of water-borne pressure-sensitive adhesives. *Polymer, 50*(7), 1654–70.

Friedrich H, F. P. (2010). Imaging of self-assembled structures: interpretation of TEM and Cryo-TEM images. *Angew Chem Int Ed, 49*(43), 7850–8.

Gardner, D. J. (2018). Theories and Mechanisms of Adhesion. In K. M. A. Pizzi, *Handbook of Adhesive Technology* (p. 3). CRC Press.

Guhl, D. (2008). *Bismuth catalysts and their performance in polyurethane applications.* Retrieved from Researchgate: https://www.researchgate.net/publication/263746144_Bismuth_Catalysts_and_their_performance_in_Polyurethane_Applications

Guhl, D. (2008). Replacing a veritable workhorse. *European Coatings Journal.*

Guhl, D. (2015). Alternatives to DBTL catalysts in polyurethanes A comparative study. *The polyurethanes for high performance coatings, European Coatings Conference.* Berlin.

Gurke, T. (2002). New advances in polymeric MDI variants. *Paint Resin Times*, 22–23.

Gurunathan, T., & Chung, J. (2016). Physicochemical properties of amino-silane-terminated vegetable oil-based waterborne polyurethane nanocomposites. *ACS Sustain. Chem. Eng.*, 4645–4653.

HB., Y. (2013). Emulsion polymerization: effects of polymerization variables on the properties of vinyl acetate based emulsion polymers. *Polym Sci In Tech*, 35–70.

He, Y., Xie, D., & Zhang, X. (2014). The structure, microphase-separated morphology, and property of

polyurethanes and polyureas. *J. Mater. Sci.*, 7339–7352.

Heintz, A., Duffy, D., Hsu, S., Suen, W., Chu, W., & Paul, C. (2003). Effects of reaction temperature on the formation of polyurethane prepolymer structures. *Macromolecules*, 2695–2704.

Heintz, A., Duffy, D., Hsu, S., Suen, W., Chu, W., & Paul, C. (2003). Effects of reaction temperature on the formation of polyurethane prepolymer structures. *Macromolecules*, 2695–2704.

Huber, M., Kelch, S., & Berke, H. (2016). FTIR investigations on hydrolysis and condensation reactions of alkoxysilane. *Int. J. Adhes. Adhes.*, 153–162.

Ionescu, M. (2005). Chemistry and Technology of Polyols for Polyurethane. *iSmithers Rapra Publishing*.

J., H. (2008). Effects of agitation in emulsion polymerization—kinetic and mechanistic study of coagulum. *Ann Arbor: Pro Quest*.

Ji W, J. Y. (2012). Design and control of soap-free hydrophilic-hydrophobic core–shell latex particles with high carboxyl content in the core of the particles. *Chin J Polym Sci, 30*(4), 595–602.

JM., A. (2004). Emulsion polymerization: from fundamental mechanisms to process developments. *PolymSci Part A: Polym Chem, 42*(5), 1025–41.

John B. Sullivan Jr. MD, G. (1999). *Clinical Environmental Health and Toxic Exposures* . Lippincott Williams & Wilkins.

K., L. (2003). *Polymer dispersions and their industrial applications.* Macromol Chem Phys.

Kajtna J, G. J. (2009). The effect of polymer molecular weight and crosslinking reactions on the adhesion properties of microsphere water-based acrylic pressure-sensitive adhesives. *Int J Adhes Adhes, 29*(2), 186–94.

Klinedinst, D., Yilgör, I., Yilgör, E., Zhang, M., & Wilkes, G. (2012). The effect of varying soft and hard segment length on the structure–property relationships of segmented polyurethanes based on a linear symmetric diisocyanate, 1,4-butanediol and PTMO soft segments. *Polymer (Guildf)*, 5358–5366.

Król, P. (2007). Synthesis methods, chemical structures and phase structures of linear polyurethanes. *Prog. Mater. Sci., 52*, 915–1015.

Lapprand, A., Boisson, F., Delolme, F., Méchin, F., & Pascault, J. (2005). Reactivity of isocyanates with urethanes: Conditions for allophanate formation. *Polym. Degrad. Stab.*, 363–373.

Lee, D.-K., Tsai, H.-B., Tsai, R.-S., & Chen, P. (2007). Preparation and properties of transparent thermoplastic segmented polyurethanes derived from different polyols. *Polym. Eng. Sci.*, 695–701.

Lehringer, C., & Gabriel, J. (2014). Materials and Joints in Timber Structures: Recent Developments of Technology. *Dordrecht*, 405–420.

Lehringer, C., & Gabriel, J. (2014). Review of Recent Research Activities on One-Component PUR-Adhesives for Engineered Wood Products. In Materials and Joints in Timber Structures: Recent Developments of Technology. *Springer*, 405–420.

Luo, S.-G., Tan, H.-M., Wu, Y., Pei, F.-K., Meng, X.-H., & Zhang, J.-G. (1997). Catalytic Mechanisms of Triphenyl Bismuth, Dibutyltin Dilaurate, and Their Combination in Polyurethane-Forming Reaction. *Appl. Polym., 65*, 1217–1225.

Ma J, L. B. (2013). Research advances in polymer emulsion based on "core–shell" structure particle design. *Adv Colloid Interface Sci*, 118–31.

Master, B. (2013). *Study of Coatings Based on Polyisocyanates of Moisture Cure Depending on Its Resins and Water Scavengers.* Barcelona, Spain: Master's thesis, Universitat Politècnica de Catalunya, BarcelonaTech.

Müller, B., & Rath, W. (2010). Formulating Adhesives and Sealants: Chemistry, Physics and Applications. *Formulating Adhesives and Sealants: Chemistry, Physics and Applications*, 100-136.

Niyogi, S., Sarkar, S., & Adhikari, B. (2002). Catalytic activity of DBTDL in polyurethane formation. *Indian J. Chem. Technol., 9*, 330–333.

Nomura, Y., Sato, A., Sato, S., Mori, H., & Endo, T. (2007). Synthesis of Novel Moisture-Curable Polyurethanes End-Capped with Trialkoxysilane and Their Application to One-Component Adhesives. *J. Polym. Sci. Part A Polym. Chem.*, 2689–2704.

Papon, E., & Villenave, J. (2000). Rheological characterization of thermoplastic polyurethane elastomers. *Polym. Int.*, 591–598.

Papon, E., & Villenave, J. (2000). Rheological characterization of thermoplastic polyurethane elastomers. *Polym. Int.*, 591–598.

Pegoraro, M., Galbiati, A., & Ricca, G. (2003). 1H nuclear magnetic resonance study of polyurethane prepolymers from toluene diisocyanate and polypropylene glycol. *J. Appl. Polym. Sci.*, 347–357.

Pérez-Carrillo L, P. M.-S. (2007). Effect of particle size on the mechanical properties of polystyrene and poly(butyl acrylate) core/shell polymers. *Polymer, 48*(5), 1212–8.

Poljanšek, I., Fabjan, E., Moderc, D., & Kukanja, D. (2014). The effect of free isocyanate content on properties of one component urethane adhesive. *Int. J. Adhes. Adhes., 51*, 87–94.

Prabhakar, A., Chattopadhyay, D., Jagadeesh, B., & Raju, K. (2005). Structural investigations of polypropylene glycol (PPG) and isophorone diisocyanate (IPDI)-based polyurethane prepolymer by 1D and 2D NMR spectroscopy. *J. Polym. Sci. Part A, 43*, 1196–1209.

Priac A, M.-C. D. (2014). Alkyl phenol and alkyl phenol polyethoxylates in water and waste water: a review of options for their elimination. *Arab J Chem.*

Qie L, D. M. (2010). Manipulation of chain transfer agent and cross-linker concentration to modify latex micro-structure for pressure-sensitive adhesives. *Eur Polym J, 46*(6), 1225–36.

Qie L, D. M. (2010). The influence of butyl acrylate/methyl methacrylate/2-Hydroxyethyl methacrylate/acrylic acid latex properties on pressure sensitive Adhesive performance. *Int J Adhes Adhes, 30*(7), 654–64.

Ravichandran, R. H. (2010). New Tin Free Organometallic Catalysts for Urethanes. *Polyurethanes Technical Conference.* Houston, TX, USA.

Rawlins JW, S. R. (2013). Waterborne: environmentally friendly coating technologies. *proceedings of the fortieth annual international waterborne, high-solids, and powder coatings symposium.* DE Stech Publications, Inc.

Ren, D., & Frazier, C. (2013). Structure-property behavior of moisture-cure polyurethane wood adhesives: Influence of hard segment content. *Int. J. Adhes. Adhes.*, 118–124.

Roberge S, D. M. (2006). The effect of particle size and composition on the performance of styrene/butyl acrylate miniemulsion-based PSAs. *Polymer, 47*(3), 799–807.

Saralegi, A., Rueda, L., Fernández-D'Arlas, B., Mondragon, I., Eceiza, A., & Corcuera, M. (2013). Thermoplastic polyurethanes from renewable resources: Effect of soft segment chemical structure and molecular weight on morphology and final properties. *Polym. Int.*, 106–115.

Sardon, H., Irusta, L., & Fernández-Berridi, M. (2009). Synthesis of isophorone diisocyanate (IPDI) based waterborne polyurethanes: Comparison between zirconium and tin catalysts in the

polymerization process. *Prog. Org. Coat., 66*, 291–295.

Sardon, H., Irusta, L., Fernández-Berridi, M., Lansalot, M., & Bourgeat-Lami, E. (2010). Synthesis of room temperature self-curable waterborne hybrid polyurethanes functionalized with (3-aminopropyl)triethoxysilane (APTES). *Polymer (Guildf.), 51*, 5051–5057.

Sardon, H., Irusta, L., González, A., & Fernández-Berridi, M. (2013). Waterborne hybrid polyurethane coatings functionalized with (3-aminopropyl)triethoxysilane: Adhesion properties. *Prog. Org. Coat., 76*, 1230–1235.

Šebenik, U., & Krajnc, M. (2007). Influence of the soft segment length and content on the synthesis and properties of isocyanate-terminated urethane prepolymers. *Int. J. Adhes. Adhes.*, 527–535.

Sheth, J., Klinedinst, D., Wilkes, G., Yilgor, I., & Yilgor, E. (2005). Role of chain symmetry and hydrogen bonding in segmented copolymers with monodisperse hard segments. *Polymer (Guildf)*, 7317–7322.

Sjöberg A, R. O. (2007). An experimental parametric study of voc from flooring systems exposed to alkaline solutions. *Indoor Air*, 450–7.

Sterley, M., Trey, S., Lundevall, Å., & Olsson, S. (2012). Influence of cure conditions on the properties of a one-component moisture-cured polyurethane adhesive in the context of green gluing of wood. *J. Appl. Polym. Sci.*, E297–E304.

Stoeckel, F., Konnerth, J., & Gindl-Altmutter, W. (2013). Mechanical properties of adhesives for bonding wood—A review. *Int. J. Adhes. Adhes.*, 32–41.

Sun S, L. M. (2013). A review on mechanical properties of pressure sensitive adhesives. *Int J Adhes Adhes*, 98–106.

Tan, C., Tirri, T., & Wilen, C.-E. (2017). Investigation on the Influence of Chain Extenders on the Performance of One-Component Moisture-Curable Polyurethane Adhesives. *Polymers, 9*, 184.

Tong Yu C, Q. P. (1997). Polymer Latex: It's Preparation, Property and Application.

Wan Q, L. Y. (2011). Preparation of raspberry shaped Styrene-butadiene-methylacrylate-acrylic acid latex particles by emulsion polymerization followed by alkali/heating method. *Appl Polym Sci, 121*(3), 1276–84.

Yokota T, K. S. (2013). Influence of water content in sub-flooring materials using adhesive on chemical compounds emission. *J Adhes Sci Technol*, 648–58.

Yoon, P., & Han, C. (2000). Effect of thermal history on the rheological behavior of thermoplastic polyurethanes. *Macromolecules*, 2171–2183.

Yuan, Y., Zhang, Y., Fu, X., & Lei, J. (2017). Molecular design for silane-terminated polyurethane applied to moisture-curable pressure-sensitive adhesive. *J. Appl. Polym. Sci.*, 45292.

Yuan, Y., Zhang, Y., Fu, X., Jiang, L., Liu, Z., Hu, K., . . . Zhou, C. (2016). Silane-terminated polyurethane applied to a moisture-curable pressure-sensitive adhesive using triethoxysilane. *RSC Adv.*, 83688–83696.

Zhou C, C. R. (2011). Effect of particle structure on the peel strength and heat resistance properties of vinyl acetate/acrylate latexes laminating adhesives. *J Appl Polym Sci, 119*, 2857–65.

ISBN 978-952-12-4197-0